Calculations with a $1s,0d$ Shell Model for $A = 34$–38 Nuclei*

B. H. Wildenthal
Michigan State University, East Lansing, Michigan 48823
and Oak Ridge National Laboratory, Oak Ridge, Tennessee 37830

and

E. C. Halbert and J. B. McGrory
Oak Ridge National Laboratory, Oak Ridge, Tennessee 37830

and

T. T. S. Kuo
Oak Ridge National Laboratory, Oak Ridge, Tennessee 37830
and State University of New York, Stony Brook, New York 11790

(Received 26 April 1971)

Results are presented of calculations made in the full space of sd-shell-model wave functions for positive-parity states in the nuclei with $A = 34$–38. We employed in this work several different effective Hamiltonians, some of which had two-body parts obtained by reaction-matrix techniques from the Hamada-Johnston scattering potential. The observables calculated were energy-level spectra, single-nucleon spectroscopic factors, and $E2$ and $M1$ moments and transition strengths. These calculations yield fair-to-good agreement with many of the observed nuclear-structure data in this mass region.

I. INTRODUCTION

This paper presents the results of shell-model calculations for positive-parity states of nuclei with mass numbers $A = 34$ through 38. The model vector space is defined by a complete set of many-particle basis states for $A - 16$ nucleons distributed among the three single-particle orbits $0d_{5/2}$, $1s_{1/2}$, and $0d_{3/2}$. The model core is $(0s)^4(0p)^{12}$. The two-body parts of most of the Hamiltonians which we use in this space are derived by reaction-matrix techniques[1] from the Hamada-Johnston nucleon-nucleon scattering potential.[2] Following the current terminology, we shall refer to such Hamiltonians as "realistic."

One purpose of our work was to test how well the experimentally determined properties of $A = 34$–38 nuclei could be reproduced by using currently available realistic interactions. Our present $A = 34$–38 study is the natural extension of a similar study made earlier for $A = 18$–22.[3,4] As tests of a realistic interaction, the $A = 18$–22 and $A = 34$–38 projects differ in that they emphasize different aspects of the interaction. For $A = 18$–22, the model nuclear wave functions tend to be dominated by components in which all active nucleons occupy the $0d_{5/2}$ and $1s_{1/2}$ orbits. Thus for $A = 18$–22, the one- and two-body matrix elements of the effective Hamiltonian which are most important (and most severely tested) are those involving only the $0d_{5/2}$ and $1s_{1/2}$ orbits, while matrix elements involving only the $0d_{3/2}$ orbit are less important. But in the $A = 34$–38 region, where the $0d_{5/2}$ orbit is "effectively" filled for most low-lying states, matrix elements which involve the $0d_{3/2}$ and $1s_{1/2}$ orbits are the most important. Thus, studies of the $A = 18$–22 and $A = 34$–38 regions complement each other as tests of realistic interactions designed for use in $(1s, 0d)^{A-16}$ shell-model calculations.

Techniques for calculating realistic shell-model effective interactions are far from perfect[5,6]; but they have improved since the time we calculated realistic interactions for this $A = 34$–38 study, and presumably they will be improved further in the future. We realized at the start of this project that there would be uncertainties and imperfections in any particular realistic Hamiltonian that we could obtain, and for that reason we decided to examine the shell-model results from several alternative Hamiltonians. We have used four different realistic effective interactions, calculated in four slightly different ways, and with each of these realistic interactions we have tried two alternative sets of single-particle energies. In addition, we have used some two-body interactions of a considerably different character, i.e., interactions derived from considerations other than nucleon-nucleon scattering data. All in all, we have calculated shell-model results from 10 different $(1+2)$-body effective Hamiltonians.

In this paper we shall compare these alternative sets of shell-model results with each other and with experimental data. These comparisons offer some information about the probable characteris-

tics of a "correct" effective Hamiltonian. Furthermore, they enable us to characterize the various observables as to their sensitivity to details of the Hamiltonian. Thus, these comparisons indicate what kinds of observed phenomena can be conveniently organized in terms of an *sd* shell model. For such observables we think it is worthwhile to display our calculated values even in cases where reliable measured values are not yet available. In discussing these displays we shall mention some experiments pertinent to further tests of *sd*-shell-model predictions.

The first major shell-model study of the nuclei $A = 34-38$ was made by Glaudemans, Wiechers, and Brussaard,[7] as part of a comprehensive treatment of the $A = 29-39$ region. Their shell-model basis consisted of the complete set of $(s_{1/2})^n(d_{3/2})^m$ states; the model core was $(0s)^4(0p)^{12}(0d_{5/2})^{12}$. An effective Hamiltonian for this $s_{1/2}$-$d_{3/2}$ vector space can be specified by 15 two-body matrix elements and the two single-particle energies. Glaudemans, Wiechers, and Brussaard determined these 17 parameters by adjusting them so as to obtain a least-square fit to observed energies for nuclei in the range $A = 29-39$. In our work we have expanded the $s_{1/2}$-$d_{3/2}$ vector space to allow for excitations from the $0d_{5/2}$ orbit to $1s_{1/2}$ and $0d_{3/2}$ orbits. The most striking improvement obtained by this expansion is the improved agreement of calculated and observed properties for $J^\pi = \frac{5}{2}^+$ states. More recently, Dieperink and Brussaard[8] have published results from a study for $A = 36-38$, in which they use the same full-*sd*-shell space that we do, but with a Hamiltonian derived from the nonlocal Tabakin two-nucleon scattering potential.[9] We shall compare some of their results with our own.

II. DETAILS OF THE CALCULATIONS

A. Model Space

As already mentioned, the present calculations employ a complete set of basis states, describing active $(1s, 0d)^{A-16}$ structures outside a closed $(0s)^4$-$(0p)^{12}$ core. These shell-model calculations involve the construction and diagonalization of Hamiltonian matrices, each matrix being characterized by A, J, and T. (All such calculations were done with the Oak Ridge-Rochester computer codes.[10]) For $A = 38$ and fixed $\{J, T\}$, the *sd*-shell Hamiltonian matrices have dimensions of about 3×3. These dimensions increase rapidly as A decreases toward the middle of the shell. For $A = 34$, the matrix dimensions range up to 537×537.

Of the various limitations on our shell-model basis, probably the most damaging is the exclusion of configurations involving the negative-parity orbits $0f_{7/2}$ and $1p_{3/2}$. Analyses of single-nucleon-stripping experiments[11-13] on $A = 34$ and $A = 36$ targets indicate that, for $A = 35$ and 37, states of $\approx$2- or 3-MeV excitation account for large fragments of the single-particle width for adding one $0f_{7/2}$ nucleon to the target state. The same statement holds for adding one $1p_{3/2}$ nucleon. Now, since negative-parity configurations do not mix with positive-parity configurations, the exclusion of negative-parity $(A - 16)$-particle basis states does not affect our shell-model results for positive-parity nuclear states. But these results *are* affected by the exclusion of positive-parity $(A - 16)$-particle basis states; in particular, those formed by excitations of 2 (or 4, 6, ...) particles from the *sd* to the *fp* shell. Using the fact that in $A = 35$ and 37, states involving at least one *fp*-shell particle occur at excitations as low as $\approx$2 MeV, and invoking a simple independent-particle approximation, we see that states involving two *fp*-shell particles can be expected to occur at excitations of $\approx$4 MeV. Thus, at excitations near and above 4 MeV, we expect the experimentally observed level spectra to be denser than that calculated from our pure-*sd*-shell models. Of course, depending on the characteristics of the "true" Hamiltonian, the true eigenfunctions will contain various mixtures of "pure-*sd*-shell states" with states involving excitations of even numbers of *fp*-shell particles; and such mixing may cause other experimental-theoretical differences besides the appearance of extra states in the observed spectra.

In later sections, we shall discuss some particular ways in which our vector-space limitations may affect the correspondence between experimental and calculated spectra. Now, in the present section, we confine ourselves to a few general remarks about "intruder states" and effective operators.

Very probably, all of the true nuclear wave functions for $A = 34-38$ include significantly large components involving *fp*-shell excitations (i.e., significantly large compared to the pure-*sd*-shell components). Many effects of these *fp*-shell excitations have presumably been built into our effective Hamiltonian operators. Similarly, for some other observables, besides energy, we need to use effective operators. For example, in calculations of quadrupole moments and $B(E2)$'s, we use effective charges different from the free-neutron and free-proton charges. Thus usage implies recognition that, when the model basis is restricted to $(0s)^4(0p)^{12}(1s, 0d)^{A-16}$ configurations, the optimized effective $E2$ operator differs from the "unrenormalized" $E2$ operator that would be appropriate for calculating matrix elements between exact wave functions. But, of course, the technique of using effective operators has its limitations: It does not

equip us to describe states whose very existence depends upon the presence of extra-model configurations. Consider, for example, the lowest $J^\pi = 0^+$, 2^+, and 1^+ states of ^{38}Ar. In their true wave functions, it may well be that components involving two fp-shell nucleons occur with intensity $\approx 50\%$ that of the "pure-sd-shell" configurations. Our shell-model calculations, though they allow no explicit occupation of fp-shell orbits, nevertheless account for many observed properties of these three levels. However, our pure-sd-shell model would not be capable of accounting for the existence of an excited 0^+ state in which the intensity of fp-excited components exceeds the pure-sd-shell intensity by a factor of ≈ 10. Nucleon-transfer experiments[13] indicate that this kind of 0^+ state lies at 3.38-MeV excitation in the real ^{38}Ar spectrum. We use the name "intruder states" for such observed levels (i.e., observed levels which defy description within our model space). The frequency of occurrence of low-lying intruder states gives some indication of the appropriateness of the shell model under consideration for use in a given nuclear-mass region.

B. Realistic Two-Body Interactions

In the full $(0s, 1d)^{A-16}$ vector space described above, we have used 10 alternative model Hamiltonians. Each is a $(1+2)$-body operator. In each case, the two-body interaction part, V, is specified by a set of 63 two-body matrix elements between normalized antisymmetrized states,

$$\langle j_a j_b JT | V | j_c j_d JT \rangle ,$$

where each j_i can be $d_{5/2}$, $s_{1/2}$, or $d_{3/2}$.

Earlier work[3,4] has shown that for $A = 18-22$, many experimentally observed features can be reproduced by shell-model calculations in a full $(1s, 0d)^{A-16}$ vector space, using a realistic effective interaction that was derived[1] for $A = 18$ from the Hamada-Johnston potential. In the present $A = 34-38$ study, several of our alternative Hamiltonians incorporate realistic interactions obtained by procedures very similar to that used in generating the aforementioned $A = 18-22$ interaction. This generation procedure is designed to convert a hard-core scattering potential into a two-body interaction that is suitable for use in shell-model calculations. The "conversion" is needed to make up for omissions in the shell-model basis. The generated realistic effective interaction has two parts:

(1) a "bare-G matrix," designed to incorporate the influence of very-high-energy independent-particle states omitted from the explicit shell-model basis; *plus*

(2) some perturbative "renormalization" corrections, designed to incorporate the influence of rather low-lying independent-particle states omitted from the shell-model basis.

First we discuss some general features of the bare-G contributions to our realistic Hamiltonians. In the generation procedure[1] which we have used, the bare-G part is calculated by a combination of reference-spectrum[14] and Moszkowski-Scott separation[15] methods. In the separation method, we have used closure approximations with effective-energy denominators, and we have made further approximations in treating the Pauli and dispersion terms. When the $A = 18$ prototype of these bare-G calculations was first performed,[1] all these approximations taken together seemed to constitute a satisfactory and economical way to evaluate bare-G matrix elements. Indeed, the calculated numerical results were very similar to results calculated by more accurate and arduous methods[16] (in the case of those matrix elements for which the more accurate answers were available). However, some time after the generation and use of our $A = 18-22$ and $A = 34-38$ realistic effective interactions, it was discovered that an error had been made in generating the bare-G contributions. In the treatment of $^3S_1$-$^3S_1$ second-order contributions from the long-range tensor force, the separation method should lead to values near 400 MeV for E_{eff}, the effective-energy denominator. But values of E_{eff} near 200 MeV were used in the $A = 18-22$ calculation, and in the present calculation. Happily, recent calculations[17] indicate that a more accurate *over-all* treatment of the tensor force (including better approximations for the Pauli operator and the $^3S_1$-$^3D_1$ cross terms) yields total matrix elements which lie within 10% of the ones used here.

Thus, it seems that fortuitous cancellations account for the agreement between the bare-G part of the $A = 18-22$ interaction and a "more properly calculated" bare-G part. But since very similar procedures were used in generating both the $A = 18-22$ and $A = 34-38$ bare-G matrix elements, we feel justified in hoping that in our $A = 34-38$ interaction too, the bare G is close to a "more properly calculated" bare-G part.

Next we discuss possible faults in the renormalization methods we have used. In the realistic $A = 18-22$ interaction[1,3,4] and in our realistic $A = 34-38$ interactions, the renormalization terms are limited to selected second-order corrections. For many years there have been uncertainties and controversy about *which parts* of a complete second-order shell-model correction should be included. (Compare for example Ref. 1 and the work of Kuo and Brown.[18]) Also, there have been doubts about whether the restriction to second-order cor-

rections is justified. Indeed, recent quantitative work[5,6] demonstrates that there is no clear justification for omitting higher-order corrections.

But again we fall back on very pragmatic considerations. We know that for $A = 18-22$, the combination of G-matrix and renormalization techniques used in Ref. 1 produced an interaction which, when used in sd-shell-model calculations, allowed good reproduction of $A = 18-22$ experimental data. Since we have used a similar combination of procedures to produce "realistic" interactions for $A = 34-38$, it seems reasonable to suppose that these new interactions could be successful when used in sd-shell models for $A = 34-38$.

In summation, we acknowledge several nontrivial faults and uncertainties in our "realistic" interactions, but we hope that these interactions have the major features of a "properly calculated" G matrix. Furthermore, since these interactions do represent an attempt to relate nucleon-nucleon scattering data with nuclear-structure data, and since we know of no other sd-shell interactions for which this attempt can be confidently declared "properly fulfilled," we shall continue to call these interactions *realistic*.

In the paragraphs below, we describe the major ways in which we changed the procedure of Ref. 1 before generating realistic interactions for $A = 34-38$. Then, at the end of this section, we tabulate the two-body matrix elements of the resulting $A = 34-38$ interactions.

In generating some of our $A = 34-38$ realistic interactions, we used a harmonic-oscillator parameter of $\hbar\omega = 12.5$ MeV. For others we used $\hbar\omega = 11.0$ MeV. These values 12.5 and 11.0 replaced the larger value $\hbar\omega = 14.0$ MeV that had been used in Ref. 1 to generate the $A = 18$ interaction. The change from $\hbar\omega = 14$ MeV was made so as to take into account an increase in nuclear size from $A \approx 18$ to $A \approx 36$. (One commonly used rule is $\hbar\omega \approx 41A^{-1/3}$ MeV.[19])

In generating some of our $A = 34-38$ realistic interactions, we used exactly the same renormalization procedure as was used in Ref. 1 for the $A = 18$ interaction. This renormalization procedure incorporates selected second-order $2\hbar\omega$ corrections, all calculated in the *particle* formalism. Figures 1(a)–1(c) show the particular corrections which were included. (These are added to the bare-G part of the realistic interaction.) We shall use the abbreviation 12.5p to denote the complete two-body realistic interaction calculated with $\hbar\omega = 12.5$ MeV and *particle*-formalism renormalizations. Similarly, we use 11.0p to denote the realistic interaction calculated with $\hbar\omega = 11.0$ MeV and *particle*-formalism renormalizations.

In generating some other $A = 34-38$ realistic interactions, we renormalized by using *hole* formalism instead of particle formalism. Figures 2(a)–2(c) show these hole-formalism corrections. Strictly speaking, the diagrams of Fig. 2 show contributions to a hole-hole interaction, rather than a particle-particle interaction. But a hole-hole interaction operator, when converted to a particle-formalism representation, generally has zero-body, one-body, and two-body parts. Hence in our renormalization calculations, we take the *two-body part* of the hole-hole interaction that is obtained by summing the operators symbolized by Figs. 2(a)–2(c). (This operation, of "taking the two-body part," is trivial to perform because the desired particle-particle matrix elements are just equal in sign and magnitude to the hole-hole matrix elements from which they are determined.) We use the abbreviation 12.5h to denote the two-body interaction calculated with $\hbar\omega = 12.5$ MeV and

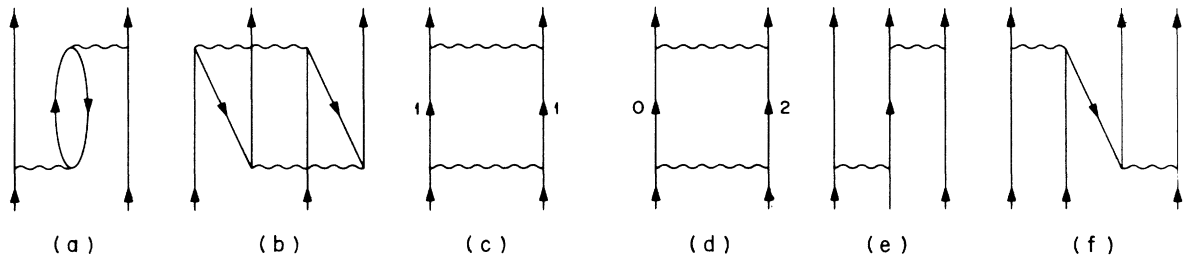

FIG. 1. Diagrams symbolizing some of the second-order $2\hbar\omega$-renormalization contributions to a realistic effective interaction appropriate for use in particle-formalism shell-model calculations. For our full-sd-shell model, all lines with upgoing arrows symbolize particles in active orbits ($0d, 1s$) or higher orbits ($0f, 1p, 1d, 2s$), while all lines with downgoing arrows symbolize holes in lower-than-active orbits ($0s, 1p$). In diagrams (c) and (d), the intermediate-state lines are labeled so as to distinguish between two related cases. In case (c), both intermediate-state particles occupy orbits $1\hbar\omega$ above the active orbits. In case (d), one intermediate-state particle occupies an active orbit while the other occupies an orbit $2\hbar\omega$ above the active orbits. Diagram (a) represents both of two related cases: the case in which the bubble symbolizes a particle $1\hbar\omega$ above the active orbits plus a hole $1\hbar\omega$ below the active orbits, and the case in which the bubble symbolizes an active particle plus a hole $2\hbar\omega$ below the active orbits.

hole-formalism renormalizations. Similarly, we use 11.0h to denote the two-body interaction calculated with $\hbar\omega = 11.0$ MeV and *hole*-formalism renormalization.

As we shall next explain, our p and h interactions are nonidentical because they exclude nonidentical subsets of all the two- and three-body terms in the complete set of second-order $2\hbar\omega$ shell-model corrections.

Figures 1(d) through 1(f) show some of the second-order $2\hbar\omega$ renormalizations which we excluded in constructing our $A = 34$–38 p interactions 12.5p and 11.0p. Figure 1(d) shows that we have omitted some two-body terms associated with the excitation of one sd-shell nucleon to the sdg shell. Figures 1(e) and 1(f) show that we have omitted all of the three-body terms. Now, three-body terms do not enter into the sd-shell calculations of energies or wave functions for $A = 18$ (two active nucleons). However, the omission of three-body terms does affect the sd-shell-model results for $A > 18$, and this omission may become more important as A (and hence the number of interacting nucleon triplets) increases. In our p interactions, the only other omitted $2\hbar\omega$ second-order terms are those which would exactly cancel each other *if* the harmonic-oscillator orbits accurately satisfied certain Hartree-Fock conditions. In practice such terms cancel each other approximately.

Our h interactions, 12.5h and 11.0h, formally exclude a different subset of $2\hbar\omega$ second-order terms. Figures 2(d) through 2(f) show some of the omitted terms. Note, for example, that our p interactions formally exclude *all* contributions from excitation of a $0d$ nucleon to the $2s$-$1d$-$0g$ shell, whereas our h interactions include *some* of the second-order contributions from this kind of excitation. Similarly, our h interactions formally exclude all contributions from excitation of a $0s$ nucleon to the $1s$-$0d$ shell, whereas our p interactions include *some* of the second-order contributions from this kind of excitation.

It could be argued that our h interactions are somewhat preferable to our p interactions when it comes to using them in $A = 34$–38 sd-shell calculations. First, in the $A = 34$–38 model nuclei the number of active "hole triplets" is much smaller than the number of active "particle triplets"; hence the neglect of three-hole terms seems preferable to the neglect of three-particle terms. Second, for $A = 34$–38 the Hartree-Fock cancellations assumed in generating the h interactions are more appropriate than those assumed in generating the p interactions. However, because of all the previously mentioned faults and uncertainties in the generation of our realistic interactions, these advantages of our h interactions over p interactions cannot be taken seriously.

Therefore we shall consider all four interactions 11.0p, 11.0h, 12.5p, and 12.5h as *a priori* equal in merit. We presume that each of them has the *flavor* of a "properly calculated" realistic interaction, and our preferences among them will be based solely on the nuclear-structure results to which they lead.

Table I lists the two-body matrix elements of the four interactions 11.0p, 11.0h, 12.5p, and 12.5h. When we use all four interactions with the same set of single-particle energies, we find noticeable differences among the resulting energy-level spectra. However, we can make these spectral differences rather small by using an appropriately different set of single-particle energies with each of these four different realistic interactions.

C. Single-Particle Energies in the Realistic Hamiltonians

To specify the one-body part of our effective Hamiltonians, we shall use these three independent

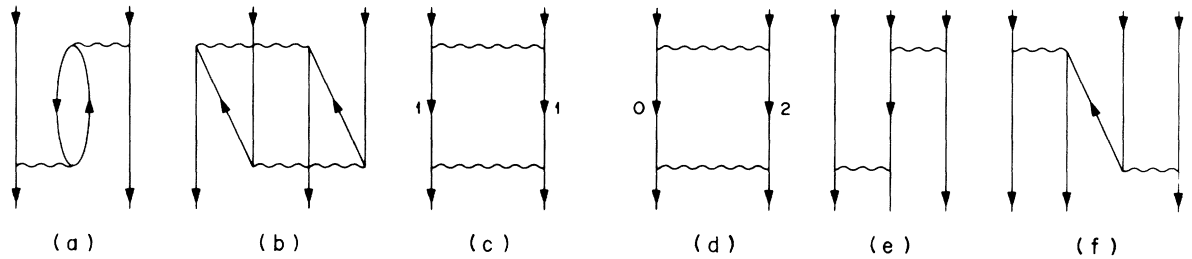

FIG. 2. Diagrams symbolizing some of the second-order $2\hbar\omega$-renormalization contributions to a realistic effective interaction appropriate for use in hole-formalism shell-model calculations. For our full-sd-shell model, all lines with downgoing arrows symbolize holes in active orbits ($0d, 1s$) or holes in lower orbits ($0s, 0p$), while all lines with upgoing arrows symbolize particles in higher-than-active orbits ($0f, 1p, 1d, 2s$). In diagrams (c) and (d) the intermediate-state lines are labeled so as to distinguish between two related cases. In case (c), both intermediate-state holes are in orbits $1\hbar\omega$ below the active orbits. In case (d), one intermediate-state hole is in an active orbit while the other hole is in an orbit $2\hbar\omega$ below the active orbits. Diagram (a) represents both of two related cases: the case in which the bubble symbolizes a hole $1\hbar\omega$ below the active orbits plus a particle $1\hbar\omega$ above the active orbits, and the case in which the bubble symbolizes a hole in an active orbit plus a particle $2\hbar\omega$ above the active orbits.

TABLE I. Values of the 63 two-body matrix elements $\langle j_1 j_2 | V | j_3 j_4 \rangle_{J,T}$ of the interactions used in the present investigation. The units are MeV. The phase conventions are explained in Ref. 4. The six numbers marked Identification show the values of $2j_1$, $2j_2$, $2j_3$, $2j_4$, $2J$, and $2T$.

	Identification			11.0h	12.5h	11.0p	12.5p	MSDI	12.5pA
1	55	55	0 2	−2.6534	−2.4698	−2.4171	−2.2766	−2.4180	−2.3408
2	55	55	2 0	−1.2465	−1.0650	−1.1729	−0.9790	−2.4351	−1.1443
3	55	55	4 2	−0.8619	−0.9611	−0.7831	−0.8799	−0.1972	−0.7016
4	55	55	6 0	−0.8230	−0.8393	−0.7327	−0.7269	−2.1643	−0.9904
5	55	55	8 2	−0.0001	−0.0471	0.0113	−0.0323	0.1866	0.2931
6	55	55	10 0	−2.8901	−3.2282	−2.7316	−3.0479	−2.3593	−2.4069
7	55	51	4 2	−0.7665	−0.8085	−0.6914	−0.7416	−0.8705	−0.8703
8	55	51	6 0	−1.2480	−1.3442	−1.2373	−1.3368	−0.5034	−0.8158
9	55	53	2 0	2.7201	2.7282	2.8367	2.8734	0.6878	1.7536
10	55	53	4 2	−0.4371	−0.4491	−0.3721	−0.3841	−0.4653	−0.4508
11	55	53	6 0	1.4337	1.5833	1.4474	1.6060	0.2251	0.9801
12	55	53	8 2	−1.0782	−1.1758	−1.0620	−1.1738	−0.5483	−1.3776
13	55	11	0 2	−1.1136	−1.0875	−0.9280	−0.8938	−1.6621	−1.0490
14	55	11	2 0	−0.7377	−0.6855	−0.6588	−0.5859	−0.4486	−0.3576
15	55	13	2 0	−0.2256	−0.2266	−0.2088	−0.2170	−0.2563	−0.1324
16	55	13	4 2	−0.6828	−0.7356	−0.6486	−0.7169	−0.7108	−0.8414
17	55	33	0 2	−3.3237	−3.4629	−3.1717	−3.3550	−2.3505	−3.9374
18	55	33	2 0	1.2420	1.2593	1.3943	1.4574	0.4458	0.8895
19	55	33	4 2	−0.7762	−0.8220	−0.7447	−0.8010	−0.5025	−0.9401
20	55	33	6 0	0.4374	0.4519	0.4127	0.4262	0.1300	0.2601
21	51	51	4 0	−0.5670	−0.5799	−0.5075	−0.5203	−2.1210	−0.8643
22	51	51	4 2	−1.0016	−1.0927	−0.9842	−1.1110	−0.6907	−0.9729
23	51	51	6 0	−2.7087	−3.0604	−2.7135	−3.0699	−2.5759	−2.4204
24	51	51	6 2	0.1788	0.1837	0.1555	0.1493	0.4608	0.5062
25	51	53	4 0	−1.0336	−1.1513	−1.1022	−1.2315	−0.4053	−0.7516
26	51	53	4 2	−0.2737	−0.2359	−0.2450	−0.2158	−0.6155	−0.2533
27	51	53	6 0	1.0170	1.0852	0.9329	0.9998	0.3875	0.6102
28	51	53	6 2	−0.0782	−0.1083	−0.0274	−0.0488	0.0	−0.0573
29	51	13	4 0	−1.8110	−2.0890	−1.8696	−2.1718	−0.3714	−1.3254
30	51	13	4 2	−1.2169	−1.3649	−1.1733	−1.3349	−0.9402	−1.5666
31	51	33	4 2	−0.6031	−0.6535	−0.5818	−0.6419	−0.6648	−0.7533
32	51	33	6 0	−0.0475	−0.0869	0.0498	0.0295	0.0839	0.0180
33	53	53	2 0	−5.4251	−5.3891	−5.3785	−5.3266	−3.1825	−3.7976
34	53	53	2 2	0.0694	0.0861	−0.1331	−0.1367	0.4608	0.1706
35	53	53	4 0	−3.4205	−3.8224	−3.4995	−3.8860	−2.3593	−2.9184
36	53	53	4 2	−0.0480	−0.0432	−0.1510	−0.1664	0.1318	0.1357
37	53	53	6 0	−0.9233	−0.9752	−0.8975	−0.9606	−2.0993	−1.1331
38	53	53	6 2	0.2600	0.1966	0.1825	0.1122	0.4608	0.4627
39	53	53	8 0	−2.8942	−3.2877	−3.1524	−3.5935	−2.3593	−2.7399
40	53	53	8 2	−1.2742	−1.3783	−1.3147	−1.4490	−0.6359	−1.3695
41	53	11	2 0	1.6025	1.5515	1.6435	1.6018	0.6782	0.9776
42	53	13	2 0	−1.6691	−1.8027	−1.5368	−1.6509	−0.3391	−1.0075
43	53	13	2 2	−0.0658	−0.1087	−0.0330	−0.0654	0.0	−0.0768
44	53	13	4 0	−1.1415	−1.2170	−1.2354	−1.3372	−0.4964	−0.8161
45	53	13	4 2	−0.5452	−0.5902	0.5912	−0.6623	−0.5025	−0.7773
46	53	33	2 0	−0.3122	−0.1808	−0.2263	−0.0712	−0.2145	−0.0435
47	53	33	4 2	−0.7898	−0.8667	−0.7775	−0.8646	−0.3553	−1.0147
48	53	33	6 0	1.5990	1.8379	1.5658	1.8108	0.1501	1.1051
49	11	11	0 2	−1.7365	−1.7098	−1.8139	−1.8186	−0.4988	−1.8033
50	11	11	2 0	−2.7802	−2.8457	−2.8372	−2.9245	−2.1968	−2.3316
51	11	13	2 0	0.5786	0.5792	0.3386	0.2866	0.0	0.1749
52	11	33	0 2	−0.7759	−0.6933	−0.7302	−0.6906	−1.3571	−0.8105
53	11	33	2 0	−0.0100	−0.1243	−0.0344	−0.1306	0.2398	−0.0797
54	13	13	2 0	−2.5384	−2.8257	−2.5181	−2.7934	−2.5759	−2.2516
55	13	13	2 2	0.2515	0.2853	0.1669	0.1668	0.4608	0.5268
56	13	13	4 0	−1.2843	−1.4193	−1.2224	−1.3606	−2.2726	−1.3772
57	13	13	4 2	−0.3724	−0.3747	−0.2827	−0.2924	−0.3069	−0.0122
58	13	33	2 0	0.9123	0.9463	0.7370	0.7384	0.4795	0.4506

TABLE I *(Continued)*

	Identification			11.0h	12.5h	11.0p	12.5p	MSDI	12.5p*A*
59	13	33	4 2	−0.3023	−0.2676	−0.2223	−0.1952	−0.5428	−0.2291
60	33	33	0 2	−1.2258	−0.9288	−1.0602	−0.8197	−1.4584	−0.6310
61	33	33	2 0	−0.5352	−0.4141	−0.5902	−0.4922	−2.2726	−0.8472
62	33	33	4 2	0.1681	0.2099	0.0556	0.0571	0.0770	0.3980
63	33	33	6 0	−2.0968	−2.3239	−1.9693	−2.1795	−2.2726	−1.8769

parameters:

$$\epsilon_{5/2}, \quad \epsilon_{1/2}-\epsilon_{5/2}, \quad \epsilon_{3/2}-\epsilon_{1/2}.$$

Here $\epsilon_{5/2}$ is a single-particle energy, while $\epsilon_{1/2}-\epsilon_{5/2}$ and $\epsilon_{3/2}-\epsilon_{1/2}$ are single-particle-energy *splittings*. This choice of parameters leads to the following convenient separation of roles. The model nuclear wave functions, and also the calculated excitation energies for fixed A, depend only on the two splittings $\epsilon_{1/2}-\epsilon_{5/2}$ and $\epsilon_{3/2}-\epsilon_{1/2}$. It is true that all three parameters affect the calculated binding energies with respect to ^{16}O. However, suppose that $\epsilon_{5/2}$ is changed by $\Delta\epsilon_{5/2}$, while $\epsilon_{1/2}-\epsilon_{5/2}$ and $\epsilon_{3/2}-\epsilon_{1/2}$ are held fixed; then every calculated binding energy is changed by $\Delta\epsilon_{5/2}\times(A-16)$, while the model nuclear wave functions and excitation energies remain unchanged.

TABLE II. Experimental energies of states used in determining the parameter values of the least-squares Hamiltonians. Energies marked b are nuclear binding energies with respect to ^{16}O. Energies marked e are excitation energies with respect to the lowest state of A, T.

A, T	J	$E_{\text{Expt.}}$ (MeV)	A, T	J	$E_{\text{Expt.}}$ (MeV)
35, $\frac{1}{2}$	$\frac{3}{2}$	216.32 b	37, $\frac{1}{2}$	$\frac{3}{2}$	240.34 b
	$\frac{1}{2}$	1.21 e		$\frac{1}{2}$	1.40 e
	$\frac{5}{2}$	1.75 e		$\frac{5}{2}$	2.78 e
	$\frac{3}{2}$	2.65 e			
	$\frac{7}{2}$	2.65 e	37, $\frac{3}{2}$	$\frac{3}{2}$	235.22 b
	$\frac{5}{2}$	3.00 e		$\frac{1}{2}$	1.73 e
				$\frac{5}{2}$	3.09 e
36, 0	0	231.57 b			
	2	1.98 e	38, 0	3	252.38 b
	4	4.43 e		1	0.45 e
	2	4.45 e		1	1.70 e
36, 1	2	224.96 b	38, 1	0	252.21 b
	3	0.79 e		2	2.17 e
	1	1.16 e		2	"4.40"e
				1	5.55 e
36, 2	0	220.67 b			
	2	3.25 e	39, $\frac{1}{2}$	$\frac{3}{2}$	265.47 b
	1	4.58 e		$\frac{1}{2}$	2.50 e
				$\frac{5}{2}$	7.50 e
			40, 0	0	281.09 b

In working with Hamiltonians having "nonadjusted" realistic two-body interactions, we deemphasize ground-state binding energies and emphasize wave functions and excitation spectra. We do this because we realize that our realistic two-body interactions are quite imperfect, and because we know that small changes in the two-body matrix elements tend to produce binding-energy changes which are larger (in MeV) than the excitation-energy changes.[4] In keeping with our emphases on wave functions and excitation spectra, we pay little attention to $\epsilon_{5/2}$ but instead concentrate on the splittings $\epsilon_{1/2}-\epsilon_{5/2}$ and $\epsilon_{3/2}-\epsilon_{1/2}$.

For $A=34$–38, the "appropriate" single-particle-energy splittings are not nearly so well defined as they were for $A=18$–22. At the lower end of the *sd* shell, there seems little reason not to use the spacings of the first $\frac{5}{2}^+$, $\frac{1}{2}^+$, and $\frac{3}{2}^+$ levels of ^{17}O as single-particle-energy splittings in *sd*-shell calculations for the next few heavier nuclei. Indeed, earlier shell-model studies have shown that, when used with realistic interactions, these ^{17}O spacings are nearly optimum for reproducing observed nuclear energy-level spectra for $A=18$–22.[4] But it is not obvious that these ^{17}O splittings remain appropriate after 20 or so particles have been added to ^{16}O. Roughly speaking: 20 added nucleons could significantly change the state of the 16-particle core, and thereby change the effective interaction between the extracore nucleons and the 16-particle core. Furthermore, because the $d_{5/2}$ shell is almost fully occupied in low-lying *sd*-model states of $A=34$–38, small errors in our realistic two-body $d_{3/2}-d_{5/2}$ and $s_{1/2}-d_{5/2}$ matrix elements might cause effects which could be roughly canceled by shifts in the single-particle energies.

We also considered the possibility of determining single-particle splittings from observed $A=39$ data rather than $A=17$ data. For a given two-body effective interaction, the observed excitation of the lowest $J=\frac{1}{2}$ state of ^{39}K-^{39}Ca allows a straight-

forward "empirical" determination of the single-particle splitting $\epsilon_{3/2} - \epsilon_{1/2}$. However, the $A = 39$ data are inadequate to allow similar determinations of $\epsilon_{1/2} - \epsilon_{5/2}$ and $\epsilon_{5/2}$. Pickup experiments[20,21] indicate that in $A = 39$ the "$d_{5/2}$ hole state" is severely fragmented and its centroid is not well determined. Thus, this simple empirical approach to fixing the one-body part of the effective Hamiltonian is not really satisfactory.

Because of such ambiguities in choosing the "correct" one-body operator, the energy-level calculations with each of our four realistic interactions were carried through with two alternative sets of single-particle splittings. First, we used splittings taken from the observed ^{17}O spectrum: $\epsilon_{1/2} - \epsilon_{5/2} = 0.87$ MeV and $\epsilon_{3/2} - \epsilon_{1/2} = 4.21$ MeV.[22] Second, we used splittings which were least-squares-adjusted so as to give a best fit, not just to the observed single-hole spectrum in $A = 39$, but rather to 23 data describing observed excitation energies in $A = 35$ to 39. These 23 excitation energies are shown in Table II; they are marked with an e. Note that each of these 23 data is an excitation energy referred to the ground state of same A, T. [All least-squares fits were done with a computer program[23] written by Glaudemans and one of us (B.H.W.).]

In labeling Hamiltonians, we use the tag ASPE to denote adjusted single-particle-energy splittings. Each complete realistic Hamiltonian operator is denoted by the combination of a two-body label (e.g., 12.5p) and a one-body label (either ^{17}O or ASPE). For example, 12.5p + ASPE denotes the Hamiltonian whose two-body part is 12.5p, and whose one-body part is the result of least-squares-adjusting the two single-particle-energy splittings.

Table III lists the optimized single-particle-energy splittings for each of our four realistic ASPE Hamiltonians. We see that for the purpose of fitting $A = 35$–39 spectra, the two 11.0 interactions "prefer" to be associated with splittings $\epsilon_{1/2} - \epsilon_{5/2} \approx 3$ MeV, while the two 12.5-MeV interactions prefer $\epsilon_{1/2} - \epsilon_{5/2} \approx 2$ MeV. However, with respect to the splitting $\epsilon_{3/2} - \epsilon_{1/2}$, the h interactions group themselves together by preferring $\epsilon_{3/2} - \epsilon_{1/2} \approx 2.4$ MeV, while the p interactions prefer $\epsilon_{3/2} - \epsilon_{1/2} \approx 3.5$ MeV. In all of these four ASPE cases, the optimized splitting $\epsilon_{1/2} - \epsilon_{5/2}$ is at least an MeV larger than the ^{17}O value 0.87 MeV, while the optimized splitting $\epsilon_{3/2} - \epsilon_{1/2}$ is 0.6 to 2.0 MeV smaller than the ^{17}O value 4.21 MeV.

Remember that these ASPE splittings have been optimized to fit 23 excitations in $A = 35$–39. It turns out that the optimized values for $\epsilon_{3/2} - \epsilon_{1/2}$ are rather different from those that would have been derived by requiring an exact fit to the observed excitation of the lowest $J = \frac{1}{2}$ state in ^{39}K-^{39}Ca, viz. 2.5 MeV. All four realistic interactions, each with its own set of ASPE splittings, yield values near 3.4 MeV. The same four interactions, when used with ^{17}O single-particle-energy splittings, yield values ranging from 4.0 to 5.2 MeV. The excitation of the "$d_{5/2}$ single-hole centroid" in ^{39}Ca is not well established experimentally. It is probably $\approx$7.50 MeV.[21] All four realistic interactions, when used either with ^{17}O or with optimized single-particle-energy splittings, yield $A = 39$ splittings which are consistent with this known experimental information about the $d_{5/2}$ centroid. (For details about the $A = 39$ shell-model results, see Table III.)

D. Hamiltonians with "Least-Squares" Interactions

Several studies[4,24–28] have indicated that shell models using the surface δ interaction (SDI) are often rather successful in reproducing observed nuclear-structure features. We have used a modified surface δ interaction[4,26–28] (MSDI) in some of our calculations for $A = 35$–39. These MSDI calculations were made partly because of our interest in this particular kind of interaction, and partly because we wanted to generate an alternative set of shell-model results, based on a Hamiltonian of completely dissimilar origin, with which to compare the results from our realistic Hamiltonians. We shall use the label MSDI to signify not just the two-body interaction, but rather the complete (1 + 2)-body Hamiltonian incorporating an MSDI two-body operator.

Both the one-body and two-body parts of the MSDI were adjusted (via the Glaudemans-Wildenthal search code[23]) so as to fit experimentally determined level energies. The complete MSDI Hamiltonian has seven adjusted parameters: the three single-particle-energy parameters, the strengths of the $T = 0$ and $T = 1$ surface δ interactions, and the $T = 0$ and $T = 1$ "monopole constants" which are added to the respective diagonal two-body matrix elements. (These two monopole constants *modify* the SDI, to yield MSDI.) The four two-body parameters are called A_0, A_1, B_0, and B_1. Their definitions are given in previous publications[4,27] as part of a precise description of the MSDI form.

During the construction of the MSDI, the two SDI strengths A_0 and A_1 and the two splittings $\epsilon_{1/2} - \epsilon_{5/2}$ and $\epsilon_{3/2} - \epsilon_{1/2}$ were all simultaneously adjusted to produce a least-squares fit to the 23 excitation energies shown in Table II. The three remaining parameters, B_0, B_1, and $\epsilon_{5/2}$, do not affect the calculated values of these 23 excitation energies. Therefore these three remaining MSDI parameters

were simultaneously adjusted to fit 11 empirically determined values for ground-state nuclear binding energies. These 11 values are listed in Table II, each marked with a b. They are all binding energies with respect to ^{16}O, and in all cases the measured total values[29] were corrected for Coulomb contributions according to a method described elsewhere.[7,4]

Finally, we constructed and used one other Hamiltonian having "least-squares" two-body matrix elements. This final Hamiltonian, called 12.5pA, incorporates an adjusted version of our realistic interaction 12.5p. The entire (1+2)-body operator 12.5pA has seven adjusted parameters. We constructed 12.5pA by exactly the same procedure that we constructed our Hamiltonian MSDI, with the following important exception. In constructing the MSDI we adjusted the strengths of the SDI $T=0$ interaction and the SDI $T=1$ interaction, but in constructing 12.5pA we adjusted the strengths of the 12.5p $T=0$ interaction and the 12.5p $T=1$ interaction.

For the MSDI, the optimized two-body parameters turned out to be $A_0=0.38$ MeV, $A_1=0.96$ MeV, $B_0=-1.82$ MeV, and $B_1=0.46$ MeV. The analogous results for 12.5pA were $A_0=0.61$ MeV, $A_1=1.17$ MeV, $B_0=-0.55$ MeV, and $B_1=0.33$ MeV. Table I shows the associated two-body matrix elements, and Table III lists the optimized single-particle-energy parameters. Note that for our Hamiltonian 12.5pA, the optimized single-particle-energy splittings $\epsilon_{3/2}-\epsilon_{5/2}$ and $\epsilon_{3/2}-\epsilon_{1/2}$ fall within the same range of values as was obtained for the realistic Hamiltonians 11.0h+ASPE, 11.0p+ASPE, 12.5h+ASPE, and 12.5p+ASPE. For our Hamiltonian MSDI, the optimized splitting $\epsilon_{3/2}-\epsilon_{1/2}$ falls within the range optained for these ASPE realistic Hamiltonians, but the optimized splitting $\epsilon_{1/2}-\epsilon_{5/2}$ is a few MeV larger. All these least-squares optimized splittings differ from the ^{17}O splittings (see Table III for details). The Hamiltonians 12.5pA and MSDI are more successful than our other Hamiltonians in fitting the observed $A=39$ excitation $E(\frac{1}{2}^+)-E(\frac{3}{2}^+)=2.50$ MeV. For both 12.5pA and the MSDI, the optimized single-particle energy $\epsilon_{5/2}$ is a few MeV more negative than the ^{17}O value.

III. RESULTS

In Sec. A we discuss only the simplest features of the energy-level spectra. In Sec. B we discuss detailed results for individual nuclei and levels.

A. Overview of Theoretical-Experimental Agreement for Level Energies

We start this section with a general comparison between the observed energy-level spectra and the spectra calculated from our eight realistic Hamiltonians. Subsequently we shall add some general remarks about the results obtained from our two more extensively adjusted Hamiltonians, 12.5pA and MSDI.

Figure 3 shows the lowest few $T=\frac{1}{2}$ energy levels for $A=35$, 37, and 39 as calculated from the eight Hamiltonians involving realistic interactions. The corresponding results for $A=36$ and 38 are shown in Fig. 4 (with $T=0$ levels shown as solid lines, and $T=1$ levels as dashed lines). In each of Figs. 3 and 4, the four columns on the left result from using single-particle-energy splittings taken from the observed ^{17}O spectrum, the four columns on the right result from using the least-squares-adjusted single-particle-energy splittings, and the central column is taken from experimental data. These figures show only the lowest few calculated and experimentally observed levels. (For $A=38$ we have drawn a *modified* version of the experimentally observed $T=1$ spectrum, as we shall discuss later.)

First, we stress the qualitative successes of the theoretical results. For all the calculated spectra in Figs. 3 and 4, there is fair-to-good agreement with the available experimental data. Thus in the experimentally observed spectrum for $A=35$ $T=\frac{1}{2}$, the lowest three levels have the sequence $\frac{3}{2}^+-\frac{1}{2}^+-\frac{5}{2}^+$, and all eight models give this sequence. For the $A=37$ $T=\frac{1}{2}$ system the experimental sequence is $\frac{3}{2}^+-\frac{1}{2}^+$-unknown-$\frac{5}{2}^+$. Five of our realistic Hamiltonians give a sequence $\frac{3}{2}^+-\frac{1}{2}^+-\frac{7}{2}^+-\frac{5}{2}^+$, consistent with experimental data. The other three realistic Hamiltonians invert two members of this sequence (either the second and third members, or the third and fourth members). In the $A=36$ $T=0$ spectrum, the calculated excitation energies of the first 0^+, 2^+, and 4^+ states are in good agreement with experimental data. The experimentally observed splitting between the $T=0$ and $T=1$ ground states of $A=36$ is reproduced within 1 MeV. For the lowest four levels of the $A=36$, $T=1$ system, seven of our eight realistic calculations give a sequence $2^+-3^+-1^+-2^+$, consistent with the available experimental data. The other calculation inverts the two upper members. For $A=38$, the $J^\pi T$ sequence of the first seven Expt. levels in Fig. 4 is reproduced by six of the eight realistic calculations. In the other two realistic calculations only one inversion mars the agreement.

Next, we mention one general way in which our realistic Hamiltonians seem to have difficulty in matching observed energy-level data. Consider the energy separation between the lowest $\frac{3}{2}^+$ and $\frac{1}{2}^+$ states in a given odd-mass nucleus ($A=35$, 37, or 39). Let Δ be the *discrepancy* (in MeV) between the calculated version of this separation, and the

observed separation. Figure 3 shows that for a fixed choice of realistic Hamiltonians, Δ increases with A. When the ^{17}O single-particle-energy splittings are used, we find $-0.1 \leq \Delta \leq 0.7$ MeV in $A = 35$, then $0.1 \leq \Delta \leq 1.4$ MeV in $A = 37$, then $1.5 \leq \Delta \leq 2.7$ MeV in $A = 39$. When the adjusted single-particle-energy splittings are used, we find smaller discrepancies but the same general trend, viz. $\Delta \approx -0.6$ MeV for $A = 35$, then $\Delta \approx -0.1$ for $A = 37$, then $\Delta \approx 0.8$ MeV for $A = 39$. Thus, when the single-particle-energy splittings are changed from their ^{17}O values, the incompatibility between the $A = 35$ and $A = 39$ results is diminished but not entirely abolished. This behavior of Δ suggests that there is no mass-independent set of single-particle energies which will work with any one of our realistic interactions to yield good fits to observed excitation energies throughout the entire region $A = 35$ through 39. Dieperink and Brussaard[9] observed something of this same difficulty when they treated $A = 37$ and $A = 39$ simultaneously, and this difficulty led them to use different single-particle-energy splittings for the different masses.

We can also consider *numerical* indices (i.e., rms deviations) for evaluating the over-all success of our models in reproducing experimentally observed energy-level data. Table III shows these numerical indices. For each of our 10 Hamiltonians, column 3 of Table III lists the rms deviation from the 23 excitation energies of Table II. Note that when ^{17}O single-particle energies are used, all four realistic interactions are qualitatively successful in fitting observed excitation energies but the two p interactions are noticeably more success-

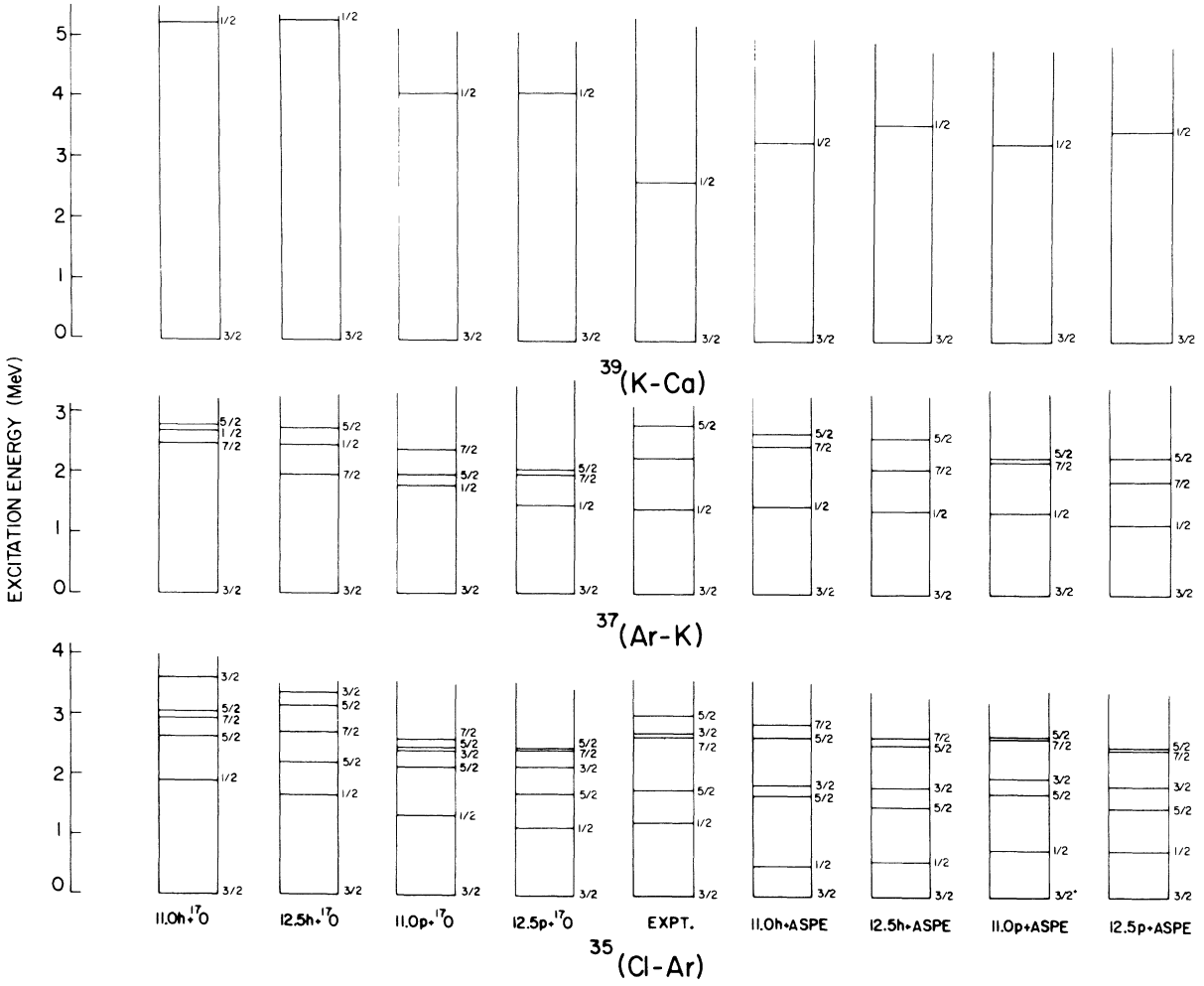

FIG. 3. The lowest few levels of the $T = \frac{1}{2}$ systems of $A = 35$, 37, and 39. This figure is intended to illustrate qualitative and general trends of the calculations. (Quantitative results for these systems are presented in other figures and in tables.) Results from the eight calculations which used realistic two-body matrix elements are presented here, in juxtaposition to schematic experimental spectra obtained by averaging results from the $T_z = +\frac{1}{2}$ and $-\frac{1}{2}$ mirror systems. Known negative-parity levels are omitted from the experimental column, as are the details at higher excitation energies.

ful than the two h interactions. When adjusted single-particle-energy splittings are allowed, this superiority of p Hamiltonians to h Hamiltonians disappears and the fits to excitation energies all become slightly better than the best fits obtained with ^{17}O single-particle energies. None of our realistic Hamiltonians was adjusted to fit binding energies, and all these realistic Hamiltonians give poor fits to the 11 ground-state binding energies listed in Table II. (Some examples are shown in later tables.)

Recall that each of our realistic ASPE Hamiltonians has only *two* free parameters affecting excitation energies, while the Hamiltonian 12.5pA has *four* free parameters affecting excitation energies. As Table III shows, these extra degrees of freedom bring some small improvement to the excitation-energy fit. The Hamiltonian MSDI, which also has *four* free parameters affecting excitation energies, gives an over-all fit that is slightly better than the 12.5pA fit. Both the MSDI and 12.5pA succeed in simultaneously fitting the spacings be-

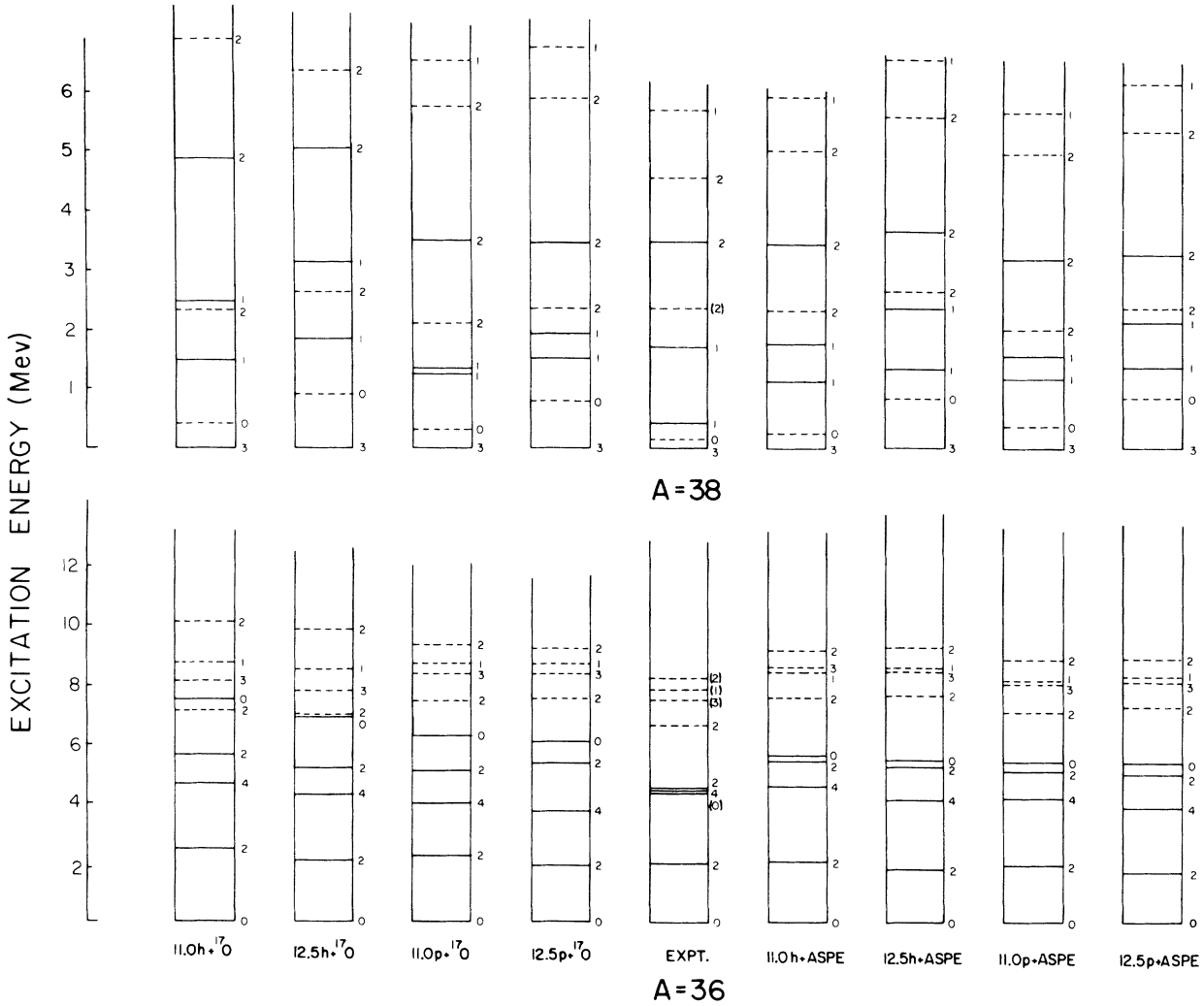

FIG. 4. The lowest few levels of the $T=0$ and $T=1$ systems of $A=36$ and 38. This figure is intended to illustrate qualitative and general trends of the calculations. (Quantitative results for these systems are presented in other figures and in tables.) Results from the eight calculations which used realistic two-body matrix elements are presented here, in juxtaposition to schematic experimental spectra taken from data on ^{36}Ar, ^{36}Cl, ^{38}K, and ^{38}Ar. Known negative-parity levels are omitted from the experimental spectra, as are the details at higher excitation energies in a given T spectrum. For each mass value, the results for $T=1$ levels are denoted by dashed lines and the $T=0$ levels by solid lines. In the experimental column, the energy splitting between $T=1$ and $T=0$ systems has been corrected by subtracting estimates of the Coulomb contributions to the measured splittings between $|T_z|=1$ and $T_z=0$ systems. The second $J^\pi=2^+$, $T=1$ level in the experimental $A=38$ column does not correspond to a single observed level but rather to a centroid of three observed levels. Also, a 0^+ state observed at 3.38 MeV has been omitted. (See Sec. III B 2 of the text.)

tween the first $\frac{3}{2}^+$ and first $\frac{1}{2}^+$ states in $A=35$, 37, and 39.

Each of the Hamiltonians 12.5pA and MSDI has two further parameters (besides the four aforementioned ones) affecting ground-state binding energies. These extra parameters allow the 12.5pA and MSDI to give excellent fits to empirically determined ground-state binding energies. (Details are given in later tables.)

There is no one choice among our 10 Hamiltonians which is markedly superior to all the others in fitting energy-level spectra. Four of the Hamiltonians were selected for more extensive investigation, in that we used their wave functions to calculate spectroscopic factors and electromagnetic observables. The four so selected were 12.5p + ^{17}O, 11.0h + ASPE, 12.5pA, and MSDI.

B. Detailed Comparison with Experimental Results

In this section we consider in detail the energies, spectroscopic factors for single-nucleon transfer, and magnetic dipole and electric quadrupole observables as calculated from the two Hamiltonians 12.5p + ^{17}O and 11.0h + ASPE. Some results from the Hamiltonians 12.5pA and MSDI will be considered too, but less thoroughly. We shall discuss each A, T system in turn, starting with $A=38$ and proceeding downward to $A=34$. By combining information about spectroscopic factors with information about excitation energies, we shall attempt to establish correspondences between model states and observed states up through about 5 MeV of excitation in each system. Also, we shall compare calculated and observed values for $E2$ and $M1$ static moments and transition strengths. During our discussions we shall refer to tables showing the dominant components of the model wave functions, for selected nuclear states, as obtained from the Hamiltonian 12.5p + ^{17}O. We emphasize the results obtained from the two Hamiltonians 12.5p + ^{17}O and 11.0h + ASPE, partly because of our interest in their realistic origins and partly because they seem to be more successful than either 12.5pA or MSDI in matching the experimental data on spectroscopic factors and electromagnetic observables.

We report $B(E2)$'s in units of $e^2\,\mathrm{F}^4$, and quadrupole moments in units of $e\,\mathrm{F}^2$. In calculating electric quadrupole moments and $E2$ transition strengths, we assume added effective charges of $0.5e$. That is, the charge of the neutron is taken to be $0.5e$, and the charge of the proton to be $1.5e$. The radial wave functions are assumed to be of the harmonic-oscillator form, with $\hbar\omega = 41A^{-1/3}$ MeV. Our main motivation for these choices was that these same assumptions yielded reasonably good agreement between calculated and measured values for the nuclei $A=18$–22. All magnetic dipole matrix elements are calculated by using the free-neutron and free-proton magnetic moments. Again, this choice was suggested by results in the $A=18$–22 region,[4] where calculations with free-nucleon magnetic moments seemed to give reasonable answers. Numerical values for $B(M1)$'s are presented as 100 times the value in units of μ_N^2.

Spectroscopic factors are presented in the isospin formalism. That is, when we say S, we mean S, not C^2S. E.g., the sum-rule limit for $d_{5/2}$ pickup is 12, not 6. Experimental S factors are presented with the experimentalist's own absolute normalization, where available.

TABLE III. Goodness-of-fit values and related parameters. In the last three columns, $E(\frac{3}{2}^+)$ is the energy of the ground state of $A=39$ relative to ^{16}O (with Coulomb contributions ignored), while $E(\frac{1}{2}^+)$ and $E(\frac{5}{2}^+)$ are excitation energies with respect to the ground state of $A=39$. The columns headed Goodness of fit refer to deviations from the 23 excitation energies listed in Table II.

Hamiltonian	Goodness of fit av. abs. dev. (MeV)	Goodness of fit rms dev. (MeV)	Single-particle-energy splittings $\epsilon_{1/2}-\epsilon_{5/2}$ (MeV)	$\epsilon_{3/2}-\epsilon_{5/2}$ (MeV)	$\epsilon_{3/2}-\epsilon_{1/2}$ (MeV)	Calculated energies of states in $A=39$ $E(\frac{3}{2}^+)$ (MeV)	$E(\frac{1}{2}^+)$ (MeV)	$E(\frac{5}{2}^+)$ (MeV)
11.0h + ^{17}O	0.96	1.22	0.87	5.08	4.21	276.54	5.20	7.71
11.0p + ^{17}O	0.58	0.71	0.87	5.08	4.21	279.05	4.09	6.56
12.5h + ^{17}O	0.89	1.15	0.87	5.08	4.21	295.34	5.22	8.46
12.5p + ^{17}O	0.51	0.64	0.87	5.08	4.21	300.87	4.03	6.99
11.0h + ASPE	0.33	0.43	2.95	5.18	2.23	267.50	3.22	7.82
11.0p + ASPE	0.32	0.41	2.80	6.14	3.34	263.96	3.23	7.62
12.5h + ASPE	0.41	0.51	2.02	4.55	2.53	294.41	3.55	7.93
12.5p + ASPE	0.44	0.51	2.26	5.86	3.60	289.83	3.43	7.77
12.5pA	0.27	0.38	2.43	5.10	2.67	265.62	3.13	7.48
MSDI	0.24	0.30	4.82	7.27	2.45	265.58	2.45	7.27

In our tabulations of wave functions, the conventions of the presentation are as follows. A particular model level is labeled by its mass number A, twice its total angular momentum J, twice its isospin T, its calculated binding energy with respect to ^{16}O, and an ordinal number denoting whether it is the 1st, 2nd, 3rd, or 4th lowest state for the particular A, J, T combination in question. Also listed is the dimensionality of the state vector. Each component whose intensity exceeds 2% (amplitude ≥ 0.1414) is then listed. Under each amplitude value is a triplet of columns, one column for each of the three sd orbits. The entries in these three columns identify the basis vector associated with the amplitude. Thus, the entries marked Configuration show the particle partition n_1, n_2, n_3 in the three orbits. The entries marked 2(S-shell J's) show the single-shell angular momenta J_1, J_2, J_3 to which the particles in the three separate orbits are coupled. The entries marked 2(coupled J's) show first the resultant angular momentum J_{12} after coupling the J_1 of shell one ($d_{5/2}$) to the J_2 of shell two ($s_{1/2}$), and then the final resultant J_{123} (which matches, of course, the J of the state under consideration). The isospin rows repeat the preceding two rows, but for isospin rather than angular momentum. The entries marked S-S seniority show the seniorities v_1, v_2, v_3 of the particles in the three separate orbits (the three *single shells*). Underneath the information about amplitudes, we show the percentage of the total wave function that is accounted for in the listed components. Finally, the line marked Occupation shows the average occupation numbers $n(d_{5/2})$, $n(s_{1/2})$, and $n(d_{3/2})$ as obtained from the complete wave function.

Unless otherwise noted, experimental results quoted in our discussion have been taken from the compilation of Endt and van der Leun.[13] Other measurements are individually referenced, usually in the tables. In each of our tables we show all observed levels which have well-established J^π, T and which fall below the highest energy listed, *except* for those levels which we very strongly suspect are "intruder states." Observed levels which do not have securely established J^π, T are tabulated only when we have good reason to suspect an association with one of our model states. Observed levels which have probable (but not established) spins or parities are indicated by enclosing their listed energies in parentheses. Observed levels for which little or no experimental foundations exist for a particular J^π assignment, but which on the basis of our model analyses we think might correspond to our model states, are indicated by enclosing their listed energies in double parentheses. In Figs. 5–7, on the other hand, we include all observed levels below the highest one shown, except for those of established negative parity. In addition, these figures show the lowest known negative-parity level in each A, T system.

We shall not discuss here the problem of deciding what quantitative uncertainties to attribute to various experimentally determined values. In general, if theory and experiment agree within 25%, then we shall regard the agreement as "acceptable." This statement holds for $B(E2)$'s and $B(M1)$'s, for static moments, and for the *relative* values of spectroscopic factors determined from a given nucleon-transfer experiment $A(x, y)B$.

1. $A = 38$, $T = 0$: ^{38}K
(See Tables IV–VI, and Fig. 4)

Our calculations place only four $T = 0$ states below 4.5-MeV excitation in ^{38}K; they are 3^+, 1^+, 1^+, and 2^+. The model wave functions of the $J = 3^+$ ground state are quite simple, being $\gtrsim 90\%$ $(d_{3/2})^{-2}$ (see Table V). Therefore it should be strongly populated by $l = 2$ pickup from ^{39}K, and this is consistent with available experimental data.[30,31] The calculated magnetic moments for the 3^+ ground state are in good agreement with the experimental value (see Table XXVII). The electric quadrupole moment of this state has not been measured.

Unlike the 3^+ state, the lowest two 1^+ states and, to a lesser extent, the lowest 2^+ state in ^{38}K have calculated characteristics which are quite sensitive to the details of the model Hamiltonian. Their wave functions are quite mixed; for example in the 12.5p + ^{17}O wave functions for each of the 1^+ states, the configuration of highest intensity, $(d_{3/2})^{-2}$, accounts for less than 50% of the total intensity. All of the realistic calculations give too high an excitation energy for the first 1^+ state. In contrast, the MSDI Hamiltonian puts the first 1^+ state too low (even below the first 3^+ state). Experimental spectroscopic factors for the lowest two 1^+ states are in fair-to-good agreement with values calculated from the realistic Hamiltonians, but are in definite disagreement with the corresponding 12.5pA and MSDI results. More precise experimental determinations of the relative spectroscopic factors $S(l = 2)$ and $S(l = 0)$ to these levels would be valuable for further discriminating between our alternative Hamiltonians. Measurements of the electromagnetic decay strengths of these states would also be helpful (see Table VI).

The lowest two 1^+ states in ^{38}K have previously been considered theoretically by Dieperink and Glaudemans.[32] Their wave functions, obtained with a modified realistic interaction based on the Tabakin potential, are similar to ours. For these 1^+ states, the wave function from earlier $d_{3/2}$-$s_{1/2}$ calculations[7] are also rather similar to those from

TABLE IV. Energies E and spectroscopic factors S for states of $A=38$. Energies of the ground states for each T value are given relative to ^{16}O, with Coulomb contributions removed. Energies of other states (J, T) are given relative to the ground state of same T. An integer subscript to an S symbol denotes an orbital angular momentum l, while a half-integer subscript denotes a total nucleon angular momentum j. The symbol pk denotes pickup, and the symbol st denotes stripping. The initial state in the pickup reaction is the $J=\frac{3}{2}$, $T=\frac{1}{2}$ ground state of ^{39}K; and the initial state in the stripping reaction is the $J=\frac{3}{2}$, $T=\frac{3}{2}$ ground state of ^{37}Cl.

States of $A=38$ J, T	Energy E (MeV) Expt.	11.0h +ASPE	12.5p +^{17}O	12.5pA	MSDI		$100\times(S_0; S_2)$ Expt.	$100\times(S_{1/2}; S_{3/2}, S_{5/2})_{calc}$ 11.0h +ASPE	12.5p +^{17}O	12.5pA	MSDI
1, 0	0.45	1.12	1.53	1.01	−0.13	pk	10; 39 [a]	15; 34, 4	11; 37, 6	2; 70, 0	2; 71, 0
	1.70	1.76	1.93	2.58	2.22	pk	0; 75 [a]	5; 34, 12	3; 32, 15	29; 4, 5	36; 3, 0
		5.02	5.17	4.99	4.69	pk		17; 6, 9	22; 5, 9	5; 0, 16	0; 0, 5
		7.13	8.34	6.81	6.64	pk		1; 0, 12	0; 0, 5	1; 0, 15	0; 0, 31
2, 0	(3.44) [a]	3.42	3.47	3.30	2.38	pk	34; 27 [a]	51; 0, 9	36; 0, 22	56; 0, 5	62; 0, 1
		7.21	6.78	6.78	7.19	pk		10; 0, 53	23; 0, 39	5; 0, 57	1; 0, 61
3, 0	252.38	252.52	283.15	252.41	252.04	pk	; 183 [a]	; 170, 2	; 167, 4	; 172, 2	; 175, 0
		8.56	7.94	8.14	7.37	pk		; 4, 59	; 6, 60	; 3, 74	; 0, 84
		11.27	10.97	10.38	9.46	pk		; 1, 24	; 1, 20	; 0, 10	; 0, 3
4, 0		7.30	5.96	6.77	7.19	pk		; , 112	; , 112	; , 112	; , 112
5, 0		15.13	13.50	14.58	14.46						
0, 1	252.21	252.25	282.35	252.28	252.02	st	; 235 [b]	; 268,	; 267,	; 267,	; 270,
						pk	; 78 [c]	; 70,	; 70,	; 68,	; 68,
	(6.61) [b]	6.88	8.03	6.46	6.81	st	; 20 [b]	; 0,	; 0,	; 0,	; 0,
						pk		; 2,	; 1,	; 2,	; 5,
1, 1	(5.55) [c]	5.59	5.96	5.55	5.17	st	4; 7 [b]	2; 3, 0	1; 2, 0	2; 3, 0	4; 6, 0
						pk	117; 0 [c]	112; 0, 0	112; 0, 0	112; 0, 0	112; 0, 0
		10.00	8.62	9.54	9.99	st		0; 1, 0	0; 2, 0	0; 2, 0	0; 0, 0
						pk		0; 0, 112	0; 0, 112	0; 0, 112	0; 0, 112
2, 1	2.17	2.02	1.56	1.90	2.03	st	2; 247 [b]	1; 243, 1	1; 245, 1	1; 234, 2	1; 232, 1
						pk	0; 374 [c]	6; 354, 2	2; 358, 4	7; 344, 5	16; 335, 1
	(4.40) [c,d]	4.75	5.09	4.58	4.38	st	5; 14 [b,d]	2; 4, 0	1; 2, 0	2; 6, 1	5; 14, 1
						pk	180; 30 [c,d]	174; 15, 1	170; 9, 5	166; 21, 2	165; 37, 1
		10.00	8.81	9.76	9.55	st		1; 1, 2	1; 1, 3	2; 2, 3	1; 0, 1
						pk		3; 4, 182	6; 5, 179	4; 6, 180	4; 2, 168
3, 1		10.19	8.86	9.83	9.99	st		; 0, 3	; 1, 4	; 1, 5	; 0, 2
						pk		; 0, 262	; 0, 262	; 0, 262	; 9, 262
4, 1		8.53	7.14	7.80	8.85	st		; , 1	; , 1	; , 1	; , 0
						pk		; , 333	; , 331	; , 330	; , 336

[a] Reference 30 (for both S_0 and S_2).
[b] Reference 34 (for both S_0 and S_2).
[c] Reference 33 (for both S_0 and S_2).
[d] The excitation energy 4.40 MeV is a centroid of three observed levels; and each of the spectroscopic factors 5, 14, 180, and 30 is a sum of experimental S factors for these three levels. (See text.)

TABLE V. Major components of the wave functions of states of $A=38$ as calculated with the $12.5p+^{17}O$ Hamiltonian. The conventions of the presentation are explained in Sec. III B of the text.

$A=38$, $2J^{\pi}=2^{+}$, $2T=0$, $E=281.619$, eigenvector 1 of this A, J, T.

Amplitude	−0.418			−0.150			−0.551			0.707		
S-shell labels	$D5$	$S1$	$D3$	$D5$	$S1$	$D3$	$D5$	$S1$	$D3$	$D5$	$S1$	$D3$
Configuration	11	4	7	12	2	8	12	3	7	12	4	6
2(S-shell J's)	5	0	3	0	2	0	0	1	3	0	0	2
2(coupled J's)		5	2		2	2		1	2		0	2
2(S-shell T's)	1	0	1	0	0	0	0	1	1	0	0	0
2(coupled T's)		1	0		0	0		1	0		0	0
S-S seniorities	1	0	1	0	2	0	0	1	1	0	0	2

Listed components account for 100.0 per cent of the wave function.
Occupation $(D5)=11.63$, $(S1)=3.65$, $(D3)=6.52$.

$A=38$, $2J^{\pi}=2^{+}$, $2T=0$, $E=281.225$, eigenvector 2 of this A, J, T.

Amplitude	0.206			−0.631			−0.196			−0.304			−0.654		
S-shell labels	$D5$	$S1$	$D3$	$D5$	$S1$	$D3$	$D5$	$S1$	$D3$	$D5$	$S1$	$D3$	$D5$	$S1$	$D3$
Configuration	10	4	8	11	4	7	12	2	8	12	3	7	12	4	6
2(S-shell J's)	2	0	0	5	0	3	0	2	0	0	1	3	0	0	2
2(coupled J's)		2	2		5	2		2	2		1	2		0	2
2(S-shell T's)	0	0	0	1	0	1	0	0	0	0	1	1	0	0	0
2(coupled T's)		0	0		1	0		0	0		1	0		0	0
S-S seniorities	2	0	0	1	0	1	0	2	0	0	1	1	0	0	2

Listed components account for 100.0 per cent of the wave function.
Occupation $(D5)=11.52$, $(S1)=3.83$, $(D3)=6.65$.

$A=38$, $2J^{\pi}=4^{+}$, $2T=0$, $E=279.682$, eigenvector 1 of this A, J, T.

Amplitude	−0.249			−0.601			−0.760		
S-shell labels	$D5$	$S1$	$D3$	$D5$	$S1$	$D3$	$D5$	$S1$	$D3$
Configuration	11	3	8	11	4	7	12	3	7
2(S-shell J's)	5	1	0	5	0	3	0	1	3
2(coupled J's)		4	4		5	4		1	4
2(S-shell T's)	1	1	0	1	0	1	0	1	1
2(coupled T's)		0	0		1	0		1	0
S-S seniorities	1	1	0	1	0	1	0	1	1

Listed components account for 100.0 per cent of the wave function.
Occupation $(D5)=11.58$, $(S1)=3.36$, $(D3)=7.06$.

$A=38$, $2J^{\pi}=6^{+}$, $2T=0$, $E=283.151$, eigenvector 1 of this A, J, T.

Amplitude	−0.207			0.978		
S-shell labels	$D5$	$S1$	$D3$	$D5$	$S1$	$D3$
Configuration	11	4	7	12	4	6
2(S-shell J's)	5	0	3	0	0	6
2(coupled J's)		5	6		0	6
2(S-shell T's)	1	0	1	0	0	0
2(coupled T's)		1	0		0	0
S-S seniorities	1	0	1	0	0	2

Listed components account for 100.0 per cent of the wave function.
Occupation $(D5)=11.96$, $(S1)=4.00$, $(D3)=6.04$.

TABLE V *(Continued)*

$A=38$, $2J^{\pi}=0^{+}$, $2T=2$, $E=282.347$, eigenvector 1 of this A, J, T.

Amplitude		−0.247			−0.963	
S-shell labels	$D5$	$S1$	$D3$	$D5$	$S1$	$D3$
Configuration	10	4	8	12	4	6
2(S-shell J's)	0	0	0	0	0	0
2(coupled J's)		0	0		0	0
2(S-shell T's)	2	0	0	0	0	2
2(coupled T's)		2	2		0	2
S-S seniorities	0	0	0	0	0	0

Listed components account for 98.8 per cent of the wave function.
Occupation $(D5)=11.88$, $(S1)=3.98$, $(D3)=6.15$.

$A=38$, $2J^{\pi}=2^{+}$, $2T=2$, $E=276.388$, eigenvector 1 of this A, J, T.

Amplitude		1.000	
S-shell labels	$D5$	$S1$	$D3$
Configuration	12	3	7
2(S-shell J's)	0	1	3
2(coupled J's)		1	2
2(S-shell T's)	0	1	1
2(coupled T's)		1	2
S-S seniorities	0	1	1

Listed components account for 99.9 per cent of the wave function.
Occupation $(D5)=12.00$, $(S1)=3.00$, $(D3)=7.00$.

$A=38$, $2J^{\pi}=4^{+}$, $2T=2$, $E=280.790$, eigenvector 1 of this A, J, T.

Amplitude		−0.977	
S-shell labels	$D5$	$S1$	$D3$
Configuration	12	4	6
2(S-shell J's)	0	0	4
2(coupled J's)		0	4
2(S-shell T's)	0	0	2
2(coupled T's)		0	2
S-S seniorities	0	0	2

Listed components account for 95.5 per cent of the wave function.
Occupation $(D5)=11.96$, $(S1)=3.98$, $(D3)=6.06$.

$A=38$, $2J^{\pi}=4^{+}$, $2T=2$, $E=277.252$, eigenvector 2 of this A, J, T.

Amplitude		−0.192			−0.162			−0.952			0.156	
S-shell labels	$D5$	$S1$	$D3$	$D5$	$S1$	$D3$	$D5$	$S1$	$D3$	$D5$	$S1$	$D3$
Configuration	11	3	8	11	4	7	12	3	7	12	4	6
2(S-shell J's)	5	1	0	5	0	3	0	1	3	0	0	4
2(coupled J's)		4	4		5	4		1	4		0	4
2(S-shell T's)	1	1	0	1	0	1	0	1	1	0	0	2
2(coupled T's)		2	2		1	2		1	2		0	2
S-S seniorities	1	1	0	1	0	1	0	1	1	0	0	2

Listed components account for 99.4 per cent of the wave function.
Occupation $(D5)=11.92$, $(S1)=3.06$, $(D3)=7.02$.

our full *sd*-shell calculations. Indeed, the $d_{5/2}$ orbit seems to be unimportant for $T=0$ ^{38}K wave functions within the first 5 MeV of excitation, with the possible exception of the 2^+ state.

2. $A=38$, $T=1$: ^{38}Ar-^{38}Ca
(See Tables IV–VI, and Fig. 4)

The $T=1$ states of $A=38$ are observed in ^{38}Ar, ^{38}Ca, and ^{38}K. Of these three, ^{38}Ar has received the most extensive experimental attention. All our models give 0^+-2^+-2^+-1^+-0^+ as the sequence of the lowest five $T=1$ states. Our model wave functions for these low-lying states are all very simple, as indicated in Table V. The $J^\pi=0^+$ ground state has $(d_{3/2})^{-2}$ as its dominant configuration. The second 0^+ state (not shown in Table V) is predominantly $(s_{1/2})^{-2}$. The first 2^+ state has $(d_{3/2})^{-2}$ as its dominant configuration, while the second 2^+ and the first 1^+ states are predominantly $(s_{1/2})^{-1}(d_{3/2})^{-1}$. These five states comprise the $d_{3/2}$-$s_{1/2}$ part of the $A=38$, $T=1$ spectrum. Their calculated spectroscopic factors, presented in Table IV, are direct

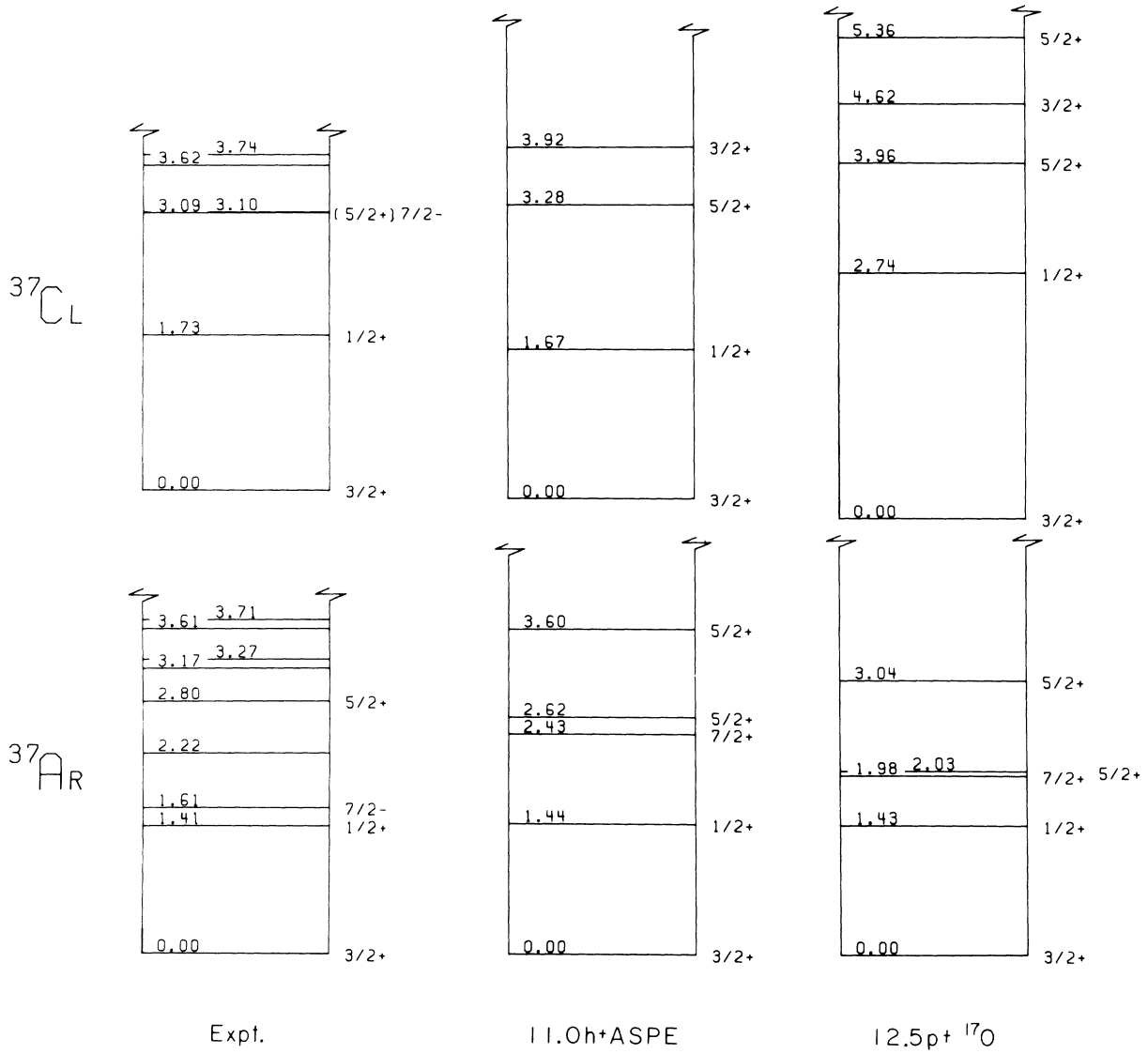

FIG. 5. Calculated and observed spectra of the $A=37$, $T=\frac{1}{2}$ system (we have used ^{37}Ar as the experimental example) and the $T=\frac{3}{2}$ system (for which we have used ^{37}Cl). All observed levels of a given T which do not have definitive negative parity are plotted up to the slash marks. In addition, the lowest-energy observed negative-parity state is plotted for each T value. In the experimental column, the energy splitting between $T=\frac{3}{2}$ and $T=\frac{1}{2}$ systems has been corrected by subtracting an estimate of the Coulomb contribution to the splitting measured between ^{37}Cl and ^{37}Ar ground states. Further information on these systems is available in Tables VII and X.

reflections of their simple wave functions.

For the lowest two states, 0^+ and 2^+, model spectroscopic factors for formation via single-nucleon pickup and stripping are completely consistent with experimental results.[33,34] Also, for the $2^+ \rightarrow 0^+$ first-to-ground-state $E2$ transition in ^{38}Ar, there is consistency between the measured[35] $B(E2)$ value $38 \pm 9\ e^2\,\mathrm{F}^4$ and the shell-model values 28 and

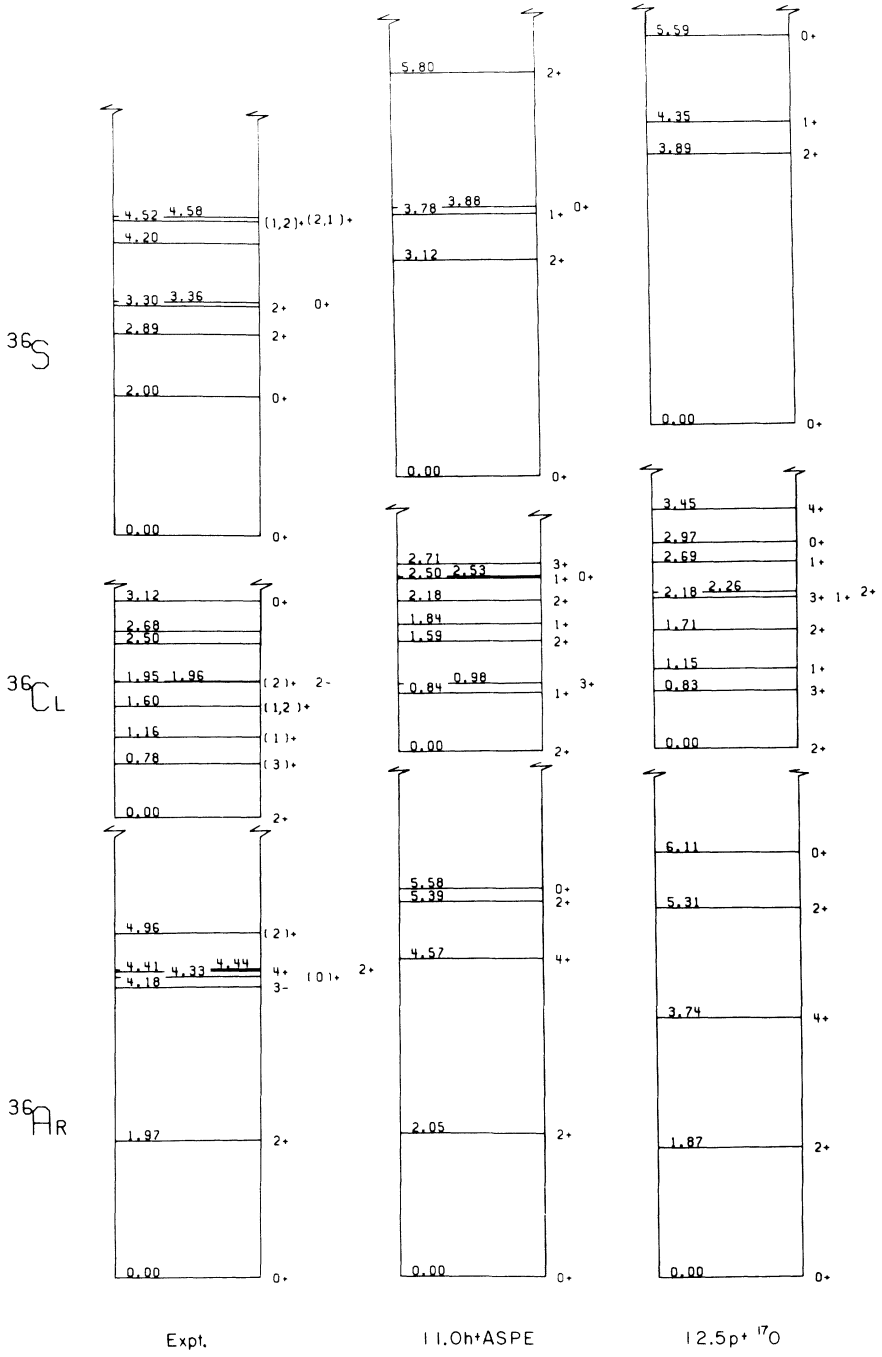

FIG. 6. Calculated and observed spectra of $A = 36$ for $T = 0$, $T = 1$, and $T = 2$. We have used ^{36}Ar, ^{36}Cl, and ^{36}S as the experimental manifestations of these systems. All observed levels of a given T which do not have definite negative parity are plotted up to the slash marks. In addition, the lowest-energy observed negative-parity state is plotted for each T value. In the experimental column, the energy splittings separating the $T = 2$, $T = 1$, and $T = 0$ systems have been corrected by subtracting estimates of the Coulomb contributions from the measured splittings that separate ^{36}S, ^{36}Cl, and ^{36}Ar ground states. Further information on these systems is available in Tables XII, XVI, and XVIII.

TABLE VI. Calculated $B(E2)$ and $B(M1)$ values for transitions between states of $A=38$. The notation J_ν, T labels the νth-lowest state of given J and T in the model spectrum.

Initial state J_ν, T	Final state J_ν, T	$B(E2)$ $(e^2\,\mathrm{F}^4)$ 12.5p+^{17}O	$B(E2)$ $(e^2\,\mathrm{F}^4)$ 11.0h+ASPE	$100\times B(M1)$ $(\mu_N{}^2)$ 12.5p+^{17}O	$100\times B(M1)$ $(\mu_N{}^2)$ 11.0h+ASPE
			^{38}K		
$1_1, 0$	$3_1, 0$	34.	38.	0	0
$1_2, 0$	$3_1, 0$	0.3	0.2	0	0
$2_1, 0$	$3_1, 0$	7.8	8.5	0.00	0.00
$2_1, 1$	$3_1, 0$	8.4	10.0		0.06
$1_1, 0$	$0_1, 1$	0	0	0.8	
$1_2, 0$	$0_1, 1$	0	0	7.7	
$2_1, 0$	$0_1, 1$	0.8	0.8	0	0
$2_1, 1$	$0_1, 1$	12.	13.	0	0
$1_2, 0$	$1_1, 0$	27.	29.		0.04
$2_1, 0$	$1_1, 0$	4.5	7.4		0.2
$2_1, 1$	$1_1, 0$	0.3	0.05		0.5
$2_1, 0$	$1_2, 0$	10.6	10.6		0.1
$2_1, 1$	$1_2, 0$	0.3	0.1		0.01
			^{38}Ar		
$2_1, 1$	$0_1, 1$	28.	29.	0	0
$2_2, 1$	$0_1, 1$	10.	8.4	0	0

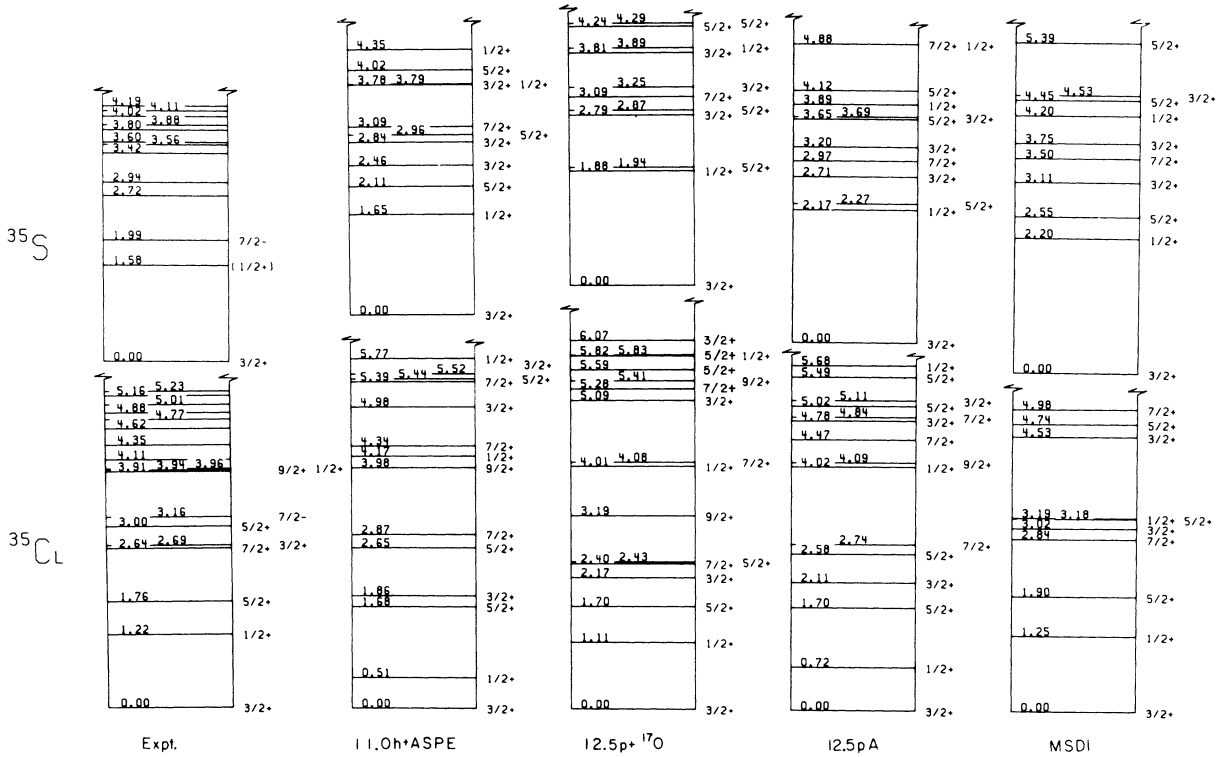

FIG. 7. Calculated and observed spectra of $A=35$, $T=\frac{1}{2}$, and $T=\frac{3}{2}$. We have used experimental data from ^{35}Cl and ^{35}S in this figure. All known levels of a given T which do not have definite negative parity are plotted up to the slash marks. In addition, the lowest-energy observed negative-parity state is plotted for each T value. In the experimental column, the energy splitting separating the $T=\frac{3}{2}$ and $T=\frac{1}{2}$ systems has been obtained by subtracting an estimate of the Coulomb contribution from the measured splitting of the ^{35}Cl and ^{35}S ground states. Further information about these systems is available in Tables XX and XXIII.

29 e^2 F^4 obtained from 12.5p + ^{17}O and 11.0h + ASPE.

At excitation energies higher than the first excited state, however, there are some significant differences between the observed spectrum and our *s-d*-shell spectra. These differences very probably arise from the importance, in the 3-to-5-MeV region, of the sort of *fp*-shell intruder states we mentioned earlier. The third observed level of ^{38}Ar, at 3.38 MeV, is assigned[13] $J^\pi = 0^+$. We have omitted this observed state from the central column of Fig. 4, and from Table IV, because it appears to be a very clear example of an $(sd)^{-4}(fp)^2$ intruder state. This characterization is suggested by several theoretical studies[36,37] and presently available experimental data.[13,38]

Above the observed 3.38-MeV level, proton transfer from a ^{39}K target yields four prominent $l = 0$ states in ^{38}Ar. These are seen at 3.94, 4.57, 5.16, and 5.55 MeV, with $S(l = 0)$ factors of 0.4, 0.9, 0.5, and 1.2, respectively.[33] But according to our models, there are only two *sd*-shell states below 9 MeV that are strongly populated by $l = 0$ pickup. These are the second *sd*-shell 2^+ state and the first *sd*-shell 1^+ state, both of which have wave functions dominated by $(d_{3/2})^{-1}(s_{1/2})^{-1}$. It has been suggested[33] that the observation of two "extra" $l = 0$ states in ^{38}Ar results from mixing of the second *sd*-shell 2^+ state with two *fp*-shell intruder states, while the observed $l = 0$, 1^+ state retains an essentially pure *sd*-shell character. In particular: The second *sd*-shell 2^+ state is thought to be fragmented into a triad comprising the 2^+ state at 3.94 MeV together with the two $(1, 2)^+$ states seen at 4.57 and 5.16 MeV, while the first *sd*-shell 1^+ state is thought to be a reasonable partner for the $(1, 2)^+$ state observed at 5.55 MeV.[33] As Table IV shows, the calculated spectroscopic factor and the excitation energy of the lowest *sd*-shell 1^+ state are in good agreement with experimental results for the observed 5.55-MeV state. Also, the calculated spectroscopic factor and the excitation energy of the second *sd*-shell 2^+ state are in good agreement with results obtained by *summing* the experimental spectroscopic factors of the lowest three observed $l = 0$ states, and using their spectroscopic-factor-weighted centroid energy as the "observed" energy. This spectroscopic-factor-weighted centroid is at 4.40 MeV. Figure 4 and Table IV each show this centroid, rather than the lowest three $l = 0$ levels actually observed.

The calculated spectrum and wave functions for the $A = 38$, $T = 1$ system are not sensitive to the choice among our model Hamiltonians. Furthermore, the results from previously reported calculations,[7,8] using other Hamiltonians, are similar to ours. If one insists on a pure *sd*-shell model,

TABLE VII. Energies E and spectroscopic factors S for states of $A = 37$, $T = \frac{1}{2}$. The initial state for the stripping factors S_{st} is the $J^\pi = 0^+$, $T = 0$ ground state of ^{36}Ar. The initial state for the pickup factors S_{pk} is the $J^\pi = 0^+$, $T = 1$ ground state of ^{38}Ar. For the meaning of E, see Table IV.

		Energy E (MeV)					$(100 \times S_{st})/(100 \times S_{pk})$			
A, J, T	Expt.	11.0h + ASPE	12.5p + ^{17}O	12.5p*A*	MSDI	Expt.[a]	11.0h + ASPE	12.5p + ^{17}O	12.5p*A*	MSDI
37, $\frac{1}{2}$, $\frac{1}{2}$	1.41	1.44	1.43	1.80	1.53	14/	11/76	9/61	9/75	9/68
		5.51	5.31	4.69	3.63		0/17	0/12	0/34	1/61
		5.98	5.95	6.69	5.69		0/0	0/2	0/2	0/3
		7.32	7.27	7.80	8.40		0/7	0/1	0/1	0/0
37, $\frac{3}{2}$, $\frac{1}{2}$	240.34	238.81	266.26	240.45	240.36	43/	33/290	30/280	36/299	42/311
		4.66	4.63	4.69	4.51		0/3	0/0	0/12	0/14
		5.75	5.97	6.32	5.52		1/14	1/24	0/2	0/0
		7.22	7.02	6.73	7.13		0/0	0/2	0/0	0/1
37, $\frac{5}{2}$, $\frac{1}{2}$	2.80	2.62	2.03	2.76	2.81		6/127	8/167	2/42	0/5
		3.60	3.04	4.04	4.64		0/10	0/12	3/94	0/23
		5.90	5.76	5.97	5.89		0/7	0/7	0/3	0/2
		7.11	6.79	6.65	6.96		0/31	0/15	1/86	0/96
37, $\frac{7}{2}$, $\frac{1}{2}$	((2.22))	2.43	1.98	2.22	2.48					
		4.89	4.67	4.75	5.06					
		8.81	7.17	8.16	9.45					
		10.11	8.94	9.85	10.17					
37, $\frac{9}{2}$, $\frac{1}{2}$		8.81	7.12	8.19	9.38					
		10.39	8.86	9.90	10.64					
37, $\frac{11}{2}$, $\frac{1}{2}$		7.80	6.02	6.88	9.20					
37, $\frac{13}{2}$, $\frac{1}{2}$		15.16	12.60	14.03	16.38					

[a] Reference 12.

then further extensive experimental investigation of the $A=38$, $T=1$ system might not be very helpful in optimizing details of the model. (This is because of fp-shell complications in the real system.) However, it would be nice to know whether the observed 4.57-, 5.16-, and 5.55-MeV states are indeed 2^+, 2^+, and 1^+ as presumed above. Another item of interest would be a measured value for the static quadrupole moment of the first 2^+ state.

3. $A=37$, $T=\frac{1}{2}$: ^{37}Ar-^{37}K
(See Tables VII–IX, and Fig. 5)

The experimental information about even-parity levels in the $A=37$, $T=\frac{1}{2}$ system is not extensive.[12,13,39-41] Of the eight levels observed[39] below 3.5 MeV, three have assigned spins and known positive parity, two have known negative parity, and three have neither spin nor parity assigned. All the models which we discuss in this section give a $\frac{3}{2}^+$ ground state, a $\frac{1}{2}^+$ first excited state at about 1.5 MeV, and a $\frac{5}{2}^+$ state at about 2.5 MeV. These results are in good agreement with the observed spectrum. The 2.22-MeV level observed in ^{37}Ar has neither assigned spin nor assigned parity. We presume it to be the lowest $\frac{7}{2}^+$ state which is predicted by all our models to lie between 1.8 and 2.5 MeV. (Above this 2.22-MeV candidate, the next possible $\frac{7}{2}^+$ state in the experimental spectrum lies at 3.17 MeV.) The remaining sd-shell state that is predicted to lie fairly low in the $A=37$, $T=\frac{1}{2}$ spectrum is the second $\frac{5}{2}^+$ state. It lies between 3.0 and 4.6 MeV, depending on the Hamiltonian used. Thus, judging from the model results, at least one of the two unknown-parity levels observed at 3.17 and 3.27 MeV probably has extra-sd-shell origins. Above 3.5-MeV excitation, the density of observed levels is clearly greater than our sd models predict. We presume that these extra observed states, also, involve essential contributions from configurations involving fp-shell single-particle orbits.

Next we consider spectroscopic factors for stripping and pickup to the various states of $A=37$, $T=\frac{1}{2}$. The S factors calculated from the four Hamiltonians of Table VII are rather similar to each other, except for the $d_{5/2}$ pickup strengths. For the lowest $\frac{3}{2}^+$ and $\frac{1}{2}^+$ levels, our model results are consistent with experimentally determined stripping S factors. For the $d_{5/2}$ pickup strengths, the two realistic Hamiltonians give similar results, but the other two Hamiltonians give results different from those of the realistic Hamiltonians. Inspection of Table VII shows that a neutron-pickup experiment on ^{38}Ar, leading to the excited levels of ^{37}Ar, would be very informative. The results would allow identification of higher-lying $\frac{3}{2}^+$ and $\frac{5}{2}^+$ states in the experimental spectrum, and could help us to evaluate our models and to discriminate among them. As Table IX indicates, experimental data on $A=37$ electromagnetic decay widths would be similarly useful.

In some ways, results from our alternative Hamiltonians resemble each other more closely than they resemble nature. For example, the Hamiltonians 11.0h + ASPE and 12.5p + ^{17}O both give ^{37}Ar ground-state magnetic moments near $1.5\mu_N$, while the experimentally measured value is $0.95\mu_N$. In a similar way, the $A=37$, $T=\frac{1}{2}$ theoretical results of Dieperink and Brussaard[8] resemble our theoretical results more than they resemble nature. There are, however, significant differences between the 3- and the 2-shell spectra[7] for this system. These differences occur due to the importance of $(d_{5/2})^{-1}$ components in the 3-shell wave functions for low-lying $J^\pi=\frac{5}{2}^+$ states (see Table VIII).

4. $A=37$, $T=\frac{3}{2}$: ^{37}Cl
(See Tables IX-XI, and Fig. 5)

Experimental information about the positive-parity level structure of ^{37}Cl is also not abundant. Aside from the assignments of $J^\pi=\frac{3}{2}^+$ to the ground state and $\frac{1}{2}^+$ to the first excited state, there is available only a tentative $\frac{5}{2}^+$ assignment to the 3.09-MeV level. Note that the lowest $\frac{7}{2}^+$ state has moved up in excitation energy, compared to its position in the $T=\frac{1}{2}$ spectrum. The calculated values for the magnetic dipole and electric quadrupole moments of the $\frac{3}{2}^+$ ground state are in fair-to-good agreement with the measured values for these quantities (see Table XXVII). There are no experimentally determined spectroscopic factors available for the levels of ^{37}Cl. As Table X[42] indicates, proton-pickup measurements on a ^{38}Ar target would yield valuable information about the $A=37$ level structure, and about the degree of success of our models.

5. $A=36$, $T=0$: ^{36}Ar
(See Tables XII–XV, and Fig. 6)

The calculated excitation energies of the lowest 2^+ and 4^+ states in ^{36}Ar are in acceptable agreement with the experimental values. In all of our models the second model 0^+ state lies $\gtrsim 1$ MeV higher in excitation than the observed $(0)^+$ state at 4.33 MeV, and in most of the calculations with *realistic* two-body matrix elements the second model 2^+ state lies about 1 MeV higher than the second observed 2^+ state (at 4.44 MeV). Above the second observed 2^+, there are no $T=0$ states having both definitely known spin and known positive parity. However, several of the states observed

TABLE VIII. Major components of the wave functions of states of $A=37$, $T=\frac{1}{2}$ as calculated with the 12.5p + ^{17}O Hamiltonian. The conventions of the presentation are explained in Sec. III B of the text.

$A=37$, $2J^{\pi}=1^{+}$, $2T=1$, $E=264.831$, eigenvector 1 of this A, J, T. Model core = 16, dimensions = 14.

Amplitude	−0.200			0.214			0.277			0.453			0.156			0.632			0.178			−0.353		
S-shell labels	$D5$	$S1$	$D3$	$D5$	$S1$	$D3$	$D5$	$S1$	$D3$	$D5$	$S1$	$D3$	$D5$	$S1$	$D3$	$D5$	$S1$	$D3$	$D5$	$S1$	$D3$	$D5$	$S1$	$D3$
Configuration	10	3	8	11	3	7	11	3	7	11	4	6	12	1	8	12	3	6	12	3	6	12	4	5
2(S-shell J's)	0	1	0	5	1	3	5	1	3	5	0	4	0	1	0	0	1	0	0	1	2	0	0	1
2(coupled J's)		1	1		4	1		4	1		5	1		1	1		1	1		1	1		0	1
2(S-shell T's)	2	1	0	1	1	1	1	1	1	1	0	2	0	1	0	0	1	2	0	1	0	0	0	1
2(coupled T's)		1	1		0	1		2	1		1	1		1	1		1	1		1	1		0	1
S-S seniorities	0	1	0	1	1	1	1	1	1	1	0	2	0	1	0	0	1	0	0	1	2	0	0	3

Listed components account for 94.8 per cent of the wave function.
Occupation $(D5)=11.50$, $(S1)=3.32$, $(D3)=6.18$.

$A=37$, $2J^{\pi}=3^{+}$, $2T=1$, $E=266.263$, eigenvector 1 of this A, J, T. Model core = 16, dimension = 20.

Amplitude	0.333			0.203			0.155			−0.859		
S-shell labels	$D5$	$S1$	$D3$	$D5$	$S1$	$D3$	$D5$	$S1$	$D3$	$D5$	$S1$	$D3$
Configuration	10	4	7	11	4	6	12	2	7	12	4	5
2(S-shell J's)	0	0	3	5	0	4	0	0	3	0	0	3
2(coupled J's)		0	3		5	3		0	3		0	3
2(S-shell T's)	2	0	1	1	0	2	0	2	1	0	0	1
2(coupled T's)		2	1		1	1		2	1		0	1
S-S seniorities	0	0	1	1	0	2	0	0	1	0	0	1

Listed components account for 91.5 per cent of the wave function.
Occupation $(D5)=11.63$, $(S1)=3.91$, $(D3)=5.46$.

$A=37$, $2J^{\pi}=3^{+}$, $2T=1$, $E=261.636$, eigenvector 2 of this A, J, T. Model core = 16, dimension = 20.

Amplitude	−0.207			0.414			0.349			−0.156			−0.289			−0.695		
S-shell labels	$D5$	$S1$	$D3$	$D5$	$S1$	$D3$	$D5$	$S1$	$D3$	$D5$	$S1$	$D3$	$D5$	$S1$	$D3$	$D5$	$S1$	$D3$
Configuration	11	3	7	11	4	6	11	4	6	12	2	7	12	3	6	12	3	6
2(S-shell J's)	5	1	3	5	0	4	5	0	6	0	0	3	0	1	2	0	1	4
2(coupled J's)		4	3		5	3		5	3		0	3		1	3		1	3
2(S-shell T's)	1	1	1	1	0	2	1	0	0	0	2	1	0	1	0	0	1	2
2(coupled T's)		2	1		1	1		1	1		2	1		1	1		1	1
S-S seniorities	1	1	1	1	0	2	1	0	2	0	0	1	0	1	2	0	1	2

Listed components account for 92.8 per cent of the wave function.
Occupation $(D5)=11.59$, $(S1)=3.28$, $(D3)=6.13$.

TABLE VIII *(Continued)*

$A=37$, $2J^{\pi}=5^{+}$, $2T=1$, $E=264.229$, eigenvector 1 of this A, J, T. Model core = 16, dimension = 22.

Amplitude	−0.170			−0.189			−0.613			−0.186			−0.297			−0.166			0.205			−0.284			0.451		
S-shell labels	$D5$	$S1$	$D3$	$D5$	$S1$	$D3$	$D5$	$S1$	$D3$	$D5$	$S1$	$D3$	$D5$	$S1$	$D3$	$D5$	$S1$	$D3$	$D5$	$S1$	$D3$	$D5$	$S1$	$D3$	$D5$	$S1$	$D3$
Configuration	9	4	8	10	4	7	11	4	6	11	4	6	11	4	6	11	4	6	12	2	7	12	3	6	12	4	5
2(S-shell J's)	5	0	0	2	0	3	5	0	0	5	0	2	5	0	4	5	0	6	0	2	3	0	1	4	0	0	5
2(coupled J's)		5	5		2	5		5	5		5	5		5	5		5	5		2	5		1	5		0	5
2(S-shell T's)	1	0	0	0	0	1	1	0	2	1	0	0	1	0	2	1	0	0	0	0	1	0	1	2	0	0	1
2(coupled T's)		1	1		0	1		1	1		1	1		1	1		1	1		0	1		1	1		0	1
S-S seniorities	1	0	0	2	0	1	1	0	0	1	0	2	1	0	2	1	0	2	0	2	1	0	1	2	0	0	3

Listed components account for 91.6 per cent of the wave function.
Occupation $(D5)=11.22$, $(S1)=3.76$, $(D3)=6.02$.

$A=37$, $2J^{\pi}=5^{+}$, $2T=1$, $E=263.227$, eigenvector 2 of this A, J, T. Model core = 16, dimension = 22.

Amplitude	0.156			0.203			0.385			−0.148			0.181			0.178			0.813		
S-shell labels	$D5$	$S1$	$D3$	$D5$	$S1$	$D3$	$D5$	$S1$	$D3$	$D5$	$S1$	$D3$	$D5$	$S1$	$D3$	$D5$	$S1$	$D3$	$D5$	$S1$	$D3$
Configuration	11	4	6	11	4	6	11	4	6	12	2	7	12	3	6	12	3	6	12	4	5
2(S-shell J's)	5	0	0	5	0	2	5	0	4	0	2	3	0	1	4	0	1	6	0	0	5
2(coupled J's)		5	5		5	5		5	5		2	5		1	5		1	5		0	5
2(S-shell T's)	1	0	2	1	0	0	1	0	2	0	0	1	0	1	2	0	1	0	0	0	1
2(coupled T's)		1	1		1	1		1	1		0	1		1	1		1	1		0	1
S-S seniorities	1	0	0	1	0	2	1	0	2	0	2	1	0	1	2	0	1	2	0	0	3

Listed components account for 96.1 per cent of the wave function.
Occupation $(D5)=11.73$, $(S1)=3.88$, $(D3)=5.40$.

$A=37$, $2J^{\pi}=7^{+}$, $2T=1$, $E=264.286$, eigenvector 1 of this A, J, T. Model core = 16, dimension = 18.

Amplitude	−0.180			−0.220			−0.246			0.897		
S-shell labels	$D5$	$S1$	$D3$	$D5$	$S1$	$D3$	$D5$	$S1$	$D3$	$D5$	$S1$	$D3$
Configuration	11	3	7	11	4	6	12	3	6	12	4	5
2(S-shell J's)	5	1	3	5	0	2	0	1	6	0	0	7
2(coupled J's)		4	7		5	7		1	7		0	7
2(S-shell T's)	1	1	1	1	0	0	0	1	0	0	0	1
2(coupled T's)		2	1		1	1		1	1		0	1
S-S seniorities	1	1	1	1	0	2	0	1	2	0	0	3

Listed components account for 94.7 per cent of the wave function.
Occupation $(D5)=11.84$, $(S1)=3.90$, $(D3)=5.26$.

TABLE IX. Calculated $B(E2)$ and $B(M1)$ values for transitions between states of $A=37$. The notation $(J)_\nu$ labels the νth-lowest state of given J in a model spectrum.

Initial state $(J)_\nu$	Final state $(J)_\nu$	$B(E2)$ $(e^2\,F^4)$ 12.5p+^{17}O	$B(E2)$ $(e^2\,F^4)$ 11.0h+ASPE	$100\times B(M1)$ $(\mu_N{}^2)$ 12.5p+^{17}O	$100\times B(M1)$ $(\mu_N{}^2)$ 11.0h+ASPE
		^{37}Ar, $T=\frac{1}{2}$			
$(\frac{4}{2})_1$	$(\frac{3}{2})_1$	62.	68.	3.6	3.3
$(\frac{3}{2})_2$	$(\frac{3}{2})_1$	2.3	2.2	8.6	6.2
$(\frac{5}{2})_1$	$(\frac{3}{2})_1$	20.	21.	87.	76.
$(\frac{5}{2})_2$	$(\frac{3}{2})_1$	6.8	4.4	10.3	9.3
$(\frac{7}{2})_1$	$(\frac{3}{2})_1$	34.	37.	0	0
$(\frac{3}{2})_2$	$(\frac{1}{2})_1$	14.	15.	0.05	0.2
$(\frac{5}{2})_1$	$(\frac{1}{2})_1$	36.	37.	0	0
$(\frac{5}{2})_2$	$(\frac{1}{2})_1$	6.3	8.0	0	0
		^{37}Cl, $T=\frac{3}{2}$			
$(\frac{1}{2})_1$	$(\frac{3}{2})_1$	17.	20.	9.3	4.3
$(\frac{3}{2})_2$	$(\frac{3}{2})_1$	7.1	7.0	3.1	0.9
$(\frac{5}{2})_1$	$(\frac{3}{2})_1$	26.	36.	16.	8.1
$(\frac{5}{2})_2$	$(\frac{3}{2})_1$	19.	11.	17.	38.
$(\frac{7}{2})_1$	$(\frac{3}{2})_1$	14.	14.	0	0
$(\frac{3}{2})_2$	$(\frac{1}{2})_1$	37.	38.	3.1	1.5
$(\frac{5}{2})_1$	$(\frac{1}{2})_1$	39.	29.	0	0
$(\frac{5}{2})_2$	$(\frac{1}{2})_1$	12.	18.	0	0

TABLE X. Energies E and spectroscopic factors S for states of $A=37$, $T=\frac{3}{2}$. The initial state for the stripping factors S_{st} is the $J^\pi=0^+$, $T=2$ ground state of ^{36}S. The initial state for the pickup factors S_{pk} is the $J^\pi=0^+$, $T=1$ ground state of ^{38}Ar. For the meaning of E, see Table IV.

A, J, T	Energy E (MeV) Expt.	11.0h+ASPE	12.5p+^{17}O	12.5pA	MSDI	$(100\times S_{st})/(100\times S_{pk})$ 11.0h+ASPE	12.5p+^{17}O	12.5pA	MSDI
37, $\frac{1}{2}$, $\frac{3}{2}$	1.73	1.67	2.74	1.71	1.55	7/250	2/239	7/238	12/242
		8.29	7.48	7.88	7.81	1/9	1/19	2/18	2/9
		10.76	10.27	10.15	11.10	0/2	0/4	0/2	0/1
		16.46	14.84	16.08	15.99	0/0	0/0	0/0	0/0
37, $\frac{3}{2}$, $\frac{3}{2}$	235.22	233.77	261.43	235.63	235.19	112/268	113/267	107/267	111/270
		3.92	4.62	3.75	3.73	2/8	1/6	3/13	3/14
		5.56	7.00	5.46	5.88	0/1	0/3	0/1	0/2
		8.85	7.84	8.44	8.59	1/4	1/4	2/7	0/2
37, $\frac{5}{2}$, $\frac{3}{2}$	(3.09) [a]	3.28	3.96	3.22	2.98	0/16	0/85	0/35	0/7
		6.00	5.36	5.55	6.30	3/709	3/592	4/645	2/751
		8.69	7.60	8.22	8.95	1/57	2/101	2/94	0/29
		10.90	10.77	10.49	10.52	0/0	0/0	0/1	0/2
37, $\frac{7}{2}$, $\frac{3}{2}$		7.49	6.31	6.77	7.97				
		9.68	9.37	8.89	9.66				
		11.91	11.64	11.50	11.68				
		14.66	12.98	13.84	15.25				
37, $\frac{9}{2}$, $\frac{3}{2}$		7.30	6.15	6.64	7.84				
		10.27	10.11	9.69	10.44				
37, $\frac{11}{2}$, $\frac{3}{2}$		14.16	12.76	13.68	15.10				

[a] Reference 42.

TABLE XI. Major components of the wave functions of the states of $A=37$, $T=\frac{3}{2}$ as calculated with the $12.5p+^{17}O$ Hamiltonian. The conventions of the presentation are explained in Sec. III B of the text.

$A=37$, $2J^{\pi}=1^{+}$, $2T=3$, $E=258.688$, eigenvector 1 of this A, J, T. Model core = 16, dimension = 5.

Amplitude		0.207			0.179			0.211			0.931	
S-shell labels	$D5$	$S1$	$D3$	$D5$	$S1$	$D3$	$D5$	$S1$	$D3$	$D5$	$S1$	$D3$
Configuration	10	3	8	11	3	7	11	4	6	12	3	6
2(S-shell J's)	0	1	0	5	1	3	5	0	4	0	1	0
2(coupled J's)		1	1		4	1		5	1		1	1
2(S-shell T's)	2	1	0	1	1	1	1	0	2	0	1	2
2(coupled T's)		3	3		2	3		1	3		1	3
S-S seniorities	0	1	0	1	1	1	1	0	2	0	1	0

Listed components account for 98.7 per cent of the wave function.
Occupation $(D5)=11.81$, $(S1)=3.06$, $(D3)=6.13$.

$A=37$, $2J^{\pi}=3^{+}$, $2T=3$, $E=261.427$, eigenvector 1 of this A, J, T. Model core = 16, dimension = 10.

Amplitude		0.186			0.960	
S-shell labels	$D5$	$S1$	$D3$	$D5$	$S1$	$D3$
Configuration	10	4	7	12	4	5
2(S-shell J's)	0	0	3	0	0	3
2(coupled J's)		0	3		0	3
2(S-shell T's)	2	0	1	0	0	3
2(coupled T's)		2	3		0	3
S-S seniorities	0	0	1	0	0	1

Listed components account for 95.6 per cent of the wave function.
Occupation $(D5)=11.89$, $(S1)=3.97$, $(D3)=5.14$.

$A=37$, $2J^{\pi}=3^{+}$, $2T=3$, $E=256.808$, eigenvector 2 of this A, J, T. Model core = 16, dimension = 10.

Amplitude		0.289			0.227			0.913	
S-shell labels	$D5$	$S1$	$D3$	$D5$	$S1$	$D3$	$D5$	$S1$	$D3$
Configuration	11	3	7	12	2	7	12	3	6
2(S-shell J's)	5	1	3	0	0	3	0	1	4
2(coupled J's)		4	3		0	3		1	3
2(S-shell T's)	1	1	1	0	2	1	0	1	2
2(coupled T's)		2	3		2	3		1	3
S-S seniorities	1	1	1	0	0	1	0	1	2

Listed components account for 96.9 per cent of the wave function.
Occupation $(D5)=11.88$, $(S1)=2.98$, $(D3)=6.14$.

$A=37$, $2J^{\pi}=5^{+}$, $2T=3$, $E=257.469$, eigenvector 1 of this A, J, T. Model core = 16, dimension = 10.

Amplitude		0.191			0.333			0.908	
S-shell labels	$D5$	$S1$	$D3$	$D5$	$S1$	$D3$	$D5$	$S1$	$D3$
Configuration	11	3	7	11	4	6	12	3	6
2(S-shell J's)	5	1	3	5	0	0	0	1	4
2(coupled J's)		4	5		5	5		1	5
2(S-shell T's)	1	1	1	1	0	2	0	1	2
2(coupled T's)		2	3		1	3		1	3
S-S seniorities	1	1	1	1	0	0	0	1	2

Listed components account for 97.2 per cent of the wave function.
Occupation $(D5)=11.80$, $(S1)=3.13$, $(D3)=6.07$.

$A=37$, $2J^{\pi}=5^{+}$, $2T=3$, $E=256.070$, eigenvector 2 of this A, J, T. Model core = 16, dimension = 10.

Amplitude		−0.149			−0.850			−0.348			0.304	
S-shell labels	$D5$	$S1$	$D3$	$D5$	$S1$	$D3$	$D5$	$S1$	$D3$	$D5$	$S1$	$D3$
Configuration	9	4	8	11	4	6	11	4	6	12	3	6
2(S-shell J's)	5	0	0	5	0	0	5	0	4	0	1	4
2(coupled J's)		5	5		5	5		5	5		1	5
2(S-shell T's)	3	0	0	1	0	2	1	0	2	0	1	2
2(coupled T's)		3	3		1	3		1	3		1	3
S-S seniorities	1	0	0	1	0	0	1	0	2	0	1	2

Listed components account for 95.8 per cent of the wave function.
Occupation $(D5)=11.02$, $(S1)=3.88$, $(D3)=6.10$.

TABLE XI *(Continued)*

$A=37$, $2J^{\pi}=7^+$, $2T=3$, $E=255.120$, eigenvector 1 of this A, J, T. Model core = 16, dimension = 6.

Amplitude		−0.206			−0.972	
S-shell labels	$D5$	$S1$	$D3$	$D5$	$S1$	$D3$
Configuration	10	4	7	11	4	6
2(S-shell J's)	8	0	3	5	0	4
2(coupled J's)		8	7		5	7
2(S-shell T's)	2	0	1	1	0	2
2(coupled T's)		2	3		1	3
S-S seniorities	2	0	1	1	0	2

Listed components account for 98.7 per cent of the wave function.
Occupation $(D5)=10.95$, $(S1)=3.99$, $(D3)=6.06$.

near and above 5 MeV have been assigned positive parity and J of 1 or 2 on the basis of stripping measurements. Aside from states which obviously have $T=1$, the experimental spectrum[34] of ^{36}Ar has at least 11 such positive-parity levels below 8.5 MeV, while only four such theoretical states tend to occur in approximately the same energy span. Thus, it appears that intruder states from the fp shell are present from perhaps ≈5-MeV excitation on up. In addition, fp excitation may be a factor in depressing the observed excitation energies of the second 0^+ and 2^+ levels.

For the $A=36$, $T=0$ system, experimental information about the nuclear wave functions is available from spectroscopic factors for the ^{35}Cl (^{3}He, d)^{36}Ar reaction,[34] and from lifetimes of the lowest four excited states. Table XII shows fair-to-good agreement between the measured and shell-model spectroscopic factors. A comparison of experimental and shell-model S factors suggests that the second observed 2^+ in ^{36}Ar, *unlike* the second observed 2^+ in ^{38}Ar, should be correlated directly to the second sd-shell-model 2^+ state. (Recall that in ^{38}Ar, the strength of the second sd-shell-model 2^+ seemed to be shared among several observed 2^+ states. This fragmentation occurs, presumably, because of the importance of fp orbits in low-lying ^{38}Ar states.) For most of the other ^{36}Ar states in Table XII, the spectroscopic factors are so small that experimental-theoretical comparisons do not provide significant tests of the model wave functions.

For the first-to-ground state $2^+ \to 0^+$ transition in ^{36}Ar, the published[35] experimental $B(E2)$ value is 59 e^2 F^4, in excellent agreement with the shell-model values 58 and 59 e^2 F^4 calculated from 12.5p + ^{17}O and 11.0h + ASPE. For transitions connecting some other ^{36}Ar states, there are experimental data giving *relative* $B(E2)$ values.[43] These measured relative values, and some shell-model results, are listed in Table XIV. (All the numbers are normalized so that the first-to-ground $2^+ \to 0^+$ transitions have unit strength.) The experimental-theoretical agreement in Table XIV is generally satisfactory; and this agreement suggests that the second model 0^+ and 2^+ states are reasonably good representations of the observed states, even though these two model states tend to appear higher than their observed counterparts.

6. $A=36$, $T=1$: ^{36}Cl
(See Tables XV–XVII, and Fig. 6)

This is the second odd-odd system we have considered in this paper. Such nuclei generally have a high density of states in the region of low excitation energy. When there are states of the same spin at nearly the same energy, then there is usually considerable sensitivity of the model wave functions to changes in the Hamiltonians. This instability hinders us when we try to find correspondences between theoretical and experimental levels, above the first few. In the particular case of ^{36}Cl there is another difficulty: the lack of firm experimental spin assignments beyond the second excited state.

The observed ground state of ^{36}Cl is assigned 2^+, and all our Hamiltonians give this result. The calculated values of the quadrupole moment of this state are small and negative, in qualitative agreement with the measured value (see Table XXVII). The calculated values of the magnetic moment are in fair agreement with experiment. The spectroscopic factor for stripping from a ^{35}Cl target to the two lowest $T=1$ states in ^{36}Ar has been experimentally[34] determined simultaneously with the S factors presented in Table XII for the $T=0$ states of $A=36$. (Thus, for the stripping S factors from Ref. 34, the same normalization of Table XII is carried over to Table XVI.[44,45]) The experimental result for the ground-state stripping S factor is in good agreement with our sd shell-model results. A measured pickup spectroscopic factor to the 2^+ ground state, from the ground state of ^{37}Cl, is also available.[46] It, too, is in good agreement with the model results. The 12.5p + ^{17}O model wave func-

TABLE XII. Energies E and spectroscopic factors S for states of $A=36$, $T=0$. The initial state for the stripping factors S_{st} is the $J^\pi=\frac{3}{2}^+$, $T=\frac{1}{2}$ ground state of ^{35}Cl. For the meaning of E, and the meanings of the numerical subscripts on S, see Table IV.

		Energy E (MeV)				$100\times(S_0;\ S_2)_{st}$				
		11.0h	12.5p				11.0h	12.5p		
A, J, T	Expt.	+ASPE	$+^{17}$O	12.5pA	MSDI	Expt.[a]	+ASPE	$+^{17}$O	12.5pA	MSDI
36, 0, 0	231.57	229.13	254.15	231.66	231.19	;473	;430,	;433,	;392,	;397,
	(4.33)	5.58	6.11	5.26	5.94	; 6	; 2,	; 0,	; 0,	; 0,
		11.11	11.04	9.88	8.42		; 0,	; 1,	; 0,	; 0,
		11.62	12.08	12.41	11.52		; 0,	; 0,	; 0,	; 0,
36, 1, 0		7.71	7.80	7.07	5.94		7; 5,0	5; 5,0	4; 6,0	4; 7,0
		9.27	8.62	8.89	7.90		1; 2,1	1; 2,1	2; 3,0	0; 0,0
36, 2, 0	1.97	2.05	1.87	1.78	1.81	;163	0;105,5	0;100,5	0;130,7	0;169,2
	4.44	5.39	5.31	4.63	4.47	8; 72	13; 45,1	10; 39,1	10; 38,1	10; 36,1
	(4.96)	8.69	8.63	7.68	6.32	1; 1	3; 2,4	1; 8,8	1; 3,3	0; 2,0
		9.23	9.20	8.80	8.58		0; 4,2	0; 0,0	0; 3,1	0; 0,0
36, 3, 0		8.99	8.69	8.13	7.43		; 2,4	; 0,8	; 3,2	; 2,0
		10.50	10.27	9.53	8.69		; 1,1	; 4,0	; 0,3	; 0,0
		10.85	10.77	10.74	10.78		; 2,0	; 0,0	; 0,1	; 0,1
		12.43	12.21	11.80	11.32		; 0,0	; 0,0	; 0,0	; 0,0
36, 4, 0	4.41	4.57	3.74	4.37	5.06	; 3	; ,5	; ,6	; ,2	; ,0
		8.07	7.55	6.99	7.35		; ,0	; ,0	; ,0	; ,0
		10.17	9.73	8.78	9.33		; ,0	; ,0	; ,0	; ,0
		12.01	12.01	10.87	10.46		; ,0	; ,0	; ,0	; ,0
36, 5, 0		11.96	10.02	10.27	12.32					
36, 6, 0		10.64	8.79	9.07	11.36					
36, 7, 0		20.81	18.44	18.86	20.38					
36, 8, 0		16.62	13.63	14.36	18.50					

[a] Reference 34.

TABLE XIII. Major components of the wave functions of states of $A=36$, $T=0$ as calculated with the 12.5p+^{17}O Hamiltonian. The conventions of the presentation are explained in Sec. III B of the text.

$A=36$, $2J^{\pi}=0^{+}$, $2T=0$, $E=254.141$, eigenvector 1 of this A, J, T. Model core=16, dimension=21.

Amplitude	0.178			−0.481			−0.177			−0.214			0.207			−0.244			0.221			−0.251			0.152			0.591		
S-shell labels	$D5$	$S1$	$D3$	$D5$	$S1$	$D3$	$D5$	$S1$	$D3$	$D5$	$S1$	$D3$	$D5$	$S1$	$D3$	$D5$	$S1$	$D3$	$D5$	$S1$	$D3$	$D5$	$S1$	$D3$	$D5$	$S1$	$D3$	$D5$	$S1$	$D3$
Configuration	9	4	7	10	4	6	10	4	6	10	4	6	11	2	7	11	3	6	11	4	5	12	2	6	12	3	5	12	4	4
2(S-shell J's)	3	0	3	0	0	0	2	0	2	4	0	4	5	2	3	5	1	4	5	0	5	0	0	0	0	1	1	0	0	0
2(coupled J's)		3	0		0	0		2	0		4	0		3	0		4	0		5	0		0	0		1	0		0	0
2(S-shell T's)	1	0	1	2	0	2	0	0	0	2	0	2	1	0	1	1	1	2	1	0	1	0	2	2	0	1	1	0	0	0
2(coupled T's)		1	0		2	0		0	0		2	0		1	0		2	0		1	0		2	0		1	0		0	0
S-S seniorities	3	0	1	0	0	0	2	0	2	2	0	2	1	2	1	1	1	2	1	0	3	0	0	0	0	1	3	0	0	0

Listed components account for 92.6 per cent of the wave function.
Occupation $\langle D5\rangle=10.98$, $\langle S1\rangle=3.61$, $\langle D3\rangle=5.41$.

$A=36$, $2J^{\pi}=0^{+}$, $2T=0$, $E=248.030$, eigenvector 2 of this A, J, T. Model core=16, dimension=21.

Amplitude	0.202			0.163			−0.379			0.333			0.243			−0.200			0.432			−0.241			0.509		
S-shell labels	$D5$	$S1$	$D3$	$D5$	$S1$	$D3$	$D5$	$S1$	$D3$	$D5$	$S1$	$D3$	$D5$	$S1$	$D3$	$D5$	$S1$	$D3$	$D5$	$S1$	$D3$	$D5$	$S1$	$D3$	$D5$	$S1$	$D3$
Configuration	10	2	8	10	3	7	11	2	7	11	3	6	11	4	5	12	0	8	12	2	6	12	2	5	12	4	4
2(S-shell J's)	0	0	0	4	1	3	5	2	3	5	1	4	5	0	5	0	0	0	0	0	0	0	1	1	0	0	0
2(coupled J's)		0	0		3	0		3	0		4	0		5	0		0	0		0	0		1	0		0	0
2(S-shell T's)	2	2	0	2	1	1	1	0	1	1	1	2	1	0	1	0	0	0	0	2	2	0	1	1	0	0	0
2(coupled T's)		0	0		1	0		1	0		2	0		1	0		0	0		2	0		1	0		0	0
S-S seniorities	0	0	0	2	1	1	1	2	1	1	1	2	1	0	3	0	0	0	0	0	0	0	1	3	0	0	0

Listed components account for 92.5 per cent of the wave function.
Occupation $\langle D5\rangle=11.44$, $\langle S1\rangle=2.81$, $\langle D3\rangle=5.75$.

$A=36$, $2J^{\pi}=4^{+}$, $2T=0$, $E=252.271$, eigenvector 1 of this A, J, T. Model core=16, dimension=56.

Amplitude	−0.193			−0.281			−0.228			−0.301			−0.181			0.208			−0.252			−0.157			−0.369			−0.459		
S-shell labels	$D5$	$S1$	$D3$	$D5$	$S1$	$D3$	$D5$	$S1$	$D3$	$D5$	$S1$	$D3$	$D5$	$S1$	$D3$	$D5$	$S1$	$D3$	$D5$	$S1$	$D3$	$D5$	$S1$	$D3$	$D5$	$S1$	$D3$	$D5$	$S1$	$D3$
Configuration	10	3	7	10	4	6	10	4	6	11	3	6	11	3	6	11	4	5	11	4	5	12	2	6	12	3	5	12	4	4
2(S-shell J's)	0	1	3	0	0	4	4	0	0	5	1	0	5	1	4	5	0	1	5	0	3	0	0	4	0	1	3	0	0	4
2(coupled J's)		1	4		0	4		4	4		4	4		4	4		5	4		5	4		0	4		1	4		0	4
2(S-shell T's)	2	1	1	2	0	2	2	0	2	1	1	2	1	1	2	1	0	1	1	0	1	0	2	2	0	1	1	0	0	0
2(coupled T's)		1	0		2	0		2	0		2	0		2	0		1	0		1	0		2	0		1	0		0	0
S-S seniorities	0	1	1	0	0	2	2	0	0	1	1	0	1	1	2	1	0	3	1	0	1	0	0	2	0	1	1	0	0	2

Listed components account for 77.0 per cent of the wave function.
Occupation $\langle D5\rangle=11.06$, $\langle S1\rangle=3.42$, $\langle D3\rangle=5.53$.

TABLE XIII (*Continued*)

$A=36$, $2J^{\pi}=8^{+}$, $2T=0$, $E=250.404$, eigenvector 1 of this A, J, T. Model core=16, dimension=44.

Amplitude	0.269			0.174			−0.200			0.166			−0.166			−0.630			0.184			−0.216			−0.207			−0.282			0.226		
S-shell labels	$D5$	S1	$D3$	$D5$	S1	$D3$	$D5$	S1	$D3$	$D5$	S1	$D3$	$D5$	S1	$D3$	$D5$	S1	$D3$	$D5$	S1	$D3$	$D5$	S1	$D3$	$D5$	S1	$D3$	$D5$	S1	$D3$	$D5$	S1	$D3$
Configuration	9	4	7	10	4	6	10	4	6	11	2	7	11	3	6	11	4	5	11	4	5	11	4	5	12	2	6	12	3	5	12	4	4
2(S-shell J's)	5	0	3	2	0	6	8	0	0	5	0	3	5	1	4	5	0	3	5	0	5	5	0	7	0	2	6	0	1	7	0	0	8
2(coupled J's)		5	8		2	8		8	8		5	8		4	8		5	8		5	8		5	8		2	8		1	8		0	8
2(S-shell T's)	1	0	1	0	0	0	2	0	2	1	2	1	1	1	2	1	0	1	1	0	1	1	0	1	0	0	0	0	1	1	0	0	0
2(coupled T's)		1	0		0	0		2	0		1	0		2	0		1	0		1	0		1	0		0	0		1	0		0	0
S-S seniorities	1	0	1	2	0	2	2	0	0	1	0	1	1	1	2	1	0	1	1	0	3	1	0	2	0	2	2	0	1	3	0	0	4

Listed components account for 84.8 per cent of the wave function.
Occupation $(D5)=10.83$, $(S1)=3.64$, $(D3)=5.52$.

tion for the $A=36$, $T=1$ ground state is dominated (70%) by the configuration $(d_{5/2})^{12}(s_{1/2})^{4}(d_{3/2})^{4}$.

The first excited state observed in ^{36}Cl (at 0.78 MeV) is assigned $(3)^{+}$. It is observed to have an $l=2$ stripping spectroscopic factor about $\frac{1}{3}$ of that to the 2^{+} ground state, and an $l=2$ pickup spectroscopic factor about 1.5 times that to the ground state. All of our models place a 3^{+} state near 0.9 MeV. For this state, the calculated spectroscopic factors (which are quite insensitive to the choice among our Hamiltonians) are in excellent agreement with experimentally determined S values for the 0.78-MeV observed $(3)^{+}$ state. The model wave function for this lowest 3^{+} state is also quite simple. The dominant configuration, $(d_{5/2})^{12}(s_{1/2})^{4}(d_{3/2})^{4}$, is the same as for the ground state and here it accounts for 75% of the total intensity.

The second excited state in the experimental spectrum is assigned $(1)^{+}$; it comes at 1.16 MeV and is appreciably excited by $l=2$ pickup. In our model spectra a 1^{+} state appears near 1 MeV, and it has S factors consistent with the experimental value for the observed 1.16-MeV $(1)^{+}$ state.

Beyond the second excited state, the calculated spectroscopic factors are sensitive to the choice among our Hamiltonians. The model spectra suggest that the next two levels in the experimental spectrum are 2^{+} and 1^{+}, for such states are calculated to lie near 1.7 and 2.0 MeV. Between 2- and 3-MeV excitation, other model states are predicted with J^{π} of 0^{+}, 1^{+}, 2^{+}, and 3^{+}.

Obviously, further experimental work on this $A=36$, $T=1$ system would be welcome. In particular, it would be good to measure the $E2$ widths between low-lying levels. Although we have not listed any MSDI or 12.5pA results in Table XV, we did calculate $B(E2)$ values for these Hamiltonians as well as for 12.5p + ^{17}O and 11.0h + ASPE. Of the various transitions listed in Table XV, only the $1^{+}\rightarrow 3^{+}$ transitions have strengths which are noticeably sensitive to the differences among our various Hamiltonians. The MSDI wave functions yield a particularly strong $B(E2)$ from the first 1^{+} to the first 3^{+}, and a particularly weak decay from the second 1^{+} to the first 3^{+}.

7. $A=36$, $T=2$: ^{36}S
(See Tables XVIII, XIX, and Fig. 6)

The levels of ^{36}S have been studied experimentally only with the ^{34}S$(t,p)^{36}$S double-nucleon stripping reaction[47] and the ^{37}Cl$(d,{}^{3}\mathrm{He})^{36}$S single-nucleon pickup reaction.[48,49] The pickup reaction excites the 0^{+} ground state of ^{36}S by $l=2$ transfer; and it excites the 3.30-, 4.52-, and 4.58-MeV states by $l=0$ transfer, the first two more strongly than the last. There is no other significant pick-

up strength observed below 6 MeV. Our *sd*-shell models match experiment by showing strong $l=2$ pickup exciting the 0^+ ground state; then they show strong $l=0$ transfer to the first 2^+ state and the first 1^+ state, both lying in the excitation-energy region 3.1 to 4.4 MeV. There is very little other pickup strength calculated below 6 MeV. For $l=2$ transfer to the 0^+ ground state, the experimental and theoretical S factors are in excellent agreement. As to the low-lying $l=0$ states: In our models the 2^+ level always comes below the 1^+ level. Therefore we speculate that the observed 2^+ state at 3.30 MeV corresponds to the lowest model 2^+, while the observed $(1, 2)^+$ state at 4.52 MeV corresponds to the lowest model 1^+.

The total number of observed levels below 5-MeV excitation in ^{36}S is eight. Our calculations can account for only four of these states: the ground state 0^+, the 2^+ and $(1)^+$ levels excited strongly with $l=0$ pickup, and the 0^+ level seen at 3.36 MeV. The third level seen with $l=0$ (weakly), and the 0^+ and 2^+ excited states seen in (t, p) at 2.00 and 2.89 MeV seem to be "intruders," and so does the unassigned level at 4.20 MeV. The observation of $l=0$ strength in the 4.58-MeV level presumably indicates mixing between an *sd*-shell level and an intruder level of the sort discussed in the case of ^{38}Ar.

8. $A=35$, $T=\frac{1}{2}$: ^{35}Cl-^{35}Ar
(See Tables XX–XXII, and Fig. 7)

We examine the $A=35$, $T=\frac{1}{2}$ system in greater detail than any other. Our reasons are: (1) that the experimental picture for this system is the clearest[11, 20, 50–56]; (2) that we think the model approximations should be better, the further removed we are from the $N=Z=20$ shell closure; and (3) that the calculations for $A=35$ are not as time consuming as for $A=34$.

We find good theoretical partners for the lowest 10 observed levels in ^{35}Cl which have established or, probable, even parity. Figure 7 shows the experimentally observed spectrum up to 5.5 MeV, together with the shell-model spectra calculated from four Hamiltonians. We shall consider the ^{35}Cl-^{35}Ar positive-parity states in three groups. *First*, we consider a four-member group comprising the lowest $\frac{3}{2}^+$, $\frac{5}{2}^+$, $\frac{7}{2}^+$, and $\frac{9}{2}^+$ states. For this group, three of the models in Fig. 7 fit the experimentally observed spacings very well, while the fourth model (MSDI) fails only for $\frac{9}{2}^+$. *Next*, we consider a three-member group comprising the lowest $\frac{1}{2}^+$, second $\frac{3}{2}^+$, and second $\frac{5}{2}^+$ states. In the experimentally observed spectrum we take, as members of this group, the $\frac{1}{2}^+$, $\frac{3}{2}^+$, and $\frac{5}{2}^+$ states seen at 1.22, 2.69, and 3.00 MeV, respectively. For these three observed states, all the models of Fig. 7 show obvious theoretical partners, though in most of these models the lowest $\frac{1}{2}^+$ and second $\frac{3}{2}^+$ lie lower in the excitation-energy spectrum than their observed partners. *Finally*, in the observed spectrum below 6.7 MeV there are just three other states having established even parity: the $\frac{1}{2}^+$ state at 3.96 MeV, and states at 5.57 and 6.01 MeV which are both strongly populated via $l=2$ transfer in the pickup reaction ^{36}Ar$(p, d)^{35}$Ar. The 3.96-MeV $\frac{1}{2}^+$ state is easily correlated with our second model $\frac{1}{2}^+$ state (see Fig. 7). To find model partners for the strong $l=2$ states at 5.57 and 6.01 MeV, we examine our calculated spectroscopic factors (see Table XX). We see that our third and fourth model $\frac{5}{2}^+$ states make obvious partners for the observed 5.57- and 6.01-MeV states. This completes our list of 10 "firm" correlations. Of these 10 correlations, 8 involve states for which we can make quantitative comparisons between shell-model and experimentally determined S factors, and Table XX shows that in general there is fair-to-good agreement between theory and experiment.

Between 4 and 6 MeV in the spectrum of ^{35}Cl there have been observed[11, 55, 56] more levels which have possible positive parity than can be accounted for in our model calculations. More experimental work in this area is needed to determine at what energy and to what extent our approach seriously breaks down.

In the rest of this $A=35$, $T=\frac{1}{2}$ subsection, we present a detailed level-by-level discussion covering electromagnetic observables as well as spectroscopic factors. Again we find it convenient to begin with the sequence of lowest $\frac{3}{2}^+$, $\frac{5}{2}^+$, $\frac{7}{2}^+$, and $\frac{9}{2}^+$ states.

From both 12.5 + ^{17}O and 11.0 + ASPE, the quadrupole moment of the $\frac{3}{2}^+$ ground state of ^{35}Cl is calculated to be about $-9\ e\ \mathrm{F}^2$ (see Table XXVII). The measured value is close to $-8\ e\ \mathrm{F}^2$. Our calculated values for the ground-state magnetic dipole moment tend to be about $+0.7\mu_N$, a little smaller than the measured value $+0.82\mu_N$. Next we consider ground-state spectroscopic factors (see Table XX). These depend not only on the ground-state wave function of ^{35}Ar, but also on the ground-state wave functions of ^{36}Ar (for pickup) and ^{34}S (for stripping). For pickup, all our calculations yield spectroscopic factors close to 4. Now in the simplest shell-model approximation, the ^{36}Ar and ^{35}Ar-^{35}Cl ground states would contain four and three $d_{3/2}$ particles, respectively, and the pickup factor $S(d_{3/2})$ would be exactly 4. More generally, the *total* of pickup factors $S(d_{3/2})$, *summed* over all final $A=35$, $T=\frac{1}{2}$ states, gives the number of $d_{3/2}$ nucleons in the ^{36}Ar ground state. Note now that for every model in Table XX, the sum of tabulated pickup

TABLE XIV. Relative $B(E2)$ values for transitions between $T=0$ states in ^{36}Ar. The notation J_ν labels the νth-lowest state of spin J in ^{36}Ar.

Initial state J_ν	Final state J_ν	Expt.[a]	11.0h+ASPE	12.5p+^{17}O	MSDI
2_1	0_1	1.00	1.00	1.00	1.00
2_2	0_1	0.035	0.008	0.00	0.023
0_2	2_1	0.33	0.46	0.46	0.35
2_2	2_1	0.44	0.29	0.34	0.54
4_1	2_1	1.29	1.21	1.17	1.06

[a] Reference 43.

factors $S(d_{3/2})$ exceeds 4. This is a consequence of the fact that the ^{36}Ar ground state does not have the pure $(d_{5/2})^{12}(s_{1/2})^4(d_{3/2})^4$ wave function that it would have in the simplest sd-shell approximation. Similarly, for stripping from ^{34}S, the total of $S(d_{5/2})$ and $S(s_{1/2})$ factors, summed over all final $A=35$ states, gives the number of $d_{5/2}$ and $s_{1/2}$ holes in the ^{34}S ground state. Thus, the appearance of nonvanishing $d_{5/2}$ and $s_{1/2}$ stripping factors in Table XX indicates that the ground state of ^{34}S does not have the pure $(d_{5/2})^{12}(s_{1/2})^4(d_{3/2})^2$ wave function that it would have in the simplest sd-shell approximation. Turning now to the $\frac{3}{2}^+$ ground state of ^{35}Ar-^{35}Cl itself: Table XXI shows that according to our 12.5p+^{17}O model, its wave function is quite far from what it would be in the simplest sd-shell approximation. The component of highest intensity (35%) is $(d_{5/2})^{12}(s_{1/2})^4(d_{3/2})^3$, the component of next highest intensity (16%) is $(d_{5/2})^{10}{}_{J=0}(s_{1/2})^4(d_{3/2})^5$, and the remaining 50% of intensity is spread over components each having an intensity $\leq 5\%$.

Next we consider the second member of the sequence comprising the lowest $\frac{3}{2}^+$, $\frac{5}{2}^+$, $\frac{7}{2}^+$, and $\frac{9}{2}^+$ states. Component intensities in the lowest $\frac{5}{2}^+$ state are shown in Table XXI. These intensities, when compared with intensities for the $\frac{3}{2}^+$ ground state, show that the lowest $\frac{3}{2}^+$ and $\frac{5}{2}^+$ states both have essentially the same $d_{5/2}$ structure but differ in their $s_{1/2}$-$d_{3/2}$ parts. Recall now that for single-nucleon pickup from ^{36}Ar, and for single-nucleon stripping on ^{34}S, there are large $S(d_{3/2})$ factors to the ground state of ^{35}Cl. These large $S(d_{3/2})$ factors indicate that in the ^{34}S, ^{35}Cl-^{35}Ar, and ^{36}Ar ground states, the $d_{5/2}$-$s_{1/2}$ structures are all similar. It follows, then, that we should expect only *weak* $S(d_{5/2})$ transfer strength to a $\frac{5}{2}^+$ state in Ar having the same $d_{5/2}$ structure as the $\frac{3}{2}^+$ ground state. An indeed, the S factors for this $\frac{5}{2}^+$ state are very small, both experimentally and from our models (see Table XX). When we turn to $B(E2)$'s (see Table XXII[57,58]), we find yet another indication of strong kinship between the lowest $\frac{3}{2}^+$ and $\frac{5}{2}^+$

TABLE XV. Calculated $B(E2)$ and $B(M1)$ values for transitions between states of $A=36$. The notation J_ν labels the νth-lowest state of spin J in a model spectrum.

Initial state J_ν	Final state J_ν	$B(E2)$ (e^2 F^4) 12.5p+^{17}O	$B(E2)$ (e^2 F^4) 11.0h+ASPE	$100\times B(M1)$ (μ_N^2) 12.5p+^{17}O	$100\times B(M1)$ (μ_N^2) 11.0h+ASPE
		Ar, $T=0$			
2_1	0_1	58.	59.	0	0
2_2	0_1	0.000	0.005	0	0
2_3	0_1	0.45	0.79	0	0
0_2	2_1	27.	27.	0	0
1_1	2_1	0.09	0.18	0.3	0.4
2_2	2_1	20.	17.	0.02	0.05
2_3	2_1	0.87	0.14	0.2	0.09
3_1	2_1	0.09	0.15	0.1	0.9
4_1	2_1	68.	71.	0	0
		^{36}Cl, $T=1$			
3_1	2_1	33.	37.	5.5	5.7
1_1	2_1	53.	47.	0.3	0.004
1_2	2_1	4.	9.	0.02	0.3
2_2	2_1	25.	23.	22.	20.
3_2	2_1	1.0	0.05	51.	30.
4_1	2_1	10.	14.	0	0
1_1	3_1	0.8	0.05	0	0
1_2	3_1	17.	19.	0	0
2_2	3_1	13.	0.03	1.4	2.4
3_2	3_1	2.4	6.9	27.	18.
4_1	3_1	18.	28.		14.

TABLE XVI. Energies E and spectroscopic factors S for states of $A=36$, $T=1$. The initial state for the stripping factors S_{st} is the $J^\pi=\frac{3}{2}^+$, $T=\frac{1}{2}$ ground state of ^{35}Cl. The initial state for the pickup factors S_{pk} is the $J^\pi=\frac{3}{2}^+$, $T=\frac{3}{2}$ ground state of ^{37}Cl. For the meaning of E, and the meanings of the numerical subscripts on S, see Table IV.

		Energy E (MeV)					$100\times(S_0; S_2)$	$100\times(S_{1/2}; S_{3/2}, S_{5/2})_{calc}$			
A, J, T	Expt.	11.0h +ASPE	12.5p $+^{17}$O	12.5pA	MSDI		Expt.	11.0h +ASPE	12.5p $+^{17}$O	12.5pA	MSDI
36, 0, 1	3.12 [a]	2.53	2.97	2.74	3.34	st		; 2,	; 1,	; 0,	; 0,
						pk		; 0,	; 0,	; 0,	; 0,
		7.31	6.71	6.56	5.78	st		; 0,	; 0,	; 0,	; 0,
						pk		; 0,	; 0,	; 1,	; 1,
36, 1, 1	(1.16)	0.84	1.15	1.17	0.82	st		7; 13, 1	6; 17, 2	6; 2, 1	6; 27, 0
						pk	; 37 [b]	3; 23, 3	5; 39, 5	6; 47, 3	7; 61, 0
		1.84	2.18	1.94	2.09	st		3; 7, 1	1; 3, 1	0; 2, 0	0; 0, 0
						pk		13; 14, 0	5; 4, 0	3; 9, 0	1; 0, 0
		2.50	2.69	3.15	3.18	st		0; 4, 0	0; 2, 0	1; 0, 0	2; 0, 0
						pk		0; 12, 2	1; 1, 2	6; 0, 0	21; 11, 0
		3.74	4.05	3.60	3.75	st		2; 0, 0	1; 0, 0	2; 0, 0	1; 0, 0
						pk		23; 12, 1	25; 4, 1	31; 13, 0	24; 1, 0
36, 2, 1	224.96	221.63	246.62	224.95	225.16	st	; 76 [c]-76 [d]	1; 67, 0	0; 60, 1	1; 72, 0	0; 88, 0
						pk	; 110 [b]	0; 109, 2	0; 104, 4	0; 112, 0	0; 116, 0
		1.59	1.71	1.61	1.80	st		2; 0, 1	7; 1, 8	1; 0, 1	2; 1, 0
						pk		6; 0, 5	28; 2, 34	2; 0, 1	5; 1, 0
		2.18	2.26	2.80	3.01	st		7; 0, 5	0; 0, 1	7; 0, 5	6; 0, 1
						pk		42; 0, 16	5; 1, 1	60; 0, 15	81; 1, 2
		3.96	4.10	4.49	5.01	st		; 0, 0	0; 0, 0	0; 0, 0	0; 0, 0
						pk		0; 0, 0	0; 0, 0	1; 0, 0	5; 0, 0
36, 3, 1	(0.78)	0.98	0.83	0.89	1.07	st	; 32 [c]-23 [d]	; 18, 2	; 17, 3	; 19, 1	; 22, 0
						pk	; 162 [b]	; 155, 2	; 149, 3	; 159, 0	; 166, 0
		2.71	2.18	3.59	4.06	st		; 0, 8	; 0, 12	; 0, 4	; 0, 0
						pk		; 1, 49	; 4, 77	; 0, 30	; 5, 1
		4.09	4.32	3.94	4.48	st		; 0, 0	; 0, 0	; 0, 1	; 0, 0
						pk		; 1, 2	; 0, 0	; 0, 4	; 0, 0
		4.86	4.83	4.84	5.87	st		; 1, 1	; 1, 0	; 0, 3	; 0, 1
						pk		; 8, 13	; 3, 19	; 6, 38	; 1, 19

TABLE XVI (*Continued*)

A, J, T	Energy E (MeV) Expt.	11.0h +ASPE	12.5p +^{17}O	12.5pA	MSDI	$100\times(S_0;S_2)$	Expt.	11.0h +ASPE	$100\times(S_{1/2};\ S_{3/2};\ S_{5/2})_{\rm calc}$ 12.5p +^{17}O	12.5pA	MSDI
36, 4, 1		3.52	3.45	3.39	3.89	st		; , 0	; , 1	; , 0	; , 0
						pk		; , 2	; , 6	; , 1	; , 0
		5.58	4.58	4.90	6.44	st		; , 0	; , 0	; , 0	; , 0
						pk		; , 1	; , 16	; , 0	; , 1
		6.88	5.49	6.47	8.14	st		; , 2	; , 2	; , 2	; , 1
						pk		; , 124	; , 116	; , 137	; , 151
36, 5, 1		7.43	5.83	6.44	8.76						
		8.50	7.20	7.90	9.23						
36, 6, 1		7.03	5.43	6.23	8.53						
		9.77	8.90	8.96	11.22						
36, 7, 1		13.94	11.23	12.76	15.63						

[a] Reference 45.
[b] Reference 46.
[c] Reference 34.
[d] Reference 44. We have normalized these results so as to match the ground-state S factor from Ref. 34.

states, viz., the $E2$ transition between these states is very strong. The measured $B(E2)$ is 78 e^2 F^4. The values calculated from 12.5p + ^{17}O, 11.0 + ASPE, and 12.5pA are all similar and average to 73 e^2 F^4, while the MSDI result is 30% smaller. The $B(M1)$ for the first-to-ground $\frac{5}{2}^+ \rightarrow \frac{3}{2}^+$ transition is measured to be smaller, by a factor of 100, than the $B(M1)$ from lowest $\frac{1}{2}^+$ to ground. Our shell-model $B(M1)$ values for the first-to-ground state $\frac{5}{2}^+ \rightarrow \frac{3}{2}^+$ transition vary widely, but they are all very small and so at least qualitatively in agreement with the observed result.

Next we consider information about the lowest $\frac{7}{2}^+$ and $\frac{9}{2}^+$ states in ^{35}Cl. For transitions connecting the lowest model $\frac{7}{2}^+$ state to the $\frac{3}{2}^+$ ground state, and connecting this lowest $\frac{7}{2}^+$ state to the lowest $\frac{5}{2}^+$ state, there is consistency between our shell-model $B(E2)$ results and the experimental information on the 2.64-MeV $\frac{7}{2}^+$ level of ^{35}Cl. Also, for $E2$ and $M1$ transitions from the lowest $\frac{9}{2}^+$ state to the lowest $\frac{7}{2}^+$ state, and from this same $\frac{9}{2}^+$ state to the lowest $\frac{5}{2}^+$ state, there is recognizable agreement between shell-model and measured strengths.

Thus far in our detailed discussion of the $A = 35$, $T = \frac{1}{2}$ system, we have covered observables involving only the four-member sequence comprising the lowest $\frac{3}{2}^+$, $\frac{5}{2}^+$, $\frac{7}{2}^+$, and $\frac{9}{2}^+$ states. We turn now to a level-by-level discussion of the sequence comprising the lowest $\frac{1}{2}^+$, second $\frac{3}{2}^+$, and second $\frac{5}{2}^+$ states. As our discussion will indicate, we find that observables involving states in this second mentioned sequence are more sensitive to the choice among our Hamiltonians than are observables involving only states in the first mentioned sequence.

For the lowest $\frac{1}{2}^+$ state, our shell-model spectroscopic factors for pickup from ^{36}Ar vary between 2 and 3. However, each of these shell-model answers is in satisfactory agreement with at least one of the several different reported experimental results. The shell-model stripping S factors vary too, but all agree at least qualitatively with the experimentally observed results. In the wave function of the $\frac{1}{2}^+$ state, the component of highest intensity (30%) is $(d_{5/2})^{12}(s_{1/2})^3(d_{3/2})^4{}_{J=0,\,T=0}$. Every other component has intensity smaller than 9%. The $B(E2)$ connecting this first $\frac{1}{2}^+$ state to the $\frac{3}{2}^+$ ground state has been measured,[57] via Coulomb excitation, to be 16 e^2 F^4. Our shell-model values for this $B(E2)$ range between 10 and 20 e^2 F^4. For the $M1$ transition from this first $\frac{1}{2}^+$ state to the $\frac{3}{2}^+$ ground state, the measured $B(M1)$ value[57] is $0.195\mu_N{}^2$. Most values for this $B(M1)$ as calculated in our different shell models are in satisfactory agreement with this value; only the MSDI result misses significantly.

TABLE XVII. Major components of the wave functions of the states of $A=36$, $T=1$ as calculated with the 12.5p + ^{17}O Hamiltonian. The conventions of the presentation are explained in Sec. III B of the text.

$A=36$, $2J^{\pi}=2^{+}$, $2T=2$, $E=245.473$, eigenvector 1 of this A, J, T. Model core = 16, dimension = 54.

Amplitude	−0.232			−0.175			−0.291			0.415			0.274			−0.654		
S-shell labels	$D5$	$S1$	$D3$	$D5$	$S1$	$D3$	$D5$	$S1$	$D3$	$D5$	$S1$	$D3$	$D5$	$S1$	$D3$	$D5$	$S1$	$D3$
Configuration	11	3	6	11	3	6	11	4	5	12	3	5	12	3	5	12	4	4
2(S-shell J's)	5	1	4	5	1	6	5	0	3	0	1	3	0	1	3	0	0	2
2(coupled J's)		4	2		4	2		5	2		1	2		1	2		0	2
2(S-shell T's)	1	1	2	1	1	0	1	0	3	0	1	1	0	1	3	0	0	2
2(coupled T's)		2	2		2	2		1	2		1	2		1	2		0	2
S-S seniorities	1	1	2	1	1	2	1	0	1	0	1	1	0	1	1	0	0	2

Listed components account for 84.5 per cent of the wave function.
Occupation $(D5)=11.59$, $(S1)=3.56$, $(D3)=4.85$.

$A=36$, $2J^{\pi}=2^{+}$, $2T=2$, $E=244.446$, eigenvector 2 of this A, J, T. Model core = 16, dimension = 54.

Amplitude	−0.158			−0.621			0.277			−0.428			0.273			−0.214		
S-shell labels	$D5$	$S1$	$D3$	$D5$	$S1$	$D3$	$D5$	$S1$	$D3$	$D5$	$S1$	$D3$	$D5$	$S1$	$D3$	$D5$	$S1$	$D3$
Configuration	11	3	6	11	4	5	12	2	6	12	3	5	12	3	5	12	4	4
2(S-shell J's)	5	1	4	5	0	3	0	2	0	0	1	3	0	1	3	0	0	2
2(coupled J's)		6	2		5	2		2	2		1	2		1	2		0	2
2(S-shell T's)	1	1	2	1	0	1	0	0	2	0	1	1	0	1	3	0	0	2
2(coupled T's)		0	2		1	2		0	2		1	2		1	2		0	2
S-S seniorities	1	1	2	1	0	1	0	2	0	0	1	1	0	1	1	0	0	2

Listed components account for 79.1 per cent of the wave function.
Occupation $(D5)=11.22$, $(S1)=3.43$, $(D3)=5.34$.

$A=36$, $2J^{\pi}=4^{+}$, $2T=2$, $E=246.622$, eigenvector 1 of this A, J, T. Model core = 16, dimension = 66.

Amplitude	−0.326			−0.184			−0.157			−0.845		
S-shell labels	$D5$	$S1$	$D3$	$D5$	$S1$	$D3$	$D5$	$S1$	$D3$	$D5$	$S1$	$D3$
Configuration	10	4	6	11	4	5	11	4	5	12	4	4
2(S-shell J's)	0	0	4	5	0	3	5	0	7	0	0	4
2(coupled J's)		0	4		5	4		5	4		0	4
2(S-shell T's)	2	0	2	1	0	3	1	0	1	0	0	2
2(coupled T's)		2	2		1	2		1	2		0	2
S-S seniorities	0	0	2	1	0	1	1	0	3	0	0	2

Listed components account for 87.8 per cent of the wave function.
Occupation $(D5)=11.59$, $(S1)=3.91$, $(D3)=4.50$.

$A=36$, $2J^{\pi}=4^{+}$, $2T=2$, $E=244.909$, eigenvector 2 of this A, J, T. Model core = 16, dimension = 66.

Amplitude	0.207			0.565			0.272			−0.313			−0.493		
S-shell labels	$D5$	$S1$	$D3$	$D5$	$S1$	$D3$	$D5$	$S1$	$D3$	$D5$	$S1$	$D3$	$D5$	$S1$	$D3$
Configuration	11	3	6	11	4	5	11	4	5	12	3	5	12	3	5
2(S-shell J's)	5	1	4	5	0	3	5	0	5	0	1	3	0	1	3
2(coupled J's)		4	4		5	4		5	4		1	4		1	4
2(S-shell T's)	1	1	2	1	0	3	1	0	1	0	1	1	0	1	3
2(coupled T's)		0	2		1	2		1	2		1	2		1	2
S-S seniorities	1	1	2	1	0	1	1	0	3	0	1	1	0	1	1

Listed components account for 77.8 per cent of the wave function.
Occupation $(D5)=11.26$, $(S1)=3.44$, $(D3)=5.30$.

$A=36$, $2J^{\pi}=6^{+}$, $2T=2$, $E=245.790$, eigenvector 1 of this A, J, T. Model core = 16, dimension = 69.

Amplitude	−0.236			−0.159			−0.159			−0.145			−0.143			−0.869		
S-shell labels	$D5$	$S1$	$D3$	$D5$	$S1$	$D3$	$D5$	$S1$	$D3$	$D5$	$S1$	$D3$	$D5$	$S1$	$D3$	$D5$	$S1$	$D3$
Configuration	10	4	6	11	3	6	11	4	5	11	4	5	11	4	5	12	4	4
2(S-shell J's)	0	0	6	5	1	4	5	0	3	5	0	3	5	0	7	0	0	6
2(coupled J's)		0	6		4	6		5	6		5	6		5	6		0	6
2(S-shell T's)	2	0	0	1	1	2	1	0	1	1	0	3	1	0	1	0	0	2
2(coupled T's)		2	2		2	2		1	2		1	2		1	2		0	2
S-S seniorities	0	0	2	1	1	2	1	0	1	1	0	1	1	0	3	0	0	2

Listed components account for 90.2 per cent of the wave function.
Occupation $(D5)=11.68$, $(S1)=3.92$, $(D3)=4.40$.

TABLE XVIII. Energies E and spectroscopic factors S for states of $A=36$, $T=2$. The initial state for the pickup factors S_{pk} is the $J^\pi=\frac{3}{2}^+$, $T=\frac{3}{2}$ ground state of ^{37}Cl. For the meaning of E, and the meaning of the numerical subscripts on S, see Table IV.

		Energy E (MeV)				$100\times(S_0;S_2)_{pk}$	$100\times(S_{1/2};S_{3/2};S_{5/2})_{pk}$			
A, J, T	Expt. (Ref. 48)	11.0h +ASPE	12.5p $+^{17}$O	12.5pA	MSDI	Expt. (Ref. 48)	11.0h +ASPE	12.5p $+^{17}$O	12.5pA	MSDI
36, 0, 2	220.67	217.28	242.07	220.65	220.45	; 132	; 112,	; 114,	; 107,	; 111,
	(3.36)	3.88	5.59	3.83	4.71		; 4,	; 2,	; 4,	; 6,
		10.71	9.65	9.84	11.16		; 0,	; 1,	; 1,	; 0,
		12.11	11.44	11.57	12.79		; 2,	; 1,	; 2,	; 1,
36, 1, 2	(4.52)	3.78	4.35	3.73	4.06	94;	87; 3, 1	85; 2, 2	83; 4, 2	85; 5, 1
		9.01	7.87	8.62	9.36		1; 1, 93	2; 1, 91	2; 1, 92	1; 0, 89
36, 2, 2	3.30	3.12	3.89	3.12	3.10	107;	142; 0, 1	135; 0, 5	132; 0, 2	142; 0, 0
	(4.58)	5.80	6.12	5.68	6.30	31;	1; 6, 3	3; 0, 132	2; 4, 17	1; 12, 2
		7.31	7.30	6.56	7.83		1; 1, 126	3; 4, 9	2; 3, 104	0; 2, 118
		8.84	8.54	8.19	9.56		2; 0, 23	1; 1, 7	3; 0, 30	2; 1, 30
36, 3, 2		7.35	6.07	6.58	8.22		; 1, 205	; 1, 204	; 2, 197	; 1, 206
		9.67	9.46	9.10	10.36		; 0, 4	; 1, 2	; 1, 6	; 0, 3
		10.56	10.19	9.93	11.06		; 2, 0		; 2, 0	; 2, 5
		12.28	11.79	11.74	12.80		; 0, 0		; 0, 0	; 0, 0
36, 4, 2		7.22	5.99	6.50	8.09		; , 269	; , 266	; , 261	; , 271
		9.87	9.34	8.98	10.34		; , 0	; , 0	; , 0	; , 5
		11.29	10.78	10.64	11.97		; , 2	; , 3	; , 4	; , 1
36, 5, 2		10.68	10.36	10.10	11.33					
36, 6, 2		14.56	12.27	13.26	15.94					

TABLE XIX. Major components of the wave functions of states of $A=36$, $T=2$ as calculated with the 12.5p+^{17}O Hamiltonian. The conventions of the presentation are explained in Sec. III B of the text.

$A=36$, $2J^{\pi}=0^{+}$, $2T=4$, $E=242.067$, eigenvector 1 of this A, J, T. Model core=16, dimension=9.

Amplitude		0.307			0.931	
S-shell labels	$D5$	$S1$	$D3$	$D5$	$S1$	$D3$
Configuration	10	4	6	12	4	4
2(S-shell J's)	0	0	0	0	0	0
2(coupled J's)		0	0		0	0
2(S-shell T's)	2	0	2	0	0	4
2(coupled T's)		2	4		0	4
S-S seniorities	0	0	0	0	0	0

Listed components account for 96.1 per cent of the wave function.
Occupation $(D5)=11.77$, $(S1)=3.95$, $(D3)=4.28$.

$A=36$, $2J^{\pi}=2^{+}$, $2T=4$, $E=237.716$, eigenvector 1 of this A, J, T. Model core=16, dimension=12.

Amplitude		−0.415			0.289			0.148			−0.924	
S-shell labels	$D5$	$S1$	$D3$	$D5$	$S1$	$D3$	$D5$	$S1$	$D3$	$D5$	$S1$	$D3$
Configuration	10	3	7	11	3	6	11	4	5	12	3	5
2(S-shell $J'S$)	0	1	3	5	1	4	5	0	3	0	1	3
2(coupled $J'S$)		1	2		4	2		5	2		1	2
2(S-shell $T'S$)	2	1	1	1	1	2	1	0	3	0	1	3
2(coupled $T'S$)		3	4		2	4		1	4		1	4
S-S seniorities	0	1	1	1	1	2	1	0	1	0	1	1

Listed components account for 98.1 per cent of the wave function.
Occupation $(D5)=11.82$, $(S1)=3.03$, $(D3)=5.15$.

$A=36$, $2J^{\pi}=4^{+}$, $2T=4$, $E=238.180$, eigenvector 1 of this A, J, T. Model core=16, dimension=21.

Amplitude		0.167			0.154			−0.153			−0.173			0.910	
S-shell labels	$D5$	$S1$	$D3$	$D5$	$S1$	$D3$	$D5$	$S1$	$D3$	$D5$	$S1$	$D3$	$D5$	$S1$	$D3$
Configuration	10	3	7	11	3	6	11	3	6	11	4	5	12	3	5
2(S-shell J's)	0	1	3	5	1	0	5	1	4	5	0	3	0	1	3
2(coupled J's)		1	4		4	4		4	4		5	4		1	4
2(S-shell T's)	2	1	1	1	1	2	1	1	2	1	0	3	0	1	3
2(coupled T's)		3	4		2	4		2	4		1	4		1	4
S-S seniorities	0	1	1	1	1	0	1	1	2	1	0	1	0	1	1

Listed components account for 93.3 per cent of the wave function.
Occupation $(D5)=11.78$, $(S1)=3.03$, $(D3)=5.19$.

$A=36$, $2J^{\pi}=4^{+}$, $2T=4$, $E=235.945$, eigenvector 2 of this A, J, T. Model core=16, dimension=21.

Amplitude		0.167			−0.163			0.242			0.867			0.188	
S-shell labels	$D5$	$S1$	$D3$	$D5$	$S1$	$D3$	$D5$	$S1$	$D3$	$D5$	$S1$	$D3$	$D5$	$S1$	$D3$
Configuration	10	4	6	10	4	6	11	3	6	11	4	5	12	2	6
2(S-shell J's)	0	0	4	8	0	4	5	1	0	5	0	3	0	0	4
2(coupled J's)		0	4		8	4		4	4		5	4		0	4
2(S-shell T's)	2	0	2	2	0	2	1	1	2	1	0	3	0	2	2
2(coupled T's)		2	4		2	4		2	4		1	4		2	4
S-S seniorities	0	0	2	2	0	2	1	1	0	1	0	1	0	0	2

Listed components account for 90.0 per cent of the wave function.
Occupation $(D5)=10.90$, $(S1)=3.80$, $(D3)=5.30$.

TABLE XX. Energies E and spectroscopic factors S for states of $A=35$, $T=\frac{1}{2}$. The initial state for the stripping factors S_{st} is the $J^\pi=0^+$, $T=1$ ground state of ^{34}S. The initial state for the pickup factors S_{pk} is the $J^\pi=0^+$, $T=0$ ground state of ^{36}Ar. For the meaning of E, see Table IV.

A, J, T	Expt. ^{35}Cl	Expt. ^{35}Ar	Energy E (MeV) 11.0h +ASPE	12.5p +^{17}O	12.5pA	MSDI	Expt.	$(100\times S_{st})/(100\times S_{pk})$ 11.0h +ASPE	12.5p +^{17}O	12.5pA	MSDI
$35, \frac{1}{2}, \frac{1}{2}$	1.22	1.18	0.51	1.11	0.72	1.25	19 [a] -28 [b] /140 [c] -210 [d] -250 [e]	27/256	12/194	/258	/312
	3.96 [a,b]		4.17	4.01	4.02	3.19	2 [a] -6 [b] /	4/30	5/64	/3	/5
			5.77	5.83	5.68	5.67	/	0/12	0/77	/61	/0
		6.62	6.28	6.75	6.35	6.91	-44 [f] -	0/51	0/19	/32	/32
$35, \frac{3}{2}, \frac{1}{2}$	216.32	2.60	212.07	234.76	216.32	216.53	108 [a] -130 [b] /340 [c] -350 [f] -290 [e]	64/430	73/433	/392	/397
	2.69 [f]		1.86	2.17	2.11	3.02	2 [a] - /≈50 [c] -60 [d]	6/63	3/83	/80	/52
			4.98	5.09	4.78	4.53		1/6	1/7	/3	/1
			5.52	6.07	5.11	5.48		0/0	0/2	/0	/0
$35, \frac{5}{2}, \frac{1}{2}$	1.76	1.70	1.68	1.70	1.71	1.90	/≤20 [c] -20 [d]	0/3	1/2	/2	/0
	3.00 [f]	2.95	2.65	2.43	2.58	3.18	4 [a] -4 [b] /260 [c] -310 [d] -250 [e]	13/335	13/483	/359	/92
		(5.57) [d,e]	5.44	5.59	5.02	4.74	/ -250 [d] -240 [e]	1/331	0/93	/290	/18
		(6.01) [d,e]	6.06	5.82	5.49	5.49	/ -160 [d] -130 [e]	1/152	2/292	/100	/77
$35, \frac{7}{2}, \frac{1}{2}$	2.64 [f]		2.87	2.40	2.74	2.84					
			4.34	4.08	4.47	4.98					
			5.39	5.28	4.84	6.20					
			7.57	6.87	6.64	7.77					
$35, \frac{9}{2}, \frac{1}{2}$	3.94 [g]		3.98	3.19	4.09	5.62					
			6.42	5.41	5.87	7.61					
$35, \frac{11}{2}, \frac{1}{2}$			8.39	6.81	7.25	9.67					
$35, \frac{13}{2}, \frac{1}{2}$			9.38	7.79	8.28	10.50					

[a] Reference 11.
[b] Reference 50.
[c] Reference 52.
[d] Reference 20.
[e] Reference 51.
[f] Reference 53.
[g] Reference 54.

TABLE XXI. Major components of the wave functions of states of $A=35$, $T=\frac{1}{2}$ as calculated with the 12.5p+^{17}O Hamiltonian. The conventions of the explanation are explained in Sec. III B of the text.

$A=35$, $2J^{\pi}=1^{+}$, $2T=1$, $E=233.653$, eigenvector 1 of this A, J, T. Model core=16, dimension=109.

Amplitude	−0.281			−0.198			−0.204			0.178			−0.269			−0.147			−0.310			0.199			0.537		
S-shell labels	$D5$	$S1$	$D3$	$D5$	$S1$	$D3$	$D5$	$S1$	$D3$	$D5$	$S1$	$D3$	$D5$	$S1$	$D3$	$D5$	$S1$	$D3$	$D5$	$S1$	$D3$	$D5$	$S1$	$D3$	$D5$	$S1$	$D3$
Configuration	10	3	6	10	3	6	10	4	5	11	3	5	11	3	5	11	3	5	11	4	4	12	1	6	12	3	4
2(S-shell J's)	0	1	0	0	1	0	4	0	3	5	1	3	5	1	3	5	1	5	5	0	4	0	1	0	0	1	0
2(coupled J's)		1	1		1	1		4	1		4	1		4	1		4	1		5	1		1	1		1	1
2(S-shell T's)	2	1	2	2	1	2	2	0	1	1	1	1	1	1	1	1	1	1	1	0	0	0	1	2	0	1	0
2(coupled T's)		1	1		3	1		2	1		0	1		2	1		2	1		1	1		1	1		1	1
S-S seniorities	0	1	0	0	1	0	2	0	1	1	1	1	1	1	1	1	1	3	1	0	2	0	1	0	0	1	0

Listed components account for 71.0 per cent of the wave function.
Occupation $(D5)=10.94$, $(S1)=3.03$, $(D3)=5.04$.

$A=35$, $2J^{\pi}=3^{+}$, $2T=1$, $E=234.764$, eigenvector 1 of this A, J, T. Model core=16, dimension=188.

Amplitude	−0.142			−0.220			−0.400			0.164			−0.156			0.174			−0.185			0.579		
S-shell labels	$D5$	$S1$	$D3$	$D5$	$S1$	$D3$	$D5$	$S1$	$D3$	$D5$	$S1$	$D3$	$D5$	$S1$	$D3$	$D5$	$S1$	$D3$	$D5$	$S1$	$D3$	$D5$	$S1$	$D3$
Configuration	9	4	6	10	4	5	10	4	5	10	4	5	11	2	6	11	3	5	12	2	5	12	4	3
2(S-shell J's)	3	0	4	0	0	3	0	0	3	4	0	3	5	2	4	5	1	3	0	0	3	0	0	3
2(coupled J's)		3	3		0	3		0	3		4	3		3	3		4	3		0	3		0	3
2(S-shell T's)	1	0	2	2	0	1	2	0	3	2	0	3	1	0	2	1	1	3	0	2	3	0	0	1
2(coupled T's)		1	1		2	1		2	1		2	1		1	1		2	1		2	1		0	1
S-S seniorities	3	0	2	0	0	1	0	0	1	2	0	1	1	2	2	1	1	1	0	0	1	0	0	1

Listed components account for 67.9 per cent of the wave function.
Occupation $(D5)=10.95$, $(S1)=3.61$, $(D3)=4.44$.

$A=35$, $2J^{\pi}=3^{+}$, $2T=1$, $E=232.593$, eigenvector 2 of this A, J, T. Model core=16, dimension=188.

Amplitude	−0.142			−0.145			−0.284			−0.169			−0.185			−0.172			0.159			−0.320			−0.195			−0.310			−0.316		
S-shell labels	$D5$	$S1$	$D3$	$D5$	$S1$	$D3$	$D5$	$S1$	$D3$	$D5$	$S1$	$D3$	$D5$	$S1$	$D3$	$D5$	$S1$	$D3$	$D5$	$S1$	$D3$	$D5$	$S1$	$D3$	$D5$	$S1$	$D3$	$D5$	$S1$	$D3$	$D5$	$S1$	$D3$
Configuration	10	2	7	10	3	6	10	4	5	10	4	5	11	2	6	11	2	6	11	3	5	11	3	5	11	3	5	12	2	5	12	3	4
2(S-shell J's)	0	0	3	0	1	4	0	0	3	4	0	3	5	2	0	5	2	6	5	1	1	5	1	3	5	1	7	0	0	3	0	1	4
2(coupled J's)		0	3		1	3		0	3		4	3		3	3		3	3		4	3		4	3		4	3		0	3		1	3
2(S-shell T's)	2	2	1	2	1	2	2	0	1	2	0	1	1	0	2	1	0	0	1	1	1	1	1	1	1	1	1	0	2	1	0	1	0
2(coupled T's)		0	1		1	1		2	1		2	1		1	1		1	1		2	1		2	1		2	1		2	1		1	1
S-S seniorities	0	0	1	0	1	2	0	0	1	2	0	1	1	2	0	1	2	2	1	1	3	1	1	1	1	1	3	0	0	1	0	1	2

Listed components account for 57.5 per cent of the wave function.
Occupation $(D5)=10.77$, $(S1)=2.91$, $(D3)=5.31$.

TABLE XXI *(Continued)*

$A=35$, $2J^{\pi}=5^{+}$, $2T=1$, $E=233.061$, eigenvector 1 of this A, J, T. Model core = 16, dimension = 223.

Amplitude	0.241			0.168			0.197			0.183			0.162			0.309			0.150			0.184		
S-shell labels	$D5$	$S1$	$D3$	$D5$	$S1$	$D3$	$D5$	$S1$	$D3$	$D5$	$S1$	$D3$	$D5$	$S1$	$D3$	$D5$	$S1$	$D3$	$D5$	$S1$	$D3$	$D5$	$S1$	$D3$
Configuration	10	3	6	10	4	5	10	4	5	10	4	5	11	3	5	11	3	5	11	3	5	11	4	4
2(S-shell J's)	0	1	4	0	0	5	4	0	3	4	0	3	5	1	3	5	1	3	5	1	7	5	0	2
2(coupled J's)		1	5		0	5		4	5		4	5		4	5		4	5		4	5		5	5
2(S-shell T's)	2	1	2	2	0	1	2	0	1	2	0	3	1	1	1	1	1	3	1	1	1	1	0	2
2(coupled T's)		1	1		2	1		2	1		2	1		2	1		2	1		2	1		1	1
S-S seniorities	0	1	2	0	0	3	2	0	1	2	0	1	1	1	1	1	1	1	1	1	3	1	0	2

Amplitude	0.164			−0.167			0.315			−0.327			0.298		
S-shell labels	$D5$	$S1$	$D3$	$D5$	$S1$	$D3$	$D5$	$S1$	$D3$	$D5$	$S1$	$D3$	$D5$	$S1$	$D3$
Configuration	11	4	4	12	1	6	12	3	4	12	3	4	12	4	3
2(S-shell J's)	5	0	6	0	1	4	0	1	4	0	1	4	0	0	5
2(coupled J's)		5	5		1	5		1	5		1	5		0	5
2(S-shell T's)	1	0	2	0	1	2	0	1	0	0	1	2	0	0	1
2(coupled T's)		1	1		1	1		1	1		1	1		0	1
S-S seniorities	1	0	2	0	1	2	0	1	2	0	1	2	0	0	3

Listed components account for 68.6 per cent of the wave function.
Occupation $(D5)=10.97$, $(S1)=3.23$, $(D3)=4.80$.

$A=35$, $2J^{\pi}=5^{+}$, $2T=1$, $E=232.335$, eigenvector 2 of this A, J, T. Model core = 16, dimension = 223.

Amplitude	−0.239			0.165			0.160			−0.187			−0.527			0.283			0.230			0.227			0.151		
S-shell labels	$D5$	$S1$	$D3$	$D5$	$S1$	$D3$	$D5$	$S1$	$D3$	$D5$	$S1$	$D3$	$D5$	$S1$	$D3$	$D5$	$S1$	$D3$	$D5$	$S1$	$D3$	$D5$	$S1$	$D3$	$D5$	$S1$	$D3$
Configuration	9	4	6	9	4	6	10	4	5	11	2	6	11	4	4	11	4	4	12	2	5	12	3	4	12	3	4
2(S-shell J's)	5	0	0	5	0	0	8	0	3	5	0	0	5	0	0	5	0	4	0	2	3	0	1	4	0	1	4
2(coupled J's)		5	5		5	5		8	5		5	5		5	5		5	5		2	5		1	5		1	5
2(S-shell T's)	1	0	2	3	0	2	2	0	1	1	2	2	1	0	0	1	0	0	0	0	1	0	1	0	0	1	2
2(coupled T's)		1	1		3	1		2	1		1	1		1	1		1	1		0	1		1	1		1	1
S-S seniorities	1	0	0	1	0	0	2	0	1	1	0	0	1	0	0	1	0	2	0	2	1	0	1	2	0	1	2

Listed components account for 62.9 per cent of the wave function.
Occupation $(D5)=10.66$, $(S1)=3.45$, $(D3)=4.88$.

TABLE XXI *(Continued)*

$A=35$, $2J^{\pi}=7^{+}$, $2T=1$, $E=232.363$, eigenvector 1 of this A, J, T. Model core = 16, dimension = 209.

Amplitude	0.209			0.196			−0.147			0.173			−0.150			0.175			0.222			−0.299		
S-shell labels	*D*5	*S*1	*D*3	*D*5	*S*1	*D*3	*D*5	*S*1	*D*3	*D*5	*S*1	*D*3	*D*5	*S*1	*D*3	*D*5	*S*1	*D*3	*D*5	*S*1	*D*3	*D*5	*S*1	*D*3
Configuration	9	4	6	10	4	5	10	4	5	10	4	5	10	4	5	11	3	5	11	4	4	11	4	4
2(S-shell J's)	5	0	4	0	0	7	2	0	5	4	0	3	8	0	3	5	1	3	5	0	2	5	0	4
2(coupled J's)		5	7		0	7		2	7		4	7		8	7		4	7		5	7		5	7
2(S-shell T's)	1	0	2	2	0	1	0	0	1	2	0	3	2	0	3	1	1	3	1	0	2	1	0	0
2(coupled T's)		1	1		2	1		0	1		2	1		2	1		2	1		1	1		1	1
S-S seniorities	1	0	2	0	0	3	2	0	3	2	0	1	2	0	1	1	1	1	1	0	2	1	0	2

Amplitude	0.402			0.277			0.383		
S-shell labels	*D*5	*S*1	*D*3	*D*5	*S*1	*D*3	*D*5	*S*1	*D*3
Configuration	11	4	4	12	3	4	12	4	3
2(S-shell J's)	5	0	4	0	1	6	0	0	7
2(coupled J's)		5	7		1	7		0	7
2(S-shell T's)	1	0	2	0	1	2	0	0	1
2(coupled T's)		1	1		1	1		0	1
S-S seniorities	1	0	2	0	1	2	0	0	3

Listed components account for 71.1 per cent of the wave function.
Occupation $\langle D5\rangle = 10.88$, $\langle S1\rangle = 3.59$, $\langle D3\rangle = 4.53$.

$A=35$, $2J^{\pi}=9^{+}$, $2T=1$, $E=231.569$, eigenvector 1 of this A, J, T. Model core = 16, dimension = 167.

Amplitude	−0.267			−0.201			0.186			−0.145			0.352			−0.473			0.396			−0.180			0.223			−0.224		
S-shell labels	*D*5	*S*1	*D*3	*D*5	*S*1	*D*3	*D*5	*S*1	*D*3	*D*5	*S*1	*D*3	*D*5	*S*1	*D*3	*D*5	*S*1	*D*3	*D*5	*S*1	*D*3	*D*5	*S*1	*D*3	*D*5	*S*1	*D*3	*D*5	*S*1	*D*3
Configuration	9	4	6	10	4	5	10	4	5	11	2	6	11	4	4	11	4	4	11	4	4	11	4	4	12	2	5	12	3	4
2(S-shell J's)	5	0	4	2	0	7	8	0	3	5	0	4	5	0	4	5	0	4	5	0	6	5	0	8	0	2	7	0	1	8
2(coupled J's)		5	9		2	9		8	9		5	9		5	9		5	9		5	9		5	9		2	9		1	9
2(S-shell T's)	1	0	2	0	0	1	2	0	3	1	2	2	1	0	0	1	0	2	1	0	2	1	0	0	0	0	1	0	1	0
2(coupled T's)		1	1		0	1		2	1		1	1		1	1		1	1		1	1		1	1		0	1		1	1
S-S seniorities	1	0	2	2	0	3	2	0	1	1	0	2	1	0	2	1	0	2	1	0	2	1	0	4	0	2	3	0	1	4

Listed components account for 80.4 per cent of the wave function.
Occupation $\langle D5\rangle = 10.71$, $\langle S1\rangle$ 3.68, $\langle D3\rangle = 4.61$.

For the second $\frac{3}{2}^+$ state, the configurations of highest intensity involve excitation from the $s_{1/2}$ to the $d_{3/2}$ orbit. Our calculated spectroscopic factor for pickup to this second $\frac{3}{2}^+$ state is only $\frac{1}{7}$ of that to the ground state. This shell-model ratio, $\frac{1}{7}$, is in nice agreement with the analogous measured ratio if we correlate the second model $\frac{3}{2}^+$ state with the observed $\frac{3}{2}^+$ state at 2.69 MeV in ^{35}Cl (2.60 MeV in ^{35}Ar). The shell-model results for electromagnetic decays of this second $\frac{3}{2}^+$ state also seem to agree approximately with results observed for the 2.69-MeV $\frac{3}{2}^+$ state of ^{35}Cl. More precise experimental data might allow us to discriminate among our various Hamiltonians.

For the second model $\frac{5}{2}^+$ state, the most important component (28% intensity) is

$$(d_{5/2})^{11}(s_{1/2})^4(d_{3/2})^4{}_{J=0,\,T=0}\,.$$

This component is responsible for the large $S(d_{5/2})$ factor calculated for production of this state via pickup from ^{36}Ar. Our various calculations differ in the amount of $(d_{5/2})^{11}$ strength in this second $\frac{5}{2}^+$ state, with MSDI yielding the smallest strength. The experimental results, which indicate a strong $l=2$ pickup transition to a state in ^{35}Ar at 2.95

TABLE XXII. Calculated and experimental $B(E2)$ and $B(M1)$ values for transitions between $T=\frac{1}{2}$ states of ^{35}Cl. The notation $(J)_\nu$ labels the νth lowest state of given J in the $T=\frac{1}{2}$ spectrum.

Initial state $(J)_\nu$ ^{35}Cl, $T=\frac{1}{2}$	Final state $(J)_\nu$ $T=\frac{1}{2}$	$B(E2)$ (e^2 F^4) Expt.	11.0h+ASPE	12.5p+^{17}O	12.5pA	MSDI	$100\times B(M1)$ ($\mu_N{}^2$) Expt.	11.0h +ASPE	12.5p +^{17}O	12.5pA	MSDI
$(\frac{1}{2})_1$	$(\frac{3}{2})_1$	16 ± 2 [a]	10.2	6.6	16.9	20.8	19.5 ± 6 [a]	16.	27.	22.	7.
$(\frac{5}{2})_1$	$(\frac{3}{2})_1$	78 ± 2 [a]	74.4	77.5	67.0	52.0	0.19 ± 0.06 [a]	0.0	1.2	0.18	1.4
	$(\frac{1}{2})_1$		29.2	18.5	24.6	10.6		0	0	0	0
$(\frac{7}{2})_1$	$(\frac{3}{2})_1$	20 ± 7 [b,c]	29.7	30.7	27.7	13.9		0	0	0	0
	$(\frac{5}{2})_1$	23 ± 10 [b,c]	23.6	34.4	26.1	22.5	2 ± 1 [b,c]	4.3	9.5	6.9	0.67
$(\frac{3}{2})_2$	$(\frac{3}{2})_1$	≥8 [c,d]; ≤72 [e]	21.1	23.3	8.8	6.9	≥7 [c,d]; ≤4 [e]	17.	30.	13.	3.1
	$(\frac{1}{2})_1$	≥32 [c,d]; ≤130 [e]	63.9	67.5	62.5	48.5	≥1.7 [c,d]; ≤2.1 [e]	11.	23.	8.4	0.21
	$(\frac{5}{2})_1$	≥20 [c,d]	16.5	7.5	21.8	18.2	≥34 [c,d]; ≤16 [e]	45.	39.	48.	50.
$(\frac{5}{2})_2$	$(\frac{3}{2})_1$	≥0.13 [c,d]; 0.7 [e]	11.3	4.9	7.1	1.9	≥3.6 [c,d]; 6.6 [e]	17.	27.	18.	5.7
	$(\frac{1}{2})_1$	≥40 [c,d]; 43 [e]	36.4	51.2	41.9	35.9		0	0	0	0
	$(\frac{5}{2})_1$		2.3	0.2	0.9	1.1			8.8	0.12	
$(\frac{1}{2})_2$	$(\frac{3}{2})_1$		13.2	11.8	6.3	0.9		12.	11.	5.0	5.5
	$(\frac{1}{2})_1$		0	0	0	0		74.	75.	19.	0.0
	$(\frac{5}{2})_1$		2.7	0.4	0.3	4.3		0	0	0	0
$(\frac{1}{2})_3$	$(\frac{3}{2})_1$		0.02	2.1	3.6	1.3		0.1	11.	17.	0.24
	$(\frac{1}{2})_1$		0	0	0	0					
	$(\frac{5}{2})_1$		2.9	6.6	8.4	2.6		0	0	0	0
$(\frac{3}{2})_3$	$(\frac{3}{2})_1$		3.3	2.6	2.9	2.6		20.	29.	5.5	0.57
	$(\frac{1}{2})_1$		0.06	0.2	0.04	1.0		9.6	26.	3.8	0.15
	$(\frac{5}{2})_1$		24.3	39.6	28.7	3.7		5.3	6.2	0.10	0.11
$(\frac{5}{2})_3$	$(\frac{3}{2})_1$		3.2	3.1	7.4	5.6		3.6	0.16	0.024	0.17
	$(\frac{1}{2})_1$		0.1	0.6	0.3	0.6		0	0	0	0
$(\frac{9}{2})_1$	$(\frac{5}{2})_1$	46 ± 12 [b]	63.1	52.0	61.7	35.0		0	0	0	0
	$(\frac{7}{2})_1$	18 ± 7 [b]	34.0	29.2	25.6	25.8	0.25 ± 0.14 [b]	0.26	0.013	1.2	5.0

[a] Reference 58.
[b] Reference 54.
[c] Reference 57.
[d] Reference 53.
[e] Reference 42.

MeV, are in good agreement with the predictions from our realistic Hamiltonians. (The Hamiltonian MSDI apparently puts the $d_{5/2}$-hole strength too high in the energy spectrum.) The experimentally determined stripping spectroscopic factors to this second $\frac{5}{2}^+$ state are larger than those to the first $\frac{5}{2}^+$ state, and this observation is consistent with our calculated results (only 12.5p + ^{17}O and 11.0h + ASPE have been treated). For $E2$ and $M1$ decay of this second $\frac{5}{2}^+$ state to the $\frac{3}{2}^+$ ground state, and from this second $\frac{5}{2}^+$ state to the first $\frac{1}{2}^+$ state, our calculated strengths are again consistent with the available experimental information. This concludes our level-by-level discussion of the sequence comprising the lowest $\frac{1}{2}^+$, second $\frac{3}{2}^+$, and second $\frac{5}{2}^+$ states.

For the higher levels of $J = \frac{1}{2}^+$, $\frac{3}{2}^+$, and $\frac{5}{2}^+$, we have already noted that there is at least qualitative agreement between shell-model and experimental S factors. In particular, the large $l = 2$ pickup strength observed in the 5–6-MeV region is reproduced by the realistic models. However, our MSDI wave functions fail to reproduce this strength.

In summary, we find that our 12.5p + ^{17}O, 11.0h + ASPE, and 12.5pA Hamiltonians yield $A = 35$, $T = \frac{1}{2}$ states having properties consistent with a wide range of experimental data on the mirror nuclei ^{35}Cl and ^{35}Ar. The shell-model results calculated from these three Hamiltonians are rather similar to each other, while the MSDI results are noticeably different, particularly in the distribution of $d_{5/2}$-hole strength. However, the distributions of $d_{3/2}$ and $s_{1/2}$ pickup strengths are essentially the same for all our Hamiltonians. Shell-model $B(E2)$ strengths, especially the strong ones, tend to be similar for all our Hamiltonians, but $B(M1)$ rates, especially for the weaker transitions, are highly sensitive to the choice among our model Hamiltonians. In many instances where different Hamiltonians yield essentially the same energies, spectroscopic factors, electromagnetic moments, and $B(E2)$'s, these Hamiltonians nevertheless yield quite different values for $B(M1)$'s. For calculated observables involving only the lowest $\frac{3}{2}^+$, $\frac{5}{2}^+$, $\frac{7}{2}^+$, and $\frac{9}{2}^+$ states, our model-to-model variations are generally weaker than for observables involving one or more states outside this sequence.

9. $A = 35$, $T = \frac{3}{2}$: ^{35}S

(See Tables XXIII, XXIV, and Fig. 7)

There is not much experimental information about the energy-level spectrum of ^{35}S. The ground state is $\frac{3}{2}^+$ and there is a $(\frac{1}{2}^+)$ state at 1.56-

TABLE XXIII. Energies E and spectroscopic factors S for states of $A = 35$, $T = \frac{3}{2}$. The initial state for the stripping factors S_{st} is the $J^\pi = 0^+$, $T = 1$ ground state of ^{34}S. The initial state for the pickup factors S_{pk} is the $J^\pi = 0^+$, $T = 2$ ground state of ^{36}S. For the meaning of E, and the meanings of the numerical subscripts on S, see Table IV.

	Energy E (MeV)					$(100 \times S_{st})/(100 \times S_{pk})$			
A, J, T	Expt.	11.0h + ASPE	12.5p + ^{17}O	12.5pA	MSDI	11.0h + ASPE	12.5p + ^{17}O	12.5pA	MSDI
35, $\frac{1}{2}$, $\frac{3}{2}$	(1.56) [a]	1.65	1.88	2.17	2.20	12/100	7/72	/115	/142
		3.79	3.89	3.89	4.20	0/2	1/11	/1	/12
		4.35	4.82	4.88	5.90	0/9	0/24	/16	/4
		5.55	5.25	5.32	7.09	0/24	0/10	/10	/0
35, $\frac{3}{2}$, $\frac{3}{2}$	210.61	205.57	227.83	210.32	211.03	30/327	31/323	/344	/374
		2.46	2.79	2.71	3.11	0/10	0/1	/8	/3
		2.84	3.25	3.20	3.75	2/6	1/1	/5	/2
		3.78	3.81	3.69	4.53	1/8	1/17	/0	/0
35, $\frac{5}{2}$, $\frac{3}{2}$		2.11	1.94	2.27	2.55	2/54	6/227	/11	/1
		2.96	2.87	3.65	4.45	1/84	0/27	/80	/0
		4.02	4.24	4.12	5.39	0/4	0/97	/80	/41
		4.77	4.29	5.32	6.80	0/83	0/1	/151	/13
35, $\frac{7}{2}$, $\frac{3}{2}$		3.09	3.09	2.97	3.50				
		4.93	4.51	4.88	6.59				
		5.95	5.45	5.64	7.36				
		6.72	5.91	6.54	8.36				
35, $\frac{9}{2}$, $\frac{3}{2}$		6.18	4.71	5.34	7.54				
		7.73	6.36	7.12	8.91				
35, $\frac{11}{2}$, $\frac{3}{2}$		6.72	5.10	5.83	8.31				
35, $\frac{13}{2}$, $\frac{3}{2}$		9.72	8.78	9.05	11.45				

[a] Reference 59.

TABLE XXIV. Major components of the wave functions of states of $A=35$, $T=\frac{3}{2}$ as calculated with the 12.5p+^{17}O Hamiltonian. The conventions of the presentation are explained in Sec. III B of the text.

$A=35$, $2J^{\pi}=1^{+}$, $2T=3$, $E=225.949$, eigenvector 1 of this A, J, T. Model core=16, dimension=75.

Amplitude	−0.254			0.162			−0.266			0.219			0.164			0.401			0.223			0.217			0.577		
S-shell labels	$D5$	$S1$	$D3$	$D5$	$S1$	$D3$	$D5$	$S1$	$D3$	$D5$	$S1$	$D3$	$D5$	$S1$	$D3$	$D5$	$S1$	$D3$	$D5$	$S1$	$D3$	$D5$	$S1$	$D3$	$D5$	$S1$	$D3$
Configuration	10	3	6	10	4	5	11	3	5	11	3	5	11	3	5	11	4	4	11	4	4	12	1	6	12	3	4
2(S-shell J's)	0	1	0	4	0	3	5	1	3	5	1	3	5	1	3	5	0	4	5	0	6	0	1	0	0	1	0
2(coupled J's)		1	1		4	1		4	1		4	1		4	1		5	1		5	1		1	1		1	1
2(S-shell T's)	2	1	2	2	0	3	1	1	1	1	1	3	1	1	3	1	0	2	1	0	2	0	1	2	0	1	4
2(coupled T's)		1	3		2	3		2	3		0	3		2	3		1	3		1	3		1	3		1	3
S-S seniorities	0	1	0	2	0	1	1	1	1	1	1	1	1	1	1	1	0	2	1	0	2	0	1	0	0	1	0

Listed components account for 82.7 per cent of the wave function.
Occupation $(D5)=11.10$, $(S1)=3.19$, $(D3)=4.71$.

$A=35$, $2J^{\pi}=3^{+}$, $2T=3$, $E=227.832$, eigenvector 1 of this A, J, T. Model core=16, dimension=129.

Amplitude	0.357			−0.214			0.182			0.791		
S-shell labels	$D5$	$S1$	$D3$	$D5$	$S1$	$D3$	$D5$	$S1$	$D3$	$D5$	$S1$	$D3$
Configuration	10	4	5	10	4	5	12	2	5	12	4	3
2(S-shell J's)	0	0	3	0	0	3	0	0	3	0	0	3
2(coupled J's)		0	3		0	3		0	3		0	3
2(S-shell T's)	2	0	1	2	0	3	0	2	1	0	0	3
2(coupled T's)		2	3		2	3		2	3		0	3
S-S seniorities	0	0	1	0	0	1	0	0	1	0	0	1

Listed components account for 83.2 per cent of the wave function.
Occupation $(D5)=11.40$, $(S1)=3.83$, $(D3)=3.77$.

$A=35$, $2J^{\pi}=5^{+}$, $2T=3$, $E=225.896$, eigenvector 1 of this A, J, T. Model core=16, dimension=148.

Amplitude	−0.202			−0.627			0.266			−0.283			0.177			−0.389			−0.194		
S-shell labels	$D5$	$S1$	$D3$	$D5$	$S1$	$D3$	$D5$	$S1$	$D3$	$D5$	$S1$	$D3$	$D5$	$S1$	$D3$	$D5$	$S1$	$D3$	$D5$	$S1$	$D3$
Configuration	9	4	6	11	4	4	11	4	4	11	4	4	12	2	5	12	3	4	12	3	4
2(S-shell J's)	5	0	0	5	0	0	5	0	2	5	0	4	0	2	3	0	1	4	0	1	6
2(coupled J's)		5	5		5	5		5	5		5	5		2	5		1	5		1	5
2(S-shell T's)	1	0	2	1	0	4	1	0	2	1	0	2	0	0	3	0	1	2	0	1	2
2(coupled T's)		1	3		1	3		1	3		1	3		0	3		1	3		1	3
S-S seniorities	1	0	0	1	0	0	1	0	2	1	0	2	0	2	1	0	1	2	0	1	2

Listed components account for 80.6 per cent of the wave function.
Occupation $(D5)=10.98$, $(S1)=3.60$, $(D3)=4.42$.

TABLE XXIV *(Continued)*

$A = 35$, $2J^{\pi} = 5^{+}$, $2T = 3$, $E = 224.963$, eigenvector 2 of this A, J, T. Model core = 16, dimension = 148.

Amplitude	0.158			0.145			−0.182			0.223			0.303			0.371		
S-shell labels	$D5$	$S1$	$D3$	$D5$	$S1$	$D3$	$D5$	$S1$	$D3$	$D5$	$S1$	$D3$	$D5$	$S1$	$D3$	$D5$	$S1$	$D3$
Configuration	10	4	5	11	3	5	11	3	5	11	4	4	11	4	4	11	4	4
2(S-shell J's)	2	0	3	5	1	3	5	1	5	5	0	0	5	0	4	5	0	6
2(coupled J's)		2	5		4	5		4	5		5	5		5	5		5	5
2(S-shell T's)	0	0	3	1	1	3	1	1	1	1	0	4	1	0	2	1	0	2
2(coupled T's)		0	3		2	3		2	3		1	3		1	3		1	3
S-S seniorities	2	0	1	1	1	1	1	1	3	1	0	0	1	0	2	1	0	2

Amplitude	−0.220			−0.570		
S-shell labels	$D5$	$S1$	$D3$	$D5$	$S1$	$D3$
Configuration	12	2	5	12	3	4
2(S-shell J's)	0	2	3	0	1	4
2(coupled J's)		2	5		1	5
2(S-shell T's)	0	0	3	0	1	2
2(coupled T's)		0	3		1	3
S-S seniorities	0	2	1	0	1	2

Listed components account for 73.2 per cent of the wave function.
Occupation $(D5) = 11.20$, $(S1) = 3.28$, $(D3) = 4.51$.

$A = 35$, $2J^{\pi} = 7^{+}$, $2T = 3$, $E = 224.740$, eigenvector 1 of this A, J, T. Model core = 16, dimension = 136.

Amplitude	−0.156			0.161			0.196			0.186			−0.409			−0.205			−0.677		
S-shell labels	$D5$	$S1$	$D3$	$D5$	$S1$	$D3$	$D5$	$S1$	$D3$	$D5$	$S1$	$D3$	$D5$	$S1$	$D3$	$D5$	$S1$	$D3$	$D5$	$S1$	$D3$
Configuration	10	3	6	11	3	5	11	3	5	11	3	5	11	4	4	11	4	4	12	3	4
2(S-shell J's)	0	1	6	5	1	3	5	1	3	5	1	5	5	0	4	5	0	6	0	1	6
2(coupled J's)		1	7		4	7		4	7		4	7		5	7		5	7		1	7
2(S-shell T's)	2	1	0	1	1	1	1	1	3	1	1	1	1	0	2	1	0	2	0	1	2
2(coupled T's)		3	3		2	3		0	3		2	3		1	3		1	3		1	3
S-S seniorities	0	1	2	1	1	1	1	1	1	1	1	3	1	0	2	1	0	2	0	1	2

Listed components account for 79.0 per cent of the wave function.
Occupation $(D5) = 11.28$, $(S1) = 3.28$, $(D3) = 4.44$.

TABLE XXV. Energies E and spectroscopic factors S for states of $A=34$, $T=0$. The initial state for the pickup factors S_{pk} is the $J=\frac{3}{2}$, $T=\frac{1}{2}$ ground state of ^{35}Cl. For the meaning of E, and the meanings of the numerical subscripts on S, see Table IV.

		Energy E (MeV)			$100\times(S_{1/2};\ S_{3/2},\ S_{5/2})_{pk}$	
A, J, T	Expt. Refs. 61, 62	12.5p + ^{17}O	11.0h + ASPE	11.0h + ^{17}O	12.5p + ^{17}O	11.0h + ASPE
34, 0, 0		3.94			; 0,	; 0,
		5.62			; 0,	; 0,
1	0.31	−0.53	−0.89	0.22	0; 15, 9	0; 2, 6
	0.43	0.51	−0.07	0.38	11; 11, 1	16; 0, 1
		0.98	0.06	1.60	2; 14, 10	0; 25, 4
		1.66	1.05	1.94	10; 6, 1	6; 7, 1
2	1.08	0.21	−0.20	0.46	; 1, 13	13; 1, 10
		1.13	0.76	1.94	; 7, 12	0; 3, 8
		2.06	1.36	2.68	; 0, 4	23; 1, 7
		2.84	2.16	3.44	; 1, 0	2; 1, 0
3	203.50	217.32	197.60	205.26	; 104, 4	; 89, 8
		0.44	0.34	0.91	; 6, 20	; 7, 3
		1.04	1.03	1.44	; 1, 19	; 12, 27
		2.21	1.68	2.91	; 2, 1	; 0, 0
4	2.25	1.71	1.34		; , 6	; , 4
		2.32	2.66		; , 45	; , 36
		2.97	2.66		; , 1	; , 0
5		2.05	3.06			
		2.43	3.20			
6		4.27	5.34			

TABLE XXVI. Energies E and spectroscopic factors S for states of $A=34$, $T=1$. The initial state for the pickup factors S_{pk} is the $J=\frac{3}{2}$, $T=\frac{1}{2}$ ground state of ^{35}Cl. For the meaning of E, and the meanings of the numerical subscripts on S, see Table IV.

		Energy E (MeV)		$100\times(S_0;S_2)_{pk}$		
	Expt.			Expt.	$100\times(S_{1/2};\ S_{3/2},\ S_{5/2})_{pk}$	
A, J, T	Ref. 63	12.5p + ^{17}O	11.0h + ASPE	(Ref. 64)	12.5p + ^{17}O	11.0h + ASPE
34, 0, 1	203.64	217.96	198.68	; 86	; 73,	; 64,
	3.92	3.62	3.66	; <7	; ,	; 25,
	5.23	6.21	5.62	;	; ,	; 0,
	5.86	7.02	6.91	;	; ,	; 2,
1	4.08	3.61	3.51	57; 28	; ,	; ,
		6.72	6.91	;	; ,	; ,
2	2.13	2.09	1.93	21; 26	; ,	16; 4, 17
	3.30	2.84	2.56	66; 52	; ,	54; 4, 29
	4.12	3.86	3.69		; ,	0; 90, 9
	4.89	5.25	5.12	;	; ,	47; 4, 27
3	(4.69)	3.93	4.05	; 41	; ,	; 7, 91
		5.33	6.07	;	; ,	; 6, 34
4	(4.88)	3.93	4.86	; 79	; ,	; , 84
		5.29	5.13	;	; ,	; , 15
		5.63	6.07	;	; ,	; , 15
		7.11				, 38

MeV excitation.[59] The only other spin-parity assignments are $\frac{7}{2}^-$ and $\frac{3}{2}^-$ to the 1.99- and 2.35-MeV states. Each model spectrum in Fig. 7 has a $\frac{3}{2}^+$ ground state, and a $\frac{1}{2}^+$ first excited state between 1.6 and 2.2 MeV. Several more positive-parity levels are calculated to lie between 2- and 3-MeV excitation, but at present there are not enough experimental data to warrant correlations between these higher predicted levels and experimental levels. In all of our realistic calculations, the spacing between the ground states of the $T=\frac{1}{2}$ and $T=\frac{3}{2}$ systems comes out too large.

For both 12.5p + ^{17}O and 11.0h + ASPE, the quadrupole moment calculated for the ^{35}S ground state is almost twice as big as the measured value. Our theoretical values for the magnetic moment are consistent with experimental data. (See Table XXVII.)

Calculated spectroscopic factors for pickup from ^{36}S are shown in Table XXIII. No experimental data are available. All our models give significant $s_{1/2}$-hole strength to the lowest $\frac{1}{2}^+$ state, and put a large fraction of the $d_{3/2}$-hole strength into the ground state. As was the case for $A=35$, $T=\frac{1}{2}$, the distribution of $d_{5/2}$-hole strength varies from model to model. In the lowest four $\frac{5}{2}^+$ states the MSDI model has substantially less $d_{5/2}$-hole strength than the other models have. These model-to-model variations are even wider for $T=\frac{3}{2}$ than they were for $T=\frac{1}{2}$. Obviously a ^{36}S$(d, t)^{35}$S experiment would yield very valuable information about the nature of the ^{35}S levels, and about the success of our models.

10. $A=34$, $T=0$ and $T=1$: ^{34}Cl and ^{34}S-^{34}Ar (See Tables XXV and XXVI)

We did not make calculations for the $A=34$ systems with the full gamut of our Hamiltonians, nor did we include $A=34$ levels as part of our least-square search criteria. This limited treatment was prompted by practical difficulties arising from the very large dimensions in the $T=1$ system, and by the lack of firm spectroscopic knowledge about the $T=0$ system at the time the calculations were carried out. Recent experimental work[60-64] has extended the knowledge available about $A=34$, $T=1$, and greatly clarified the situation for ^{34}Cl, $T=0$ and $T=1$. This new experimental situation calls for a more extended treatment than we present here, and a more detailed study is planned. However, comparison of experimental $A=34$ data with the present limited results is quite instructive as regards evaluation of the Hamiltonians we have used in the present investigation.

The 12.5p + ^{17}O and 11.0h + ASPE spectra which we have calculated for $A=34$, $T=1$ are in quite acceptable agreement with the observed ^{34}S spectrum, and are rather similar to each other (as has been the case for the other even-even systems we have discussed). The calculated spectroscopic factors for pickup to the $A=34$, $T=1$ states are also in rather good agreement with experimental data. The most evident problems in the $T=1$ spectrum, both for level energies and S factors, concern the 3^+ and 4^+ states.

We have calculated at least partial $T=0$ spectra

TABLE XXVII. Static electric quadrupole and magnetic dipole moments for states of $A=34-38$. The notation $(J)_\nu$ labels the νth-lowest state of spin J in the spectrum of a nucleus.

Nucleus	$(J)_\nu$	Static electric quadrupole moment (e F^2) Expt.	12.5p + ^{17}O	11.0h + ASPE	Magnetic dipole moment (μ_N) Expt.	12.5p + ^{17}O	11.0h + ASPE
^{34}S	$(2)_1$			+11.9			
	$(2)_2$			−9.7			
^{35}Cl	$(\frac{3}{2})_1$	−7.9	−9.0	−9.2	+0.82	+0.72	+0.68
	$(\frac{1}{2})_1$	...	...	...		+1.09	+1.55
	$(\frac{5}{2})_1$		+2.3	+2.4		+1.05	
^{35}S	$(\frac{3}{2})_1$	+4	+7.5	+8.1	±1.0	+1.20	+1.21
^{36}Ar	$(2)_1$		+14.3	+14.7			
	$(2)_2$		−7.9	−7.2			
	$(4)_1$		+20.9	+20.8			
^{36}Cl	$(2)_1$	−1.7	−0.94	−0.75	+1.28	+1.77	+1.55
	$(3)_1$		−2.21	−1.95		+1.41	+1.43
^{37}Ar	$(\frac{3}{2})_1$		+8.7	+8.7	+0.95	+1.53	+1.43
^{37}Cl	$(\frac{3}{2})_1$	−6.2	−8.4	−8.4	+0.68	+0.68	+0.59
^{38}K	$(3)_1$		+10.9	+10.8	+1.37	+1.23	+1.24
	$(1)_1$		+3.6	+3.7			+0.35
	$(1)_2$		−0.97	−0.73			+0.70
^{38}Ar	$(2)_1$		+1.29				

with each of the Hamiltonians 12.5p + ^{17}O, 11.0h + ASPE, and 11.0h + ^{17}O. The comparison between model results and experiment for this odd-odd six-hole system is reminiscent of the results[4] for its odd-odd six-particle analog in the lower part of the *sd* shell, ^{22}Na. In both ^{34}Cl and ^{22}Na, the lowest-energy $T=0$ level is observed to be $J^\pi = 3^+$, and in each case this state is followed by two $J^\pi = 1^+$ levels. The $A = 18-22$ realistic shell-model calculations,[4] like the present $A = 34-39$ calculations, yield energies of the 1^+ levels which are too depressed relative to the 3^+. In addition to the general problem of lack of agreement between shell-model and observed energies, the shell-model results exhibit some significant differences from one Hamiltonian to the other. The 12.5p + ^{17}O results seem superior to those from 11.0h + ASPE. Also, the use of ^{17}O single-particle energies with the 11.0h two-body matrix elements yields better results then are obtained with 11.0h + ASPE.

IV. CONCLUSIONS AND SUMMARY

We have investigated four different but related versions of "realistic" shell-model effective interactions by using them to calculate energy-level spectra for $A = 35-39$ nuclei. First the observed single-particle energy spectrum from ^{17}O was used with each of the four different two-body interactions to make four different (1 + 2)-body Hamiltonians. Next, a new set of single-particle energies was obtained for each of the four interactions, by adjusting the single-particle spacings so as to best fit observed excitation energies in the $A = 35-39$ region. All eight sets of calculated spectra are in qualitative agreement with the experimentally determined level sequences. However, detailed examination of the spectra and of spectroscopic factors indicates that there are disagreements with experiment which adjustment of the single-particle energies cannot significantly ameliorate. When the ^{17}O values are used for single-particle energies, the observed features of the lighter nuclei ($A = 35-36$) are better reproduced by the calculations than those of the heavier nuclei ($A = 37-39$). In particular, the calculated $A = 38$ and $A = 39$ results show significant deviations from the experimentally observed separation of the $d_{3/2}$ and $s_{1/2}$ centroids. Alteration of the single-particle energies, so as to minimize the mean square deviation from observed energy levels in $A = 35-39$, shifts the region of best agreement from $A \approx 35$ to $A \approx 37$.

Over all, however, the main features of the spectra are not highly sensitive to the choice among our eight realistic Hamiltonians. The coupling of the effects of the one- and two-body parts of each Hamiltonian upon the multiparticle spectra, the essential similarity of the results from the different Hamiltonians, and the present incomplete state of experimental knowledge made it impossible for us to select, on the basis of the calculated spectra, a best Hamiltonian from among these eight realistic Hamiltonians. Two of the eight were chosen, rather arbitrarily, for further study. Single-nucleon spectroscopic factors and $E2$ and $M1$ observables were calculated from the wave functions obtained with these two "realistic" Hamiltonians.

In addition, we calculated spectra, spectroscopic factors, and $E2$ and $M1$ observables from the wave functions obtained with two "least-squares" Hamiltonians, each constructed by varying a parametrized two-body interaction as well as the single-particle energies in an attempt to fit experimentally observed level energies. One of these two least-squares Hamiltonians incorporated a modified surface δ interaction (MSDI). The other incorporated a modified version of one of our realistic interactions, least-squares-adjusted in a way that was suggested by the parametric form of the MSDI Hamiltonian.

In our investigation of spectroscopic factors and $E2$ and $M1$ observables, we found that the two realistic Hamiltonians (i.e., those with unadjusted realistic two-body interactions) gave similar results, just as they had given similar results for energy-level spectra. However, the two least-squares Hamiltonians gave results noticeably different from the realistic results, and appeared to agree less well with the experimentally determined spectroscopic factors and electromagnetic observables. (This is to be contrasted with the slightly better agreement to observed level energies that these two least-squares Hamiltonians gave.)

According to the spectroscopic factors calculated from the two realistic Hamiltonians, the $d_{3/2}$, $s_{1/2}$, and $d_{5/2}$ single-particle and single-hole strengths are distributed over the model levels in a way that agrees with available stripping and pickup data, to within the experimental and DWBA uncertainties. Observed electric quadrupole and magnetic dipole moments are reproduced with fair-to-good accuracy; the results are summarized in Table XXVII. Large experimental $B(E2)$ and $B(M1)$ values are correctly estimated by the calculations. Small observed $B(E2)$'s and $B(M1)$'s are accounted for only qualitatively. That is, a small-to-vanishing experimental strength usually has as its theoretical counterpart a small-to-vanishing model strength, but the two small numbers often differ by a factor of ≈ 10.

We have emphasized comprehensiveness and a unified approach in this investigation, rather than highly accurate theoretical-experimental agree-

ment either for a particular spectrum or a particular kind of observable. The results of our investigation indicate that with an A-independent Hamiltonian, one can get good if not spectacular agreement for about 10 different mass-isospin systems. This agreement is achieved not only for level energies, but also for spectroscopic factors and $E2$ and $M1$ observables. Finally, this agreement is achieved with "realistic" effective interactions.

---

*Research jointly sponsored by the U. S. Atomic Energy Commission under contract with Union Carbide Corporation, and by the National Science Foundation.

[1]T. T. S. Kuo, Nucl. Phys. A103, 71 (1967).
[2]T. Hamada and I. D. Johnston, Nucl. Phys. 34, 382 (1962).
[3]E. C. Halbert, J. B. McGrory, and B. H. Wildenthal, Phys. Rev. Letters 20, 1112 (1968); E. C. Halbert, in *Proceedings of the Third Symposium on the Structure of Low-Medium Mass Nuclei*, edited by J. P. Davidson (University of Kansas Press, Lawrence, Kansas, 1968).
[4]E. C. Halbert, J. B. McGrory, B. H. Wildenthal, and S. P. Pandya, in *Advances in Nuclear Physics*, edited by E. Vogt and M. Baranger (Plenum Press, Inc., New York, 1971), Vol. 4.
[5]B. R. Barrett and M. W. Kirson, Nucl. Phys. A148, 145 (1970).
[6]L. Zamick, Phys. Rev. Letters 23, 1406 (1969).
[7]P. W. M. Glaudemans, G. Wiechers, and P. J. Brussaard, Nucl. Phys. 56, 529 (1964).
[8]A. E. L. Dieperink and P. J. Brussaard, Nucl. Phys. A128, 34 (1969).
[9]F. Tabakin, Ann. Phys. (N.Y.) 30, 51 (1964).
[10]J. B. French, E. C. Halbert, J. B. McGrory, and S. S. M. Wong, in *Advances in Nuclear Physics*, edited by E. Vogt and M. Baranger (Plenum Press, Inc., New York, 1969), Vol. 3.
[11]A. Graue, L. H. Herland, J. R. Lien, G. E. Sandvik, E. R. Cosman, and W. H. Moore, Nucl. Phys. A136, 577 (1969).
[12]B. Rosner and E. J. Schneid, Phys. Rev. 163, 1219 (1967).
[13]P. M. Endt and C. van der Leun, Nucl. Phys. A105, 1 (1967).
[14]H. A. Bethe, B. H. Brandow, and A. G. Petschek, Phys. Rev. 129, 225 (1963).
[15]B. L. Scott and S. A. Moszkowski, Ann. Phys. (N.Y.) 14, 107 (1961).
[16]C. W. Wong, Nucl. Phys. A91, 399 (1967).
[17]T. T. S. Kuo, in Proceedings of the Fourth Symposium on the Structure of Low-Medium Mass Nuclei, edited by J. P. Davidson (University of Kansas Press, Lawrence, Kansas, to be published).
[18]T. T. S. Kuo and G. E. Brown, Nucl. Phys. 85, 40 (1966).
[19]S. A. Moszkowski, in *Handbuch der Physik*, edited by S. Flügge (Springer-Verlag, Berlin, Germany, 1957), p. 411.
[20]R. L. Kozub, Phys. Rev. 172, 1078 (1968).
[21]J. C. Hiebert, E. Newman, and R. H. Bassel, Phys. Rev. 154, 898 (1967).
[22]I. M. Naquib and L. L. Green, Nucl. Phys. A112, 76 (1968).
[23]P. W. M. Glaudemans and B. H. Wildenthal, unpublished. A brief description of this computer program is given in the Appendix of Ref. 4.
[24]R. Arvieu and S. A. Moszkowski, Phys. Rev. 145, 830 (1966).
[25]P. W. M. Glaudemans, B. H. Wildenthal, and J. B. McGrory, Phys. Letters 21, 427 (1966).
[26]P. W. M. Glaudemans, P. J. Brussaard, and B. H. Wildenthal, Nucl. Phys. A102, 593 (1967).
[27]B. H. Wildenthal, J. B. McGrory, E. C. Halbert, and P. W. M. Glaudemans, Phys. Letters 27B, 611 (1968).
[28]B. H. Wildenthal, Phys. Rev. Letters 22, 118 (1969).
[29]F. Everling, L. A. König, J. H. E. Mattauch, and A. H. Wapstra, Nucl. Phys. 18, 1529 (1960).
[30]H. T. Fortune, N. G. Puttaswamy, and J. L. Yntema, Phys. Rev. 185, 1546 (1969).
[31]L. M. Blau, W. P. Alford, D. Cline, and H. E. Gove, Nucl. Phys. 76, 45 (1965).
[32]A. E. L. Dieperink and P. W. M. Glaudemans, Phys. Letters 28B, 531 (1969).
[33]B. H. Wildenthal and E. Newman, Nucl. Phys. A118, 347 (1968).
[34]M. A. Moinester and W. P. Alford, Nucl. Phys. A145, 143 (1970).
[35]H. Graue and K. P. Lieb, Nucl. Phys. A127, 13 (1969).
[36]F. C. Erne, Nucl. Phys. 84, 91 (1966).
[37]G. A. P. Engelbertink and P. W. M. Glaudemans, Nucl. Phys. A123, 225 (1969).
[38]G. A. P. Engelbertink, H. Lindeman, and M. J. N. Jacobs, Nucl. Phys. A107, 305 (1968).
[39]J. H. McNally, Nucl. Phys. 88, 257 (1966).
[40]C. H. Holbrow, P. V. Hewka, J. Wiza, and R. Middleton, Nucl. Phys. 79, 505 (1965).
[41]D. R. Goosman, Phys. Rev. 163, 1219 (1967).
[42]D. D. Duncan, K. H. Buerger, R. L. Place, and B. D. Kern, Phys. Rev. 185, 1515 (1969).
[43]M. C. Mermaz and G. T. Garvey, private communication.
[44]A. M. Hoogenboom, E. Kashy, and W. W. Buechner, Phys. Rev. 128, 305 (1962).
[45]J. C. Hardy, H. Brunnader, and J. Cerny, Phys. Rev. Letters 22, 1439 (1969).
[46]L. Broman, C. M. Fou, and B. Rosner, Nucl. Phys. A112, 195 (1968).
[47]S. Hinds and R. Middleton, private communication quoted in Ref. 13.
[48]W. S. Gray, P. J. Ellis, T. Wei, R. M. Polichar, and J. Janecke, Nucl. Phys. A140, 494 (1970).
[49]N. G. Puttaswamy and J. L. Yntema, Phys. Rev. 177, 1624 (1969).
[50]R. A. Morrison, Nucl. Phys. A140, 97 (1970).
[51]R. R. Johnson and R. J. Griffiths, Nucl. Phys. A108, 113 (1968).
[52]C. A. Whitten, Jr., M. C. Mermaz, and D. A. Bromley, Phys. Rev. C 1, 1455 (1970).
[53]P. Taras and J. Matas, Can. J. Phys. 48, 603 (1970).
[54]F. Ingebretsen, C. Broude, and J. S. Forster, Phys.

Letters 31B, 297 (1970).
[55]D. D. Watson, private communication.
[56]B. W. Hooton, O. Hausser, F. Ingebretsen, and T. K. Alexander, Can. J. Phys. 48, 1259 (1970).
[57]O. Hausser, D. Pelte, T. K. Alexander, and H. C. Evans, Can. J. Phys. 47, 1065 (1969).
[58]F. Ingebretsen, T. K. Alexander, O. Hausser, and D. Pelte, Can. J. Phys. 47, 1295 (1969).
[59]L. K. ter Veld and T. W. van der Mark, Phys. Rev. 173, 1101 (1968).
[60]C. E. Moss, Nucl. Phys. A131, 235 (1969).
[61]H. D. Graber and G. I. Harris, Phys. Rev. 188, 1685 (1969).
[62]P. M. DeLucca, J. C. Lawson, and P. R. Chagnon, Bull. Am. Phys. Soc. 15, 566 (1970); and private communication.
[63]C. E. Moss, R. V. Poore, N. R. Roberson, and D. R. Tilley, Nucl. Phys. A144, 577 (1970).
[64]B. H. Wildenthal and E. Newman, Phys. Rev. 174, 1431 (1968.

PHYSICAL REVIEW C VOLUME 4, NUMBER 4 OCTOBER 1971

$E1$ and $M1$ Radiative Strength in ^{53}Cr, ^{57}Fe, and ^{61}Ni from Threshold Photoneutron Cross Sections*

H. E. Jackson and E. N. Strait†
Argonne National Laboratory, Argonne, Illinois 60439
(Received 5 May 1971)

The photoneutron cross sections for ^{53}Cr, ^{57}Fe, and ^{61}Ni have been measured near threshold with high resolution. Nuclear states of interest were excited by photon absorption from a bremsstrahlung beam whose end-point energy was sufficient only for neutron decay to the ground state of the daughter. Spins of resonances were assigned on the basis of angular distributions determined from the spectra for neutron emission at angles of 90 and 135°; the ground-state radiation widths $\Gamma_{\gamma 0}$ for most resonances were determined from the observed yields. Parity assignments were based on a comparison of data with total neutron cross sections of the daughter nuclei. The central feature of the results is an intense p-wave component whose integrated strength for all targets is greater than that of the s-wave component. In addition, an anomalous concentration of $M1$ strength is observed in an intense doublet with $J^\pi = \frac{3}{2}^-$ at $E_n = 230$ keV in the cross section for ^{57}Fe. The reduced widths for $E1$ and $M1$ radiation are consistent with the values $\bar{k}_{E1} = 0.0012$ and $\bar{k}_{M1} = 0.019$, respectively.

No evidence is found in the reactions ^{53}Cr(γ,n) and ^{57}Fe(γ,n) near threshold for doorway states which have been proposed in the literature. The data were also tested for a correlation between the reduced neutron width for s-wave resonances in each target and the corresponding ground-state radiation widths. In no case is there evidence for a significant correlation. Therefore the strong correlation reported between the reduced neutron widths and total radiation widths for s-wave resonances in even-even target nuclei in this mass region should not be attributed to the ground-state transition.

I. INTRODUCTION

One of the principal objectives in the study of γ-ray decay from individual highly excited nuclear states is observation of the influence of nuclear structure on the intensity of primary transitions. Among the nuclear-structure effects expected are rapid variations with excitation energy and atomic mass of the mean intensities for both electric and magnetic dipole transitions. The physical quantity which is expected to reflect these phenomena is the radiative strength function $\bar{\Gamma}/D$ for the appropriate multipole, where $\bar{\Gamma}$ is the average radiative width for transitions of a given multipolarity and D is the mean spacing of excited states whose spins and parities are such that these transitions are allowed. Because this parameter describes the average properties of radiative transitions, including any energy or mass dependence, experimental efforts have frequently focused on its measurement and comparison with various theoretical models.

Extensive experimental information is already available for electric dipole transitions. Although the small number of experimental samples still prevents decisive comparison of data with various predictions for mass dependence, the influence of the giant dipole resonance on $E1$ radiative strength has been observed[1] in several nuclei; specifically, the strength function varies more sharply with photon energy than would be expected from single-particle estimates. More detailed phenomena, such as the existence of relatively sharp variations in the strength of $E1$ transitions in the mass region $180 < A < 208$ and the energy region $E_\gamma \approx 5.5$ MeV,